Georgia Water Resources Institute
Annual Technical Report
FY 2003

Introduction

The GWRI mission is to foster the creation of partnerships, resources, and knowledge base necessary to address current water resources challenges in the state of Georgia, the U.S., and the world. Specific GWRI goals include:

a) Develop new research methods and scientific knowledge to support sustainable river basin planning and management;

b) Educate scientists, engineers, and water professionals in state-of-the-science methods and their potential applications; and

c) Disseminate useful information to policy makers, water managers, industry stakeholders, citizen groups, and the general public.

In keeping with the above-stated mission and goals, during Fiscal Year 2003, the Georgia Water Resources Institute (GWRI) was involved in a wide range of activities at the state, national and international levels. The following sections summarize these activities as they pertain to research, education, technology transfer, and professional and policy impact.

RESEARCH PROJECTS:

1. Decreasing Irrigation Volumes While Maintaining Crop Yields, sponsored by GWRI/USGS104B;

2. A Combined Hydrological , Geochemical and Isotopic Approach to Understanding the Effects of Basin Scale on Base Flow Systematics in the Georgia Piedmont, sponsored by GWRI/USGS104B;

3. Assessment of In-Stream Processes in the Development of Sediment TMDLs for Urban Streams, sponsored by GWRI/USGS104B;

4. Mid Infrared Water Quality Sensors for the Detection of Organic Pollutants, sponsored by GWRI/USGS104G;

5. INFORM: Integrated Forecast and Reservoir Management System for Northern California, sponsored by NOAA, California Energy Commission, and CalFed;

6. Epidemiological and Environmental Malaria Information System for East Africa, sponsored by GIT and CDC.

EDUCATION AND TECHNOLOGY TRANSFER:

1. USGS Graduate Student Internship,Groundwater Modeling for Coastal Aquifers;

2. Nile Decision Support Tool Applied Training Program, sponsored by the Food and Agriculture Organization of the United Nations (FAO/UN);

3. Hydrologic Engineering for Dam Design, continuing education course;

PROFESSIONAL AND POLICY IMPACT:

GWRIs continuing involvement in Africa (Nile DST) and California (INFORM) has had and continues to have significant policy impact. The Nile DST has now been disseminated to all 10 Nile countries (Burundi, Congo, Egypt, Eritrea, Ethiopia, Kenya, Rwanda, Sudan, Tanzania, and Uganda) and is being used to generate the information base for policy dialogue among the Nile partners. In the course of FY 2003, GWRI personnel worked closely with country engineers and scientists to increase the human resource base that is familiar and can effectively use the Nile DST technology. The technology transfer process included extensive (90 hour) instruction and hands-on training as well as an internet forum for Nile DST users.

In the US, INFORM is a project that is motivated by the water and energy shortages in California. INFORM brings together all relevant agencies and stakeholder groups associated with the Sacramento and American Rivers in Northern California. Participating agencies include the National Weather Service, the US Army Corps of Engineers, the US Bureau of Reclamation, the Sacramento Flood Control Authority, US EPA, California Department of Water Development, and the California Energy Commission. The project aims at developing the institutional framework and technical tools necessary to support integrated river basin management.

At the state level, GWRI is supporting the state water resources planning effort through involvement in the Water Council for the State Attorney General and various other Committees.

Research Program

Decreasing Irrigation Volumes While Maintaining Crop Yields

Basic Information

Title:	Decreasing Irrigation Volumes While Maintaining Crop Yields
Project Number:	2003GA38B
Start Date:	3/1/2003
End Date:	2/28/2004
Funding Source:	104B
Congressional District:	GA 2nd
Research Category:	Not Applicable
Focus Category:	Irrigation, Agriculture, Water Use
Descriptors:	
Principal Investigators:	Calvin D Perry

Publication

1. Perry, C. and S. Pocknee, 2003. Precision Pivot Irrigation Controls To Optimize Water Application. In Understanding & Addressing Conservation and Recycled Water Irrigation, the Proceedings of the 2003 Irrigation Association Meeting, San Diego, CA. pp. 86-92.
2. Perry, C., S. Pocknee, and O. Hansen, 2003. A variable rate pivot irrigation control system. In J. Stafford and A. Werner (eds), ECPA 2003, Proceedings of the Fourth European Conference on Precision Agriculture, pp. 539-544.
3. Perry, C., S. Pocknee, and K. Harrison, 2003. Optimizing Irrigation Water Application. The Precision Ag Guide, pp 10-11, insert in the July issues of The Peanut Grower and Cotton Farming trade magazines, July 2003.
4. Perry, C., S. Pocknee, C. Kvien, and G. Vellidis, 2004. "Decreasing Irrigation Volumes While Maintaining Crop Yields." Georgia Water Resources Institute, Georgia Tech, Atlanta, GA., 5p.

DECREASING IRRIGATION VOLUMES WHILE MAINTAINING CROP YIELDS

Georgia Water Resources Institute
Final Report

Calvin Perry[1,2], Stuart Pocknee[2], Craig Kvien[2], George Vellidis[1,2]
[1]Biological and Agricultural Engineering Dept.
[2]National Environmentally Sound Production Agriculture Laboratory (NESPAL)
The University of Georgia - Tifton Campus

Background

VRI is an innovative technology that enables a center pivot irrigation (CP) system to match field variability with an appropriately variable irrigation application, differentially applying irrigation water to match the needs of individual management zones within a field. VRI technology can lead to substantial water conservation while optimizing application efficiency. Additionally, crop yield should increase because every field area receives the right amount of water. NESPAL and its commercial partner Farmscan have developed a VRI system that is now ready for commercial deployment. The system is currently installed on 6 CP systems (4 farmer-owned, 2 University-owned).

The NESPAL system, which retrofits on existing CP systems, integrates GPS positioning into a control system which cycles individual sprinklers or groups of sprinklers OFF and ON (seconds ON per minute) and varies travel speed to achieve desired rates within management zones. In doing so, the system also avoids off-target water applications onto roads, waterways and non-cropped areas, boggy spots, and overlapping pivot areas. The pivot covers the field at optimum speed, as variable speed control allows pivot to move quickly over boggy spots and waterways and will slow down over the sandy spots, rather than running them twice. Poorly drained spots are less boggy, aiding tillage and spraying operations.

Initial testing with these systems has shown the NESPAL VRI system to be robust and user-friendly. We have been contacted by numerous researchers, county agents, and producers from other regions that have various needs that a technology like VRI could help address.

Results

Application Maps

We developed and implemented irrigation application maps for the six installed VRI systems. Application maps for the 4 farmer-owned CP systems are shown in Figs. 1 - 4. For each of the six systems, the application map was unique as each field had site-specific variabilities to be addressed with VRI. For example, in Fig. 1, the Screven County pivot covers a field with a sandy area that does not hold much soil moisture as well as low, poorly-drained areas that become boggy during normal irrigation applications. The majority of the field (shown in dark green) requires “normal” amounts of irrigation.

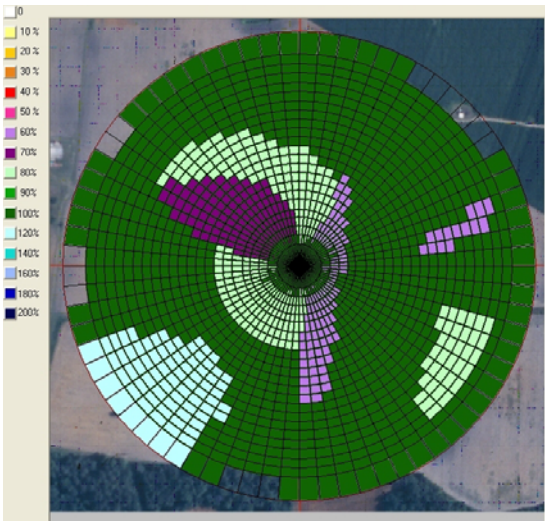

Figure 1. Application map for Screven County VRI pivot.

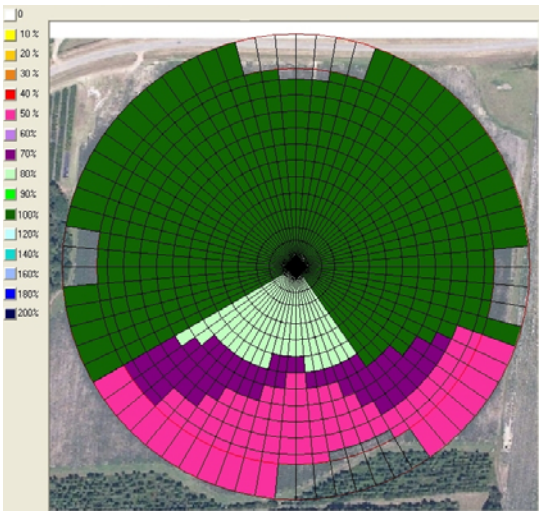

Figure 2. Application map for Colquitt County VRI pivot.

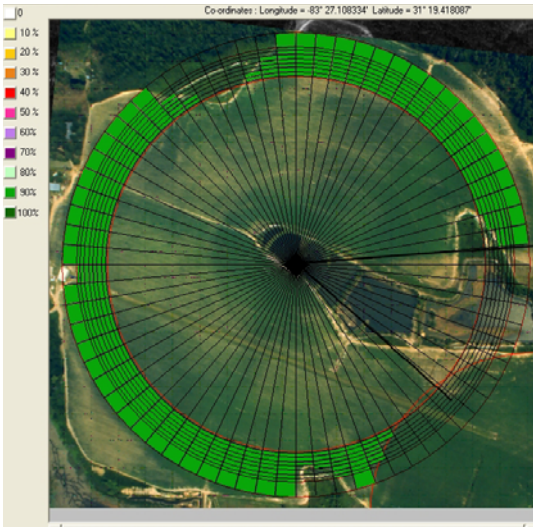

Figure 3. Application map for Cook County VRI pivot.

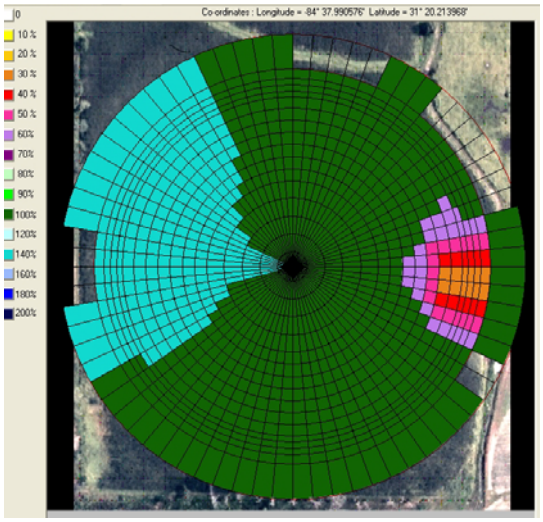

Figure 4. Application map for Baker County VRI pivot.

Water Savings

To determine the potential water savings from VRI for each system, calculations were made based on the application maps. For the following pivots, we calculated the percent water savings compared to “normal” application:

Baker Co. – 0%, Colquitt Co. - 36%, Cook Co. - 8%, Screven Co. – 7%.

To verify the water savings, flow tests were conducted on the Baker Co. and Colquitt Co. pivots. The two systems were operated with VRI engaged for one complete pass (circle) while actual water use was being monitored by a Polysonic DCT-7088 ultrasonic flow meter mounted on the mainline (Fig. 5). Results are shown in Table 1. The two pivots were operated at higher than normal travel speeds to reduce the time personnel had to remain on site during the testing. With VRI controls, the Colquitt Co. pivot used considerably less water in one pass. However, the Baker Co. pivot used slightly more water under VRI controls. This is common with many precision agriculture tools. Each field is a unique situation that has its own variability to be addressed.

Figure 5. Ultrasonic flow meter.

Yield Impacts

To evaluate the effect of variable-rate water application on crop yield, the Baker Co. field was divided into two halves (Fig. 6) with conventional application on the south half and variable application on the north half (ie. a split-map). We planned to have the grower irrigate using the split-map for the entire ’03 growing season and then harvest the peanuts and make a yield map to determine any effects of irrigation on yield. However, the field received more than average rainfall and the farmer only irrigated once.

We were able to harvest the field with a peanut combine equipped with a yield monitor. A yield map (Fig. 8) was created from the data collected during harvest.

Even though a split-map irrigation schedule was not followed (due to rainfall), the yield map does provide useful information. When compared to the 2002 corn yield map (Fig. 7) (which was representative of yield variation for several years prior), the ’03 yield map showed that, with ample soil moisture, areas with low yields (center left and upper left) can be brought up to yield levels comparable with the majority of the field that usually yields in the “high” category.

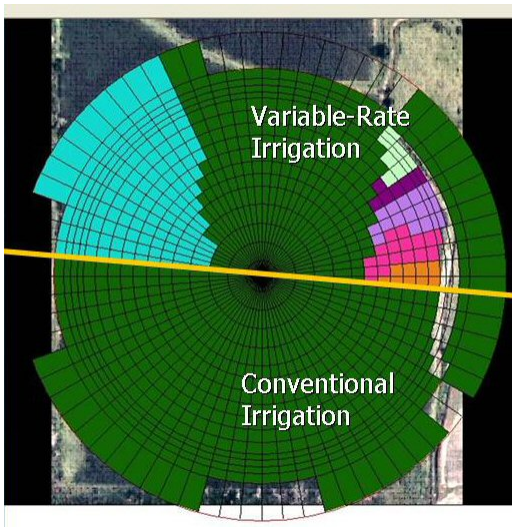

Figure 6. Split-map irrigation application map.

Table 1. Results of actual water use testing.

Pivot	Measured non-VRI water use (gallons)	Measured VRI water use (gallons)	Calculated VRI water use (gallons)	Percent Timer Setting	Time for one pass (hours)
Baker Co.	188,800	195,300	197,600	90%	4.4
Colquitt Co.	68,400	43,800	52,900	100%	4

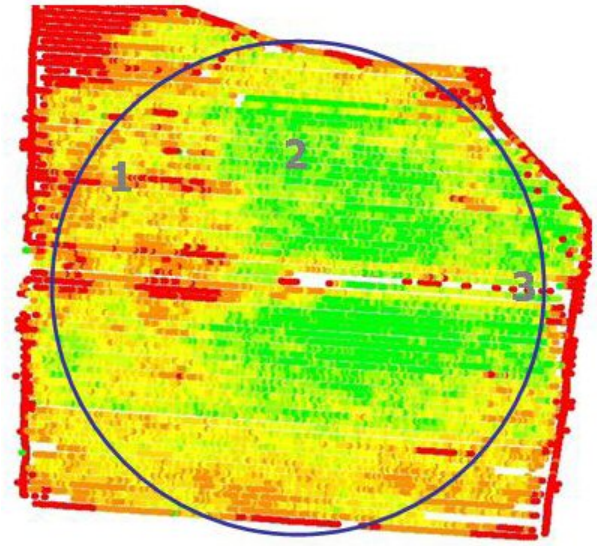

Figure 7. 2002 corn yield map. Circle indicates approx. pivot diameter. Red indicates low yield, yellow medium yield, green high yield.

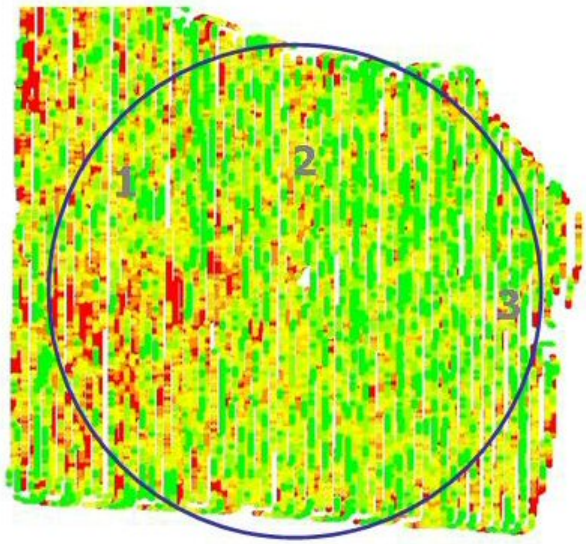

Figure 8. 2003 peanut yield map. Circle indicates approx. pivot diameter.

Web site

A web site was developed to give interested persons a better understanding of how variable-rate irrigation can benefit growers as well as rural communities. More information on this is available at http://www.nespal.org/irreff .

Publications/Presentations

Perry, C. and S. Pocknee. 2003. Precision Pivot Irrigation Controls To Optimize Water Application. In Understanding & Addressing Conservation and Recycled Water Irrigation, the Proceedings of the 2003 Irrigation Association Meeting, San Diego, CA. pp. 86-92.

Perry, C., S. Pocknee, and O. Hansen. 2003. A variable rate pivot irrigation control system. In J. Stafford and and A. Werner (eds), ECPA 2003, Proceedings of the Fourth European Conference on Precision Agriculture, pp. 539-544.

Perry, C., S. Pocknee, and K. Harrison. 2003. Optimizing Irrigation Water Application. The Precision Ag Guide, pp 10-11, July 2003. The Precision Ag Guide was an insert in the July issues of The Peanut Grower and Cotton Farming trade magazines.

Perry, C.D., S. Pocknee, O. Hansen, C. Kvien, G. Vellidis, and E. Hart. 2002. Development and testing of a variable-rate pivot irrigation control system. ASAE Paper No. 02-2290, ASAE, St. Joseph, MI.

Perry, C.D., and S. Pocknee. 2002.Variable-Rate Irrigation. The Peanut Grower Precision Ag. Guide, p.14, July 2002. The Peanut Grower is a peanut industry trade magazine.

Kvien, C., G. Vellidis, T. Wells, S. Pocknee, G. Rains, G. Hart, C. Perry, and D. Thomas. 2002. Precision management for improving crop quality in peanut and cotton. In Proceedings of the 6th International Conference on Prec. Agriculture, Minneapolis, MN. ASA-CSSA-SSSA. Pg. 567.

Perry, C.D., S. Pocknee, E. Hart, G. Vellidis, D. Thomas, N. Wells, and C. Kvien. 2002. Precision pivot irrigation. In Proceedings of the 6th International Conference on Prec. Agriculture, Minneapolis, MN. ASA-CSSA-SSSA. pp. 969-983.

"A Combined Hydrological , Geochemical and Isotopic Approach to Understanding the Effects of Basin Scale on Base Flow Systematics in the Georgia Piedmont"

Basic Information

Title:	"A Combined Hydrological , Geochemical and Isotopic Approach to Understanding the Effects of Basin Scale on Base Flow Systematics in the Georgia Piedmont"
Project Number:	2003GA40B
Start Date:	3/1/2003
End Date:	2/28/2004
Funding Source:	104B
Congressional District:	5th
Research Category:	None
Focus Category:	Surface Water, Water Quality, Water Quantity
Descriptors:	None
Principal Investigators:	Seth E. Rose

Publication

1. Rose, Seth, 2004. "A Combined Hydrological, Geochemical and Isotopic Approach to Understanding the Effects of Basin Scale on Base Flow Systematics in the Georgia Piedmont Province." Georgia Water Resources Institute, Georgia Tech, Atlanta, GA., 93p.

A Combined Hydrological, Geochemical and Isotopic Approach to Understanding the Effects of Basin Scale on Base Flow Systematics in the Georgia Piedmont Province

Principal Investigator:
Seth Rose[1]

Technical Completion Report
for the:

Georgia Water Resources Institute
FY 2003

Contract No. B-02-645/01HQGR0139

June, 2004

[1]Department of Geology
Georgia State University
P.O. Box 4105
Atlanta, GA 30302-4105

Phone: 404-463-9549
E-mail:geoser@panther.gsu.edu

TABLE OF CONTENTS

TABLE OF CONTENTS (Continued)

LIST OF TABLES

LIST OF FIGURES

ABSTRACT

The major ion geochemistry and isotopic (^{3}H concentrations, $\delta^{18}O$, and $^{87}Sr/^{86}Sr$ ratios) variability was investigated for the period between March, 2003 and March, 2004 in the Middle Oconee River basin near Arcade, Georgia. Tritium concentrations were higher in base flow and shallow ground water than in recent rainfall indicating that the ground water is stored within these Piedmont Province watersheds for several decades prior to its release as base flow. The lack of appreciable $\delta^{18}O$ variability indicates that there is not a significant component of seasonal rainfall within stream base flow and therefore the increased rate of base flow that occurs during the cooler winter and early spring months in Piedmont stream basins can not be directly related to seasonal influx. There was some geochemical variation within base flow in all four stream basins; however F-tests indicate that the greatest variability was associated with the 3.9 km^2 Indian Creek watershed which was the smallest of the basins analyzed and most subjected to contaminant input. The major ion geochemistry (e.g. alkalinity and magnesium ion concentrations) of base flow did not vary strictly as a function of basin scale or seasonal water fluctuations; however, mass balance models that assume the chemical composition of base flow is constant on a year-round basis are not correct.

The strontium isotopic data collected for this study likely represents the first of its kind for this region. Strontium isotope ratios were virtually temporally invariant at a given stream location and each stream basin was characterized by its unique range of $^{87}Sr/^{86}Sr$ ratios. The $^{87}Sr/^{86}Sr$ ratios increased with basin scale although strontium ion concentration varied over a similar range in all base flow. The unique $^{87}Sr/^{86}Sr$ ratio is likely the best parameter that can used

in future studies involving mixing processes in Piedmont Province watersheds, aquifers, lakes, and reservoirs.

PROJECT DESCRIPTION

Introduction and Overview:

One of the critical areas emerging in hydrological science that has been identified by the National Research Council (National Academy of Science, 1991) involves improvement in our understanding of how spatial and temporal scales are linked in converting rainfall to runoff (Hornberger and Boyer, 1995). Most studies of the hydrological, hydrochemical and isotopic dynamics of watersheds are done on a small scale (i.e. watershed area < 1.0 km^2) and emphasize the dynamics of storm flow. Integrating the dynamics of small watersheds to larger drainage networks is rarely undertaken and therefore it is not clear whether results gleaned from small upstream watersheds apply to the larger downstream basins that are often used for surface water resources by municipalities. In one of the few studies which considered spatial scales, Turner and Macphersen (1990) concluded that the processing of stable isotopes and major ions within a rural Western Australia catchment were very different on the 1 to 30 km^2 scale. It is implicit that understanding the spatial scale effects upon major ion and isotopic processing will also lead to a better understanding of the meaning of temporal variations within watersheds.

During most years base flow provides a perennial source of stream flow and is the dominant water resource for municipalities located within the Piedmont Province of Georgia (see information that follows in this report). A significant shortcoming of the present state of hydrological science is that base flow variation (both seasonal and spatial) has not been given sufficient attention in that most previous watershed studies have intensively focused upon storm

period dynamics. This limitation is unfortunate in that ground water sustains a year-round water resource in humid regions and provides a significant component to the storm hydrograph (see references in the literature review). Furthermore, in many hydrological settings such as the Piedmont Province, yearly base flow rates vary widely (e.g. by a factor ▣3-5) which strongly suggests that multiple mechanisms and/or source areas are involved in sustaining stream flow on a year-round basis. A better understanding of base flow generation and the associated variability with respect to flow rates can be derived using isotopic and geochemical tracers. The environmental isotopic investigation of base flow was initiated in the Georgia Piedmont by the Principal Investigator a decade ago (Rose, 1993 and Rose, 1996). However, much more work needs to be done in this area, particularly in terms of relating base flow geochemical and isotopic variation to basin scale.

This study investigated the isotopic and geochemical variation of base flow within a Piedmont basin (the Middle Oconee River, near Arcade, GA which is ▣35 km northeast of the Atlanta metropolitan region and 10 km north of Athens, GA) on spatial scales that range between ▣1.0 and ▣1,000 km^2. The spatial and temporal investigation of the isotopic variability of base flow (along with rainfall and ground water) has led to a better understanding of how variable source areas contribute to stream flow in the Piedmont setting and perhaps elsewhere.

Objectives:

Broader Hydrological Objectives: The primary objectives of this investigation were as follows:

1) To investigate the scale at which the major ion geochemistry and isotopic ($\delta^{18}O$, strontium isotope ratios, and environmental tritium) homogenization processes affect the

composition of base flow in an integrated drainage basin. This is an important question that has not been systematically addressed within the hydrological sciences to date.

2) To develop a better understanding of how the isotopic and geochemical characteristics and variability of base flow compare to that of ground water within a drainage basin. [Base flow in this report is defined as stream flow that appears on a hydrograph following storm recessions and before storm events which mostly consists of ground water discharge; after Pionke et al., 1988].

3) To investigate how the combined use of strontium and stable oxygen isotope ratios, environmental tritium, and major ion geochemistry might collectively be used to identify variable source areas, mixing processes, and residence times which control the hydrodynamic and hydrochemical dynamics of base flow in the southeastern Piedmont Province.

4) To develop a better understanding of how strontium isotope systematics can be used with the meteoric isotopes (stable oxygen ratios and tritium) in watershed science.

5) To broaden our understanding of how the isotopic study of watershed dynamics conducted on small drainage basins (i.e. ▣<1-10 km^2) relate to those of larger, more integrated basins on the scale of several hundred square kilometers.

The above-stated objectives are all interrelated in that base flow might be regarded as a mixture of ground water (and possibly vadose zone water) derived from various sources within a watershed. These sources include ground water from the near-stream zone as well as from more distal portions of the watershed. An understanding of these isotope systematics will in turn lead to a better understanding of how the variable source areas within a watershed contribute to stream flow between storm periods under a range of hydrological conditions.

Objectives Specific to the Study Area:

1) To better define the seasonal variability of environmental isotopes (i.e. tritium, stable oxygen isotopes, strontium-87/strontium-86) in rainfall, base flow and ground water and how this variation relates to sources of water in Piedmont Province watersheds. To my knowledge, strontium isotope ratios have not yet been used within this hydrological setting and it is therefore possible that the proposed research can break new ground in this area.

2) To integrate the results of this study with previous related studies in the Piedmont Province (e.g Rose, 1993; Rose, 1996; and Wenner et al., 1991) in order to better define regional isotopic trends and their possible hydrological significance.

3) To investigate the effects of scale upon base flow generation within Piedmont Province watersheds.

4) To determine whether the increased base flow rates that occur in the late winter and early spring in Piedmont watersheds are the result of the contribution of new, seasonally-derived water or some other mechanism.

5) To facilitate the rational development of a Piedmont Province watershed by providing an in-depth analysis while the study basin is in a relatively undeveloped state. The proposed Middle Oconee River study basin is juxtaposed in between three growth regions - Gainesville, GA; Athens, GA; and the eastern Atlanta metropolitan region - and will likely become a prime site for future residential development.

BACKGROUND AND LITERATURE REVIEW

The following section presents a summary of some of the major research directions that have occurred in watershed science during the past several decades. These topics are presented

in terms of how they are relevant to the research described herein and no attempt is made in the limited space available to exhaustively cover these topics on their own merits.

Hydrograph Separation:

The detailed utilization of environmental isotopic tracers for water sources within watersheds has primarily focused upon the stable isotopes of oxygen and hydrogen within storm runoff. These studies have most often been undertaken in watersheds with areas that are less than 10 km^2 (Table 10.1 in Genereux and Hooper, 1998). Such an approach has unquestionably advanced our knowledge of watershed dynamics by allowing the careful comparison of inputs (rainfall and snow melt) and outputs (stream flow). The primary focus of most watershed studies that have used isotope and geochemical systematics has been upon >hydrograph separation= which assesses the relative contribution of ground water, soil water, and direct surface water runoff to total storm runoff.

Two of the key assumptions that are inherent within the geochemical and isotopic hydrograph separation method are that the ground water or >pre-event= component is geochemically distinct form the >event= water and that both the >pre-event= and >event= components remain geochemically or isotopically constant during the course of the storm and after (Sklash and Farvolden, 1979). If the vadose zone contribution is isotopically or geochemically distinct from that of the ground water, the storm hydrograph can be separated into three components (Dewalle et al., 1988). The major conclusion drawn from these studies is that >old= or >pre-event= water comprises a significant (i.e. ▣20-60%) proportion of the total storm flow. However, chemical and isotopic methods of hydrograph separation are hampered by the

lack of knowledge regarding both the temporal and spatial isotopic and geochemical variability of those sources contributing to storm flow (Kendall, 2001).

End-Member Mixing Models:

An often-used method of analyzing possible source area contributions to stream flow involves end-member mixing analysis (Christopherson et al., 1990; Hooper et al., 1990; Katsuyama et al., 2001; and Burns et al., 2001). This involves graphical analysis in which two chemical and/or isotopic parameters are used to represent the designated end members (often these are throughfall, vadose zone ground water or interflow, and saturated zone ground water; Katsuyama et al., 2001). Such a method is very useful in demonstrating that mixing has occurred; however, the *a priori* designation of end members along with their chemical and isotopic composition can be problematic (e.g. different sets of end members have been used to model the stream water chemistry for the same small Panola Mountain catchment in the Georgia Piedmont; Hooper et al., 1990 and Burns et al., 2001). Furthermore, these models are based upon the assumed chemical and/or isotopic constancy of the components involved in the mixing process (Hooper et al., 1990). The assumption of constancy has been questioned by numerous investigators in that the chemical composition of all components including ground water can change during and after a storm (Anderson et al., 1997 and Kendall et al., 2001).

It is possible that base flow itself represents a seasonally changing mixture of different end members from various source areas which include but are not necessarily limited to the riparian saturated zone, the riparian vadose zone, and the hillslope saturated zone. The simple graphical procedures which have been developed to analyze the components of storm water can be used to analyze possible *components* of the base flow mixture. If the end-member compositions are not known with great confidence, such plots could still reveal whether water

samples fall within a mixing triangle which is indicative of three end-member mixing), on a mixing line (two end-member mixing) or cluster around a point, suggesting stream flow evolves from one more-or-less temporally invariant source.

Seasonal Variation of Stream Water Chemistry and Isotopic Composition:

The variation of solute chemistry and isotopic composition of stream water has been shown to vary on many drainage basin scales (e.g. Piñol et al, 1992; Taylor and Hamilton, 1993 and DeWalle et al., 1997). One of the major factors responsible for this variation include the contribution of variable proportions of ground water with its characteristically longer residence times. This usually results in increased solute concentrations (Ohrui and Mitchell, 1999) and less isotopic variability. Other factors include the seasonal variation of the isotopic composition of rainfall, changes in the water balance related to seasonal evapotranspiration rates, and the diminished contribution of chemically dilute vadose zone water during the dry season.

Rose (1995 and1996) found the $\delta^{18}O$ composition of both base flow and ground water within the southern Georgia Piedmont regolith to be variable and not equivalent to one another. Frederisckson and Criss (1999) derived similar findings in their study of a karstic watershed in eastern Missouri. Rose (1994) found that base flow alkalinity and base cation concentrations showed systematic temporal variation within the Falling Creek basin (southern Georgia Piedmont) as a result of the influx of additional water that occurs during the late autumn to early spring. However, Wenner et al. (1991) concluded that the $\delta^{18}O$ variations are substantially dampened at rather shallow depths and that $\delta^{18}O$ composition of base flow in a small Georgia Piedmont watershed is virtually time-invariant. Therefore, more comprehensive and exhaustive

studies are required to define the range of seasonal isotopic variation within shallow ground water and base flow and to discern its hydrological significance within the Piedmont setting.

Mechanisms for Base Flow Generation and Possible Causes of Spatial and Temporal Isotopic Variation in Stream Base Flow:

Ground-water discharge has long been cited as the dominant mechanism responsible for the generation of base flow, or that water which sustains stream flow between storm events (Freeze, 1974). The literature is not replete with discussion regarding the systematics of isotopic or geochemical variation within base flow; however, McDonnell et al. (1991) showed that stable hydrogen isotope ratios in the ground water contribution to stream flow varied in a spatially systematic manner along hillslopes within a small, steep New Zealand watershed. Gat (1974) showed that the stable isotopic ($\delta^{18}O$) composition of ground water in an Israeli coastal aquifer is greater than analytical error and that ground water within a mountain aquifer displayed a wide range of spatial and temporal isotopic variability.

In their mathematical analysis of base flow generation, Ophori and Tóth (1990) concluded that the contribution of base flow to total stream flow increases with basin area. Furthermore, their stream line analyses indicate that ground water which evolves from a specific recharge area can bypass local tributaries and eventually discharge into a higher order stream (Figure 6, Ophori and Tóth, 1990). Harris et al. (1995), on the basis of isotopic analysis, divided saturated zone contributions to stream flow into two distinct sources: a near-stream reservoir which mixes with direct precipitation and an upslope reservoir which does not mix with another water source. These analyses are consistent with the variable source area concept and imply that there are many flow paths to streams which differentially process the isotopic variation inherent within rainfall or recharge. Hewlett and Nutter (1970) developed the concept of the areally

expanding watershed for storm runoff and it is possible that those source areas which contribute to base flow also seasonally expand and contract. Very little attention has been paid to the spatial variability of pre-event water (i.e. that water which makes up base flow and ground water) over a suitably wide range of watershed scales (Genereux and Hooper, 1998) and therefore our knowledge of variable source area contributions to >pre-event water= or base flow is limited.

If we can assume that base flow is generated from variable source areas within a watershed that are at least partially characterized by transient conditions (Hewlett and Hibbert, 1963), it is likely that both the isotopic and geochemical composition vary co-systematically with these transient conditions. Furthermore, it is possible that the >inverse method= can be invoked and the seasonal and spatial variability of base flow along with the relative degree of isotopic homogenization can be utilized to identify possible source areas and the mechanisms that are responsible for its generation.

Residence Times:

Quantification of the mean residence times of ground water, soil water, and base flow can lead to a better understanding of the origins of stream flow and mixing processes that occur within watersheds. Most studies of this type (e.g. McGuire et al., 2002 and Stewart and McDonnell,1991) rely upon seasonal differences with respect to the $\delta^{18}O$ or δD inputs (precipitation) contrasted with the stable isotope output (stream flow) for the analysis of residence time. Similar studies have also utilized environmental tritium inputs and outputs (e.g. Maloszewski et al., 1992). Mathematical models typically involve the utilization of the >convolution integral= and rely upon *a priori* assumptions regarding the nature of ground-water flow through a basin (i.e. whether it is >piston=,>dispersive= or some other type of flow)

[Maloszewski and Zuber, 1992]. Frederickson and Criss (1999), using a >damped average= model of $\delta^{18}O$ values, showed that there is a large discrepancy between the modeled residence times between river water and spring water in the Meramec River Basin in eastern Missouri.

Rose (1993,1995, and 1996) has shown through a model based upon decay-corrected tritium input concentrations that the mean residence time of base flow and ground water in the Georgia Piedmont is ▣15-40 years. Burns et al. (2003) recently concluded on the basis of tritium-helium and chlorofluorocarbon dating that deeper ground water within the riparian zone of the Panola Mountain research watershed was 26-27 years old. Furthermore, Burns et al. (2003) concluded that stream flow becomes progressively older downstream. The relationship between the mean residence time of base flow, ground water and spatial scale within Piedmont watersheds has not been systematically addressed as of yet. One important question related to residence times that has not been answered is whether the additional base flow that occurs within Piedmont basins during the late winter and spring is comprised of >new=, seasonally-derived water.

Strontium Isotopes:

$^{87}Sr/^{86}Sr$ ratio analyses have been utilized only to a limited extent in catchment hydrology and to my knowledge there have not been previous studies that have incorporated strontium isotope systematics within Piedmont Province watersheds. Strontium isotope ratios or *signatures* are derived from mineral-water interactions, rather than from the atmosphere (Ninz, 1998). Hence, they serve as perfect complementary information to stable oxygen ratios ($\delta^{18}O$ and δD) and tritium which are atmospherically derived tracers. Strontium-87 is produced from the beta decay of rubidium-87; therefore, alkali-rich minerals such as mica commonly produce higher or

more *radiogenic* $^{87}Sr/^{86}Sr$ ratios than other non-radiogenic minerals such as calcite. Typically, $^{87}Sr/^{86}Sr$ ratios are used to identify ground water flow paths and mixing ratios in aquifers (e.g. Musgrove and Banner, 1993 and Lyons et al., 1995). Wadleigh et al. (1995) used strontium isotope ratios to assess the contribution of different watershed areas to stream flow and stream water chemistry. The mixing of water bodies from various sources can be discerned by plotting $^{87}Sr/^{86}Sr$ ratios versus strontium ion concentrations (Faure, 1986).

There are numerous other controls upon $^{87}Sr/^{86}Sr$ ratios in addition to source minerals that when properly interpreted can lead to a better understanding of the hydrodynamics of watersheds and aquifers. The $^{87}Sr/^{86}Sr$ ratio of rainwater compositions is usually much different than that of a solution derived from mineral weathering and therefore the isotopic composition might indicate the relative contribution of recent precipitation to natural water (Bailey, 1996; Hogan et al., 2000 and Douglas et al., 2002). There is often a strong correlation between the rates of discharge or water flux and strontium isotope composition. Aubert et al.(2002) found that strontium isotope ratios correlated positively with discharge rates in the Strengbach catchment of the Vosges mountains of France and attributed this relationship to a variable source area effect (i.e. the relative contribution from hillslopes).Variable discharge rates are often controlled by soil water-ground water and other mixing processes that also control the isotopic composition of strontium (Négrel and Lachassagne, 2000).

Biotite is the most radiogenic of the common aluminosilicate minerals in that rubidium is a common substitute for potassium (Bullen and Kendall, 1988) and other radiogenic sources include K-feldspar, garnet and hornblende (Bailey et al., 1996). Strontium isotopic rations within natural waters typically better reflect the ratio of individual minerals rather than whole rock ratios because of different weathering rates (Aubert et al., 2002). The degree of weathering is

one factor that controls strontium isotope ratios; however, other less cited but potentially important controls include discharge rates (Aubert et al., 2002) and the degree to which Sr^{+2} is absorbed upon clay soils (Katz and Bullen, 1996). The age of minerals is another control upon the $^{87}Sr/^{86}Sr$ ratio in that the isotopic composition of strontium within minerals has changed with time and the susceptibility to weathering of various minerals is also a function of time (Goldstein and Jacobsen, 1987 and Blum et al., 1994).

Nakano et al. (2001) reported that $^{87}Sr/^{86}Sr$ ratios within soil water in central Japan were highly variable (partially as the result of ion exchange) while the ratios in base flow were nearly constant. These studies suggest that $^{87}Sr/^{86}Sr$ ratios can potentially be used to trace water emanating from the vadose zone as opposed from deeper (more isotopically homogenized) ground-water flow paths. The co-systematic interpretation of strontium isotope ratios and Sr ion concentrations with major ion geochemical parameters, stable oxygen isotope ratios, and environmental tritium offers a potentially powerful means of identifying and quantifying contributions from variable source areas (e.g. near-stream zone versus longer and deeper ground water flow paths) to stream flow in the Piedmont Province and elsewhere.

STUDY AREA

Land Use and Geology:

The 860 km^2 Middle Oconee River basin study area (Figure 1) in northeastern Georgia was chosen for this study in that it is relatively undeveloped and can be readily accessed for monthly sampling from Atlanta. The basin which is predominantly within Jackson County, Georgia is comprised of ≈95% forest and pasture land (determined on the basis of the digital images in Alhadeff, 2001) and only a few small municipalities that include Pendergrass, Jefferson, and Braselton are located within its boundaries. However the basin is far from pristine

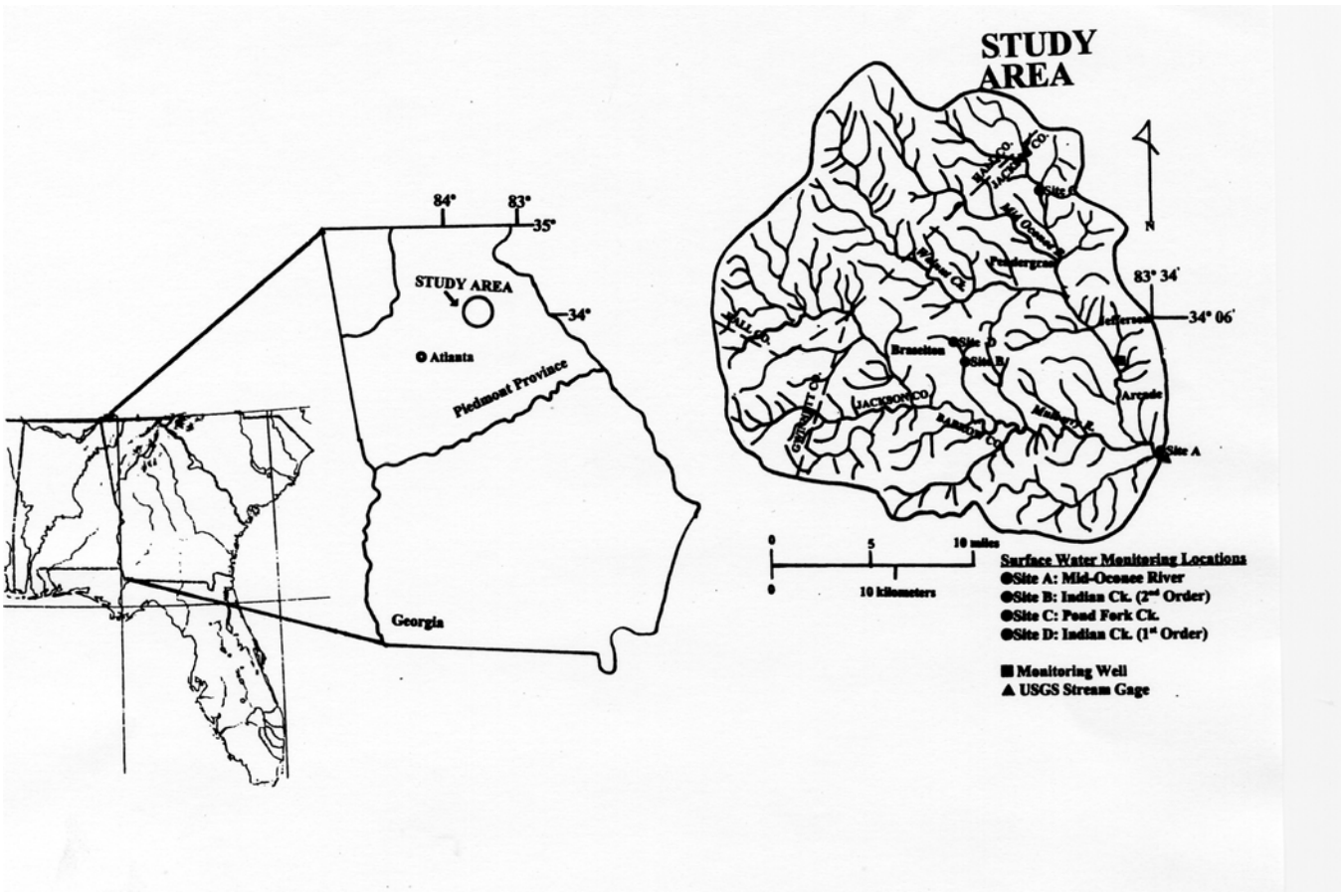

Figure 1. Map of the study area showing sampling locations

in that the Middle Oconee River currently receives effluent from a few relatively low-capacity sewage treatment plants and numerous septic tanks are present throughout the basin. Historically, the basin has been used for agricultural activities, leaving hundreds of acres of clear-cut land.

As is typical of the Georgia Piedmont, the Middle Oconee River study basin is underlain by Paleozoic metamorphic rocks that are dominantly biotite gneiss, mica schist and amphibolite schists (Figure 2). Thick columns of well-weathered, dark brown silty-clay soils (dominantly ultisols) overly the bedrock in most locations. The basin is well-incised with a complex network of streams that range from first to fifth order (Figure 1). The bedrock in this region is mantled by

0-50 meters of regolith with an average thickness of 20 meters (LeGrand, 1967). The regolith consists predominantly of ultisols (sandy clay soils with abundant iron oxyhydroxides), saprolites and alluvium near stream channels (Heath, 1964). Slopes within the Middle Oconee River basin are gradual (generally < 4%) which is typical of the Piedmont Province region as a whole. Stream flow within forested regions in the Georgia Piedmont has been approximated as a mixture of water stored from a shallow organic horizon, hill-slope ground water and deeper ground water within the soil mantle (Hooper et al., 1990). Deeper hillslope ground water stored near the bedrock surface - soil contact has been shown to be an important water source to streams in this setting (McDonnell et al., 1996).

Four stream locations (Indian Creek - first order tributary, Indian Creek - second order tributary, Pond Fork Creek, and the Middle Oconee River near Arcade, Georgia) were chosen as sampling sites in that they represent watershed areas between 3.9 - 860 km^2 (Figure 1 and Table 1). Of the four stream basins, Pond Fork Creek (watershed area = 54 km^2) in the northwestern portion of the study area is the least developed. The Middle Oconee River (watershed area = 860 m^2) which is the terminal basin of the study area is the only stream directly impacted by water treatment plant effluent. The small first-order Indian Creek watershed (watershed area = 3.9 km^2) is used as a horse pasture and is therefore the stream that is most significantly impacted by potential contamination from land use practices.

Table 1
Description of Sampling Sites

	Middle Oconee River near Arcade, Ga[1]	Pond Fork Creek	Indian Creek (1st order)	Indian Creek (2nd order)	Shallow Ground Water Monitoring Well[2,3]	Rainfall Collection Site
Latitude	34° 01'	34° 12'	34° 05'	34° 05'	34° 05'	33° 49'
Longitude	83° 34'	83° 40'	83° 44'	83° 44'	83° 35'	84° 16'
County	Jackson	Jackson	Jackson	Jackson	Jackson	Dekalb
Watershed Area (km^2)	860	54	3.9	12.7	-----	-----
Elevation (masl)[4]	210	235	270	255	240	-----
Bedrock Lithology	biotite gneiss mica schist amphibolite schist amphibolite	biotite gneiss mica schist amphibolite	Amphibolite Schist	Amphibolite Schist	biotite gneiss mica schist amphibolite	-----

[1]USGS gage site: 022174745;
[2]Well Depth = 17 meters, average water table depth = 8.4 meters below land surface;
[3]well completed in dark red brown sandy, silty, clay soils
[4]meters above mean sea level

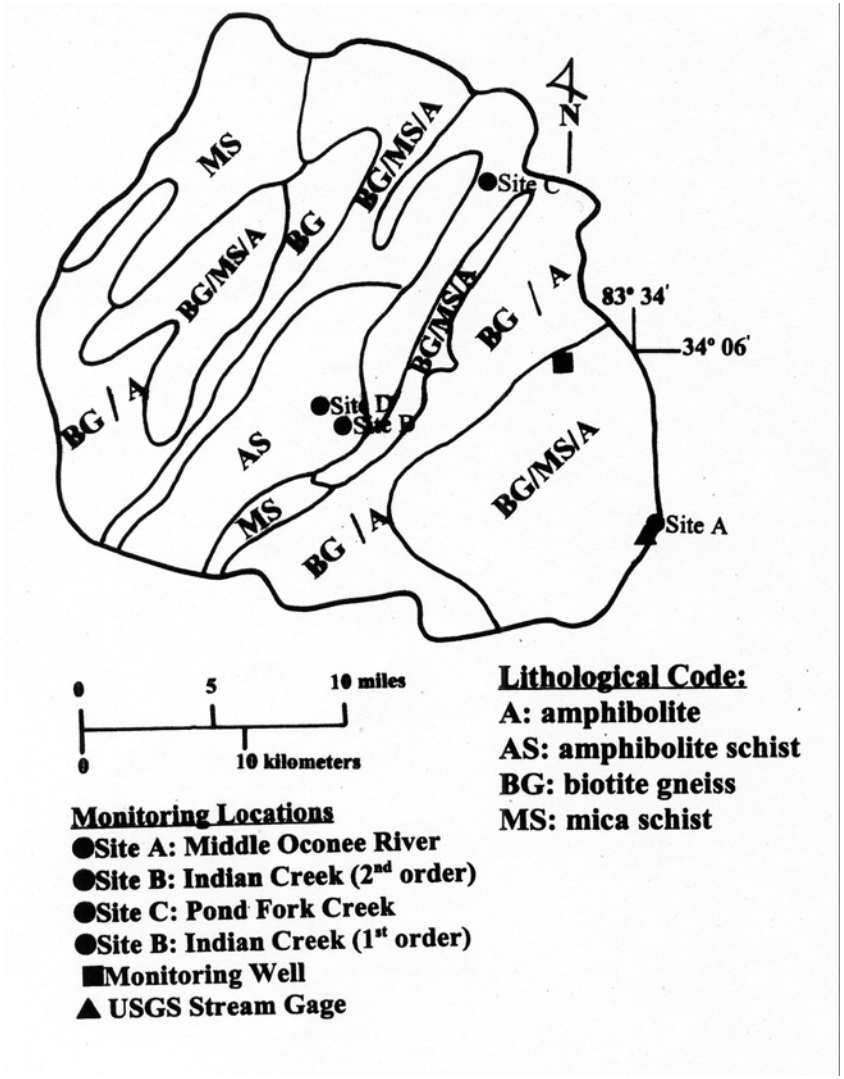

Figure 2. Geological map of the study area (after Alhadeff et al., 2001)

Hydrology:

The study area receives an average annual rainfall total of ▣1215 millimeters (mm) as determined from a U.S. Department of Agriculture gaging site located ▣15 km south of the basin (see Methods section). The average runoff for the Middle Oconee basin for the period of record between 1987 - 2002 was 438 mm or ▣36% of total precipitation. The average annual rate of base flow during this period as determined from hydrographic analysis is estimated to be 226 mm or ▣50% of total stream flow. This estimate of base flow interestingly is almost identical to the rate of *effective recharge* which was independently calculated for the Blue Ridge and Piedmont Provinces in Virginia (Nelms et al., 1997). Base flow rates within the study basin and in the region vary greatly and during wet years base flow provides ▣40% of the total stream flow and during dry years ▣70-80%.

Stream runoff and base flow in the study area are seasonal with the highest rates occurring during the Winter and Spring months when evapotranspiration rates are the lowest. The seasonal water balance for the Watkinsville, Georgia atmospheric monitoring site (▣10km southeast of the study basin) is shown on Figure 3 and it is clear that a potential water deficit (potential evaporation rates > precipitation rates) exists during the period between May through September (data from the Georgia Automated Environmental Monitoring Network, 2004). Average monthly low flow rates (an approximation of base flow) for the Middle Oconee River

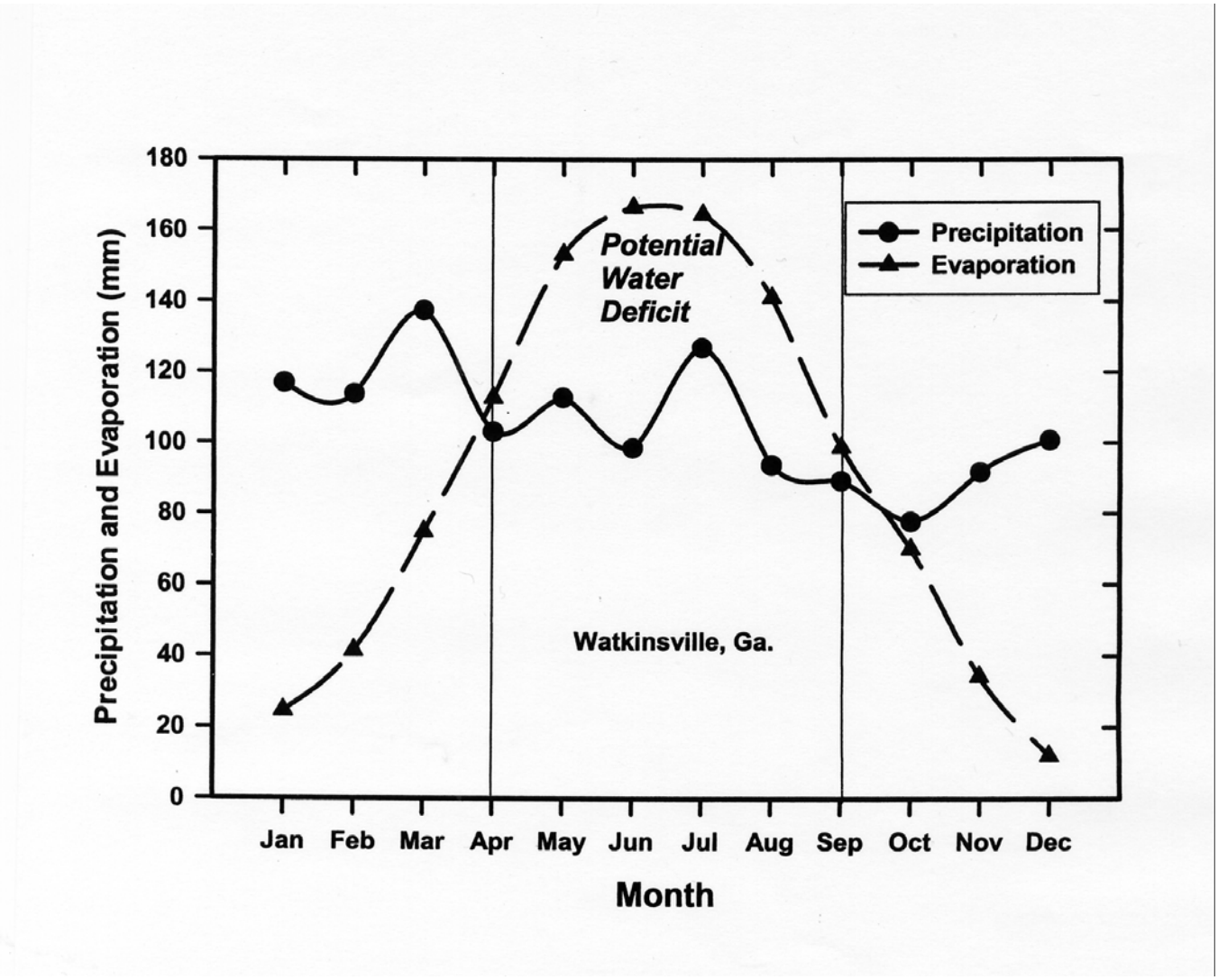

Figure 3. Monthly water budget for the study area

reach their minimum value of 10 mm during September and October and their maximum value of ▣28 mm in March. This approximate three-fold increase in the rate of base flow is very typical of the hydrodynamics of most streams in the Georgia Piedmont Province (Figure 4; data from U.S. Geological Survey, 2004a). The most important aspect of base flow is perhaps not the absolute magnitude; rather it is the estimated 75-90% of the year in which it provides the sole surface water resource. In short, base flow is the dominant water resource of the region (Rose, unpublished data).

METHODS

Data Collection, Field Methods and Sampling Methods:

Time-series samples of rainfall, shallow ground water, and stream base flow were typically collected on a monthly basis during the period between March, 2003 and March, 2004. In order to facilitate storm-by-storm collection and to minimize evaporation effects, rainfall was collected at the principal investigator=s residence in Decatur, Georgia ▣50 km east of Middle Oconee River watershed. Rainfall was collected in polyethylene sampling bottle attached to a funnel. Rainfall was gaged at the site in order to weight the precipitation samples by the amount of rainfall collected. The rainfall samples were thought to be collected sufficiently close to the study area as to be representative of conditions within the watershed. Daily precipitation values were obtained from the Georgia Automated Environmental Network (2004) for the U.S. Department of Agriculture weather station located ▣10 km south of the study basin at Watkinsville, Georgia.

Stream discharge values were obtained on a daily basis from a U.S. Geological Survey automated stream gage emplaced on the Middle Oconee River near Arcade, Georgia (U.S.

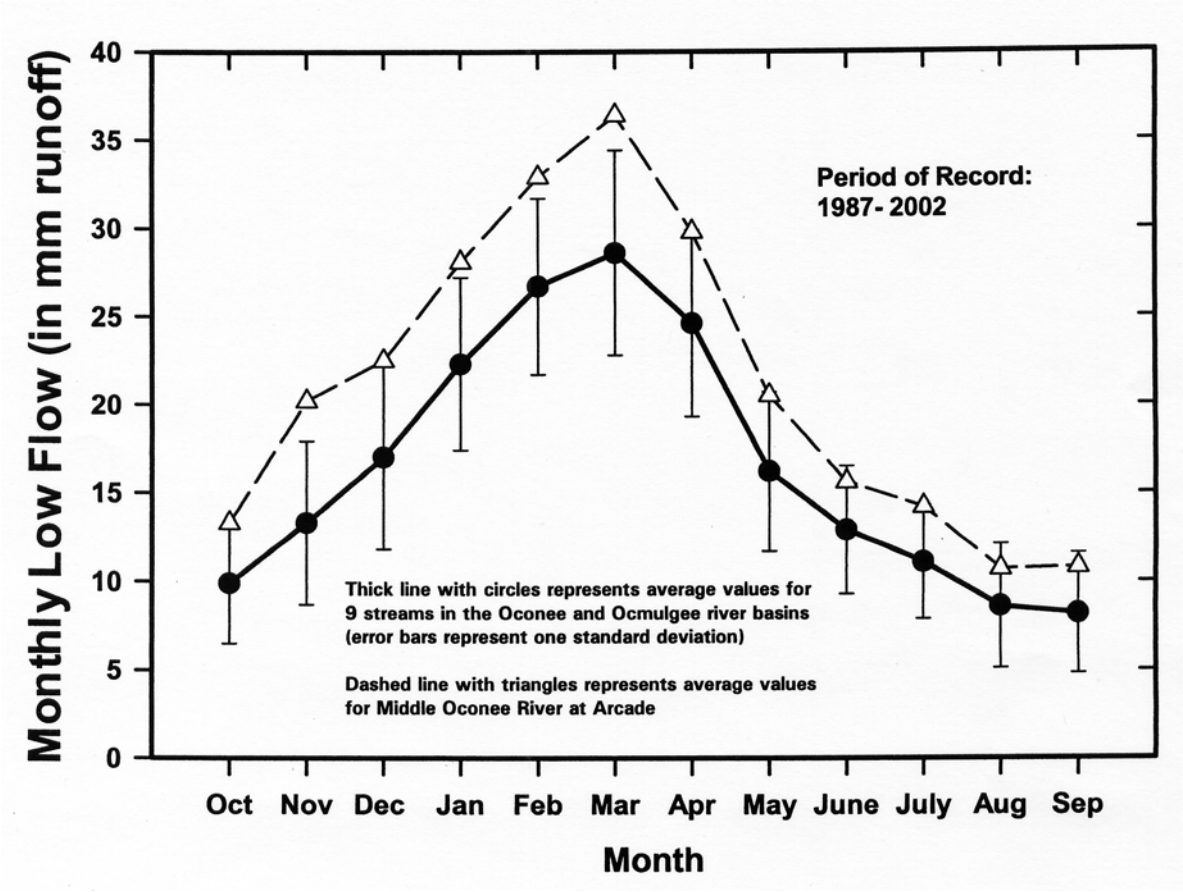

Figure 4. Monthly low flow runoff values for the study area (data compiled from U.S. Geological Survey, 2004a)

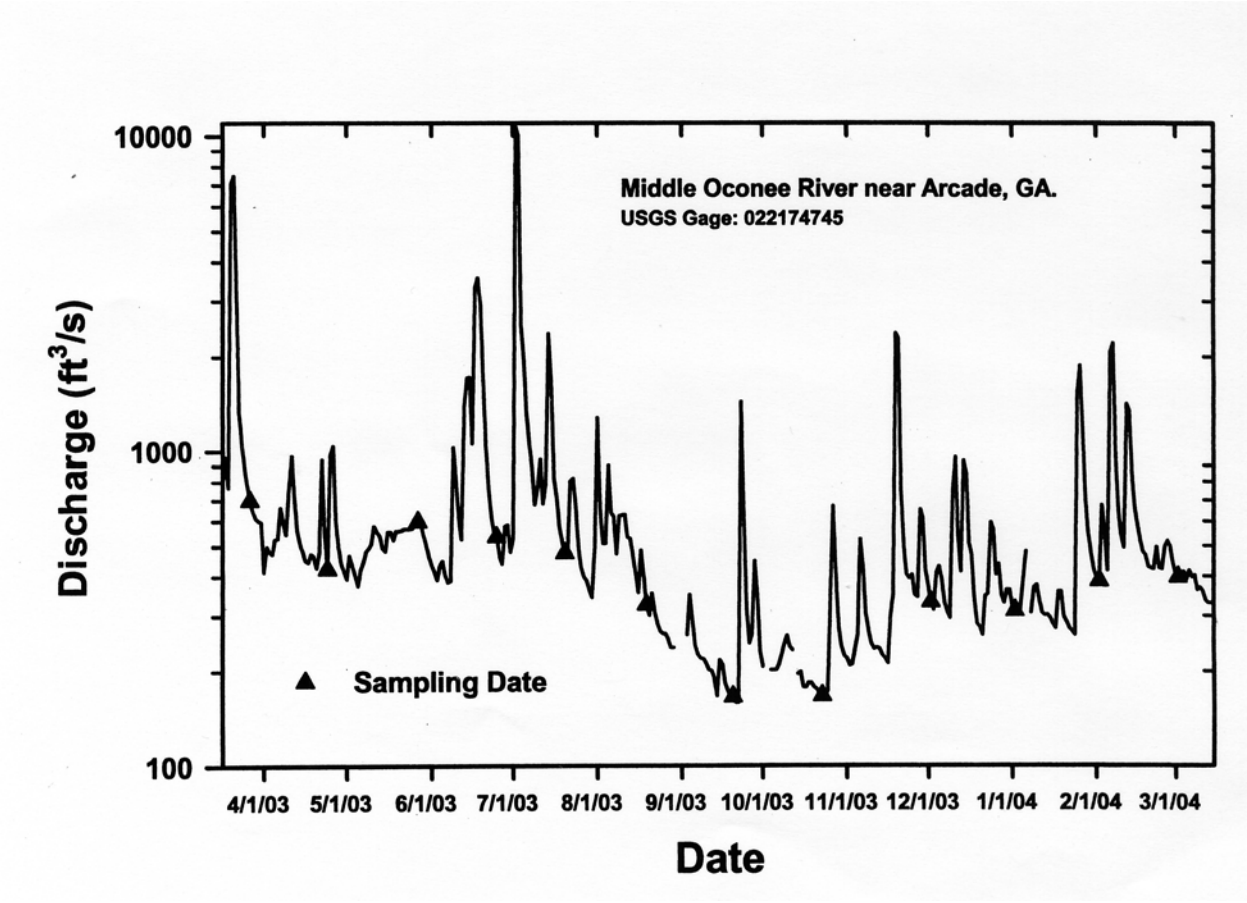

Figure 5. Hydrograph for Middle Oconee River near Arcade, Ga. during the study period showing sampling dates

Geological Survey, 2004b; Figure 5). Discharge values are transmitted from this site on a continuous basis through telemetry which facilitated sampling the Middle Oconee River and its tributaries under base flow or near-base flow conditions (i.e. periods between storm events when discharge was at a minimum; Figure 5). An assumption made for this study is that relative rates of discharge for the Middle Oconee River (the gaged stream) also apply to the three other ungaged stream locations that were monitored. This assumption is believed to be valid in that the streams are within ▣15 km of one another (Figure 1) and none of the discharge within this basin is regulated by dams. Stream water samples were collected using a weighted acid-washed, 18 MΩ DI-rinsed polyethylene collection vessel placed near the centroid of low. Both stream water and ground water samples were transferred to acid-washed, DI-rinsed, sample-rinsed polyethylene sampling bottles and refrigerated until the analyses could be made.

A 5-centimeter diameter PVC monitoring well was installed to a depth of 17 meters on a wooded site adjacent to the Middle Oconee River near Jefferson, Georgia (Figure 1). This was the one undeveloped location permitted for drilling by the Jackson County Water and Sewage Authority. The well was auger-drilled and a 5-meter long, 20-slot PVC well screen was installed at the bottom of the well. No extraneous fluids were introduced for its construction or development. The water table was located at a depth of approximately 8 meters below land surface and varied by < 1 meter during the duration of this study. Soil samples were taken from the auger bore at 1.5-meter intervals and were found to be uniformly comprised of dark brownish red sandy clay, characteristic of ultisols. The newly installed well was allowed to equilibrate with ground water for one month and during each sampling period one well volume was extracted with a polyethylene bailer immediately before the final sample was taken.

Major Ion Analytical Methods:

The specific conductance of the ground water and stream water was measured in the field using a YSI conductivity meter. The pH and alkalinity was measured on unfiltered samples using an Orion 720 pH meter (buffered at pH = 4.0 and 7.0) and 0.02N H_2SO_4 titrant. The precision associated with the titration was 6% as one relative standard deviation (rsd) [A relative standard deviation = 1 standard deviation/mean]. Non-acidified samples were used for anion analyses and were filtered first through 0.45μ acetate membrane and then through a 0.20μ membrane. Chloride and sulfate concentrations were determined using a Lachat 5000 ion chromatograph (bicarbonate/carbonate eluent; rapid anion method). The precision associated with these measurements was better than 5% (1 rsd). Cation concentrations (K, Na, Ca, Mg) were measured upon 0.45μ filtered, acidified (pH < 2.0) samples using a Perkin Elmer 3110 atomic absorption spectrophotometer. Magnesium ion concentrations were focused upon in this present study in that the precision associated with these measurements is better than 4% (1 rsd).

Tritium and Stable Oxygen Isotopes:

Tritium concentrations were measured at the University of Waterloo=s Environmental Isotope Laboratory by a beta particle counting method following electrolytic pre-concentration of tritium within the samples. Tritium concentrations are reported in tritium units (T.U.), where 1 T.U. = 1 tritium atom in 10^{18} hydrogen atoms in water. Replicate measurements of several water samples indicated a repeatability within 1.5 T.U. Stable oxygen isotopes were measured at the Geochron Laboraties using a CO_2 equilibration method. The precision associated with these measurements is ▣ 0.2 per mil. The results are reported as $\delta^{18}O$ per mil relative to SMOW (Standard Mean Ocean

Water) where:

$\delta^{18}O_{(SMOW)} = \{[^{18}O/^{16}O_{Sample} - {}^{18}O/^{16}O_{SMOW}] \times [^{18}O/^{16}O_{SMOW}]^{-1}\} \times 1000$

Strontium Ion Concentrations and Strontium Isotope Ratios:

Strontium ion concentrations and isotopic ratios were measured at the University of North Carolina-Chapel Hill mass spectrometry laboratory under the direction of Dr. Paul Fullagar. The determinations were performed on a Micromass Sector 54 thermal ionization mass spectrometer (TIMS). Typically this laboratory is able to measure strontium (Sr) ion concentrations with a precision and accuracy of better than 1% (Woods et al., 2000). $^{87}Sr/^{86}Sr$ ratios were adjusted using National Bureau of Standards #987 as to conform to a well-recognized standard. The percentage error associated with these measurements is <0.0010 and therefore the isotopic ratios are typically significant to the 5th decimal place (however in most cases they are reported only to the fourth decimal place).

RESULTS

Hydrology:

The study area received 57.8 inches (1467 mm) of precipitation between April 1, 2003 and March 31, 2004 (Appendix 1). This is 21% greater than normal for an annual period and most of the excess precipitation occurred during June and July, 2003 when precipitation was three to five times greater than normal. Average daily discharge for the Middle Oconee River near Arcade during the study period varied between 167 cubic feet per second (cfs) and 10,800 cfs (Appendix 2). The total discharge for the study period was 37% greater than normal with the excess primarily limited to the exceptionally wet period between June and July, 2003 (Figure 6).

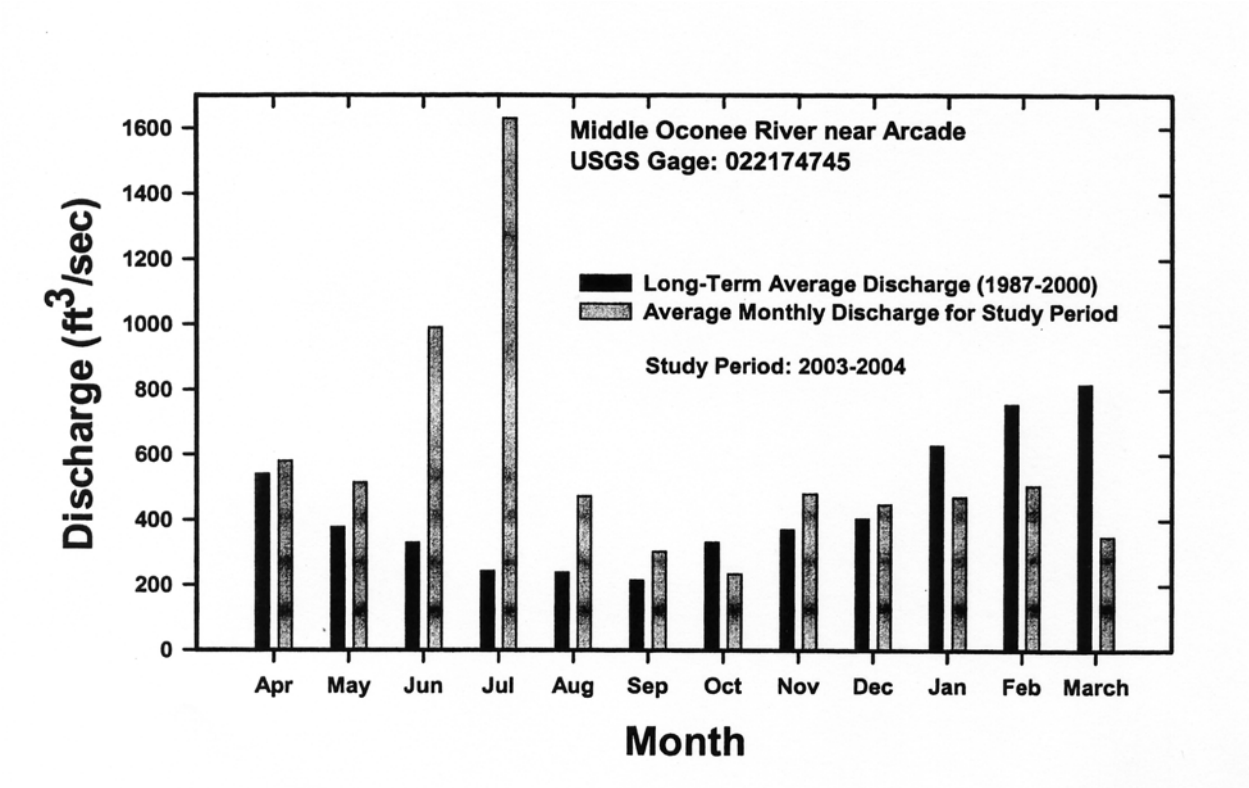

Figure 6. Monthly discharge data for the Middle Oconee River near Arcade, Georgia

During the later portion of the study period, between September, 2003 - March, 2004, discharge rates were near or below normal (Figure 6) and it was during this period that base flow dominated. Average base flow rates during the first four months of the study period (April-July, 2003) were ▣400 cfs and then declined by nearly a factor of two to 200 cfs during the period Monthly discharge data for the Middle Oconee River near Arcade, Georgia between August-December, 2003 (Figure 5). During the later part of the study period base flow rates rose to near their level at the beginning of the study period. As previously discussed, this decline in base flow rates during the hot summer months is a defining characteristic of stream flow in this region and is a result of potential evaporation exceeding precipitation. However, due to the excessive summer rain during this study period, the decline in base flow rates was slightly less than average for both the Middle Oconee River and the region as a whole (as defined by the nine Piedmont streams for the period 1987-2002; Figure 4).

Tritium(^{3}H) Concentrations:

Tritium concentrations varied between 7.3 and 16.6 T.U. and the average was 10.2 T.U. for base flow in the four stream basins (Table 2, Appendix 3). The average concentration in shallow ground water was 15.8 T.U. In contrast, the average weighted rainfall concentration for the study period was 7.2 T.U. and 5.1 T.U. for the period between 1999 - 2002 in the Panola Mountain research watershed located ▣45 km southeast of the study area (written communication, Robert L. Michel, 2003). Environmental tritium values within base flow and shallow ground water that are higher than precipitation values are consistent with the presence of some pre-bomb and bomb-period water (Rose, 1993 and Rose, 1996) as will be subsequently discussed. Tritium concentrations were also approximately 10 units lower within these stream

Table 2
Statistical Summary of Major Ion Chemistry and Isotopic Parameters

Middle Oconee River near Arcade, Georgia (USGS gage number: 022174745)								
	Specif. Cond.(µS/cm)	**pH**	**Alkalinity (mg/L)**	**Magnesium (mg/L)**	**Sulfate (mg/L)**	**Chloride (mg/L)**	**$\delta^{18}O$ SMOW**	**^{3}H (T.U.)**
Low	70.0	6.00	24.4	1.8	2.1	4.8	-6.0	7.3
High	92.3	7.08	33.3	2.0	8.7	11.0	-5.1	14.0
Average	81.9	6.70	27.7	1.9	5.4	7.7	-5.4	9.1
Standard Deviation	6.1	0.29	2.9	0.1	1.8	2.5	0.3	2.3
Rel. Std. Dev. (RSD)	7.4%	4.4%	10.5%	5.7%	32.8%	33.2%	5.7%	25.0%
Number	12	12	12	12	12	12	11	8
Pond Fork Creek								
	Specif. Cond.(µS/cm)	**pH**	**Alkalinity (mg/L)**	**Magnesium (mg/L)**	**Sulfate (mg/L)**	**Chloride (mg/L)**	**$\delta^{18}O$ SMOW**	**^{3}H (T.U.)**
Low	66.2	6.36	22.7	1.6	1.8	4.8	B5.7	9.0
High	76.9	7.06	30.5	1.9	3.8	10.1	-4.9	11.1
Average	74.3	6.82	26.5	1.8	2.1	7.3	-5.2	10.1
Standard Deviation	3.8	0.22	2.7	0.1	0.6	2.1	0.3	0.8
Rel. Std. Dev. (RSD)	5.1%	3.2%	10.2%	5.6%	29.9%	30.7%	5.0%	7.5%
Number	12	12	12	12	12	12	8	6

Table 2 (continued)
Statistical Summary of Major Ion and Isotopic Parameters

Indian Creek (1st order)								
	Specif. Cond.(μS/cm)	**pH**	**Alkalinity (mg/L)**	**Magnesium (mg/L)**	**Sulfate (mg/L)**	**Chloride (mg/L)**	**$\delta^{18}O$ SMOW**	**^{3}H (T.U.)**
Low	86.9	6.53	30.5	1.4	1.1	5.1	-5.4	7.6
High	112.2	7.06	47.2	1.8	3.7	14.4	-4.8	16.6
Average	92.6	6.56	35.9	1.6	2.1	10.5	-5.1	15.8
Standard Deviation	9.9	0.25	4.7	0.2	0.7	3.4	0.2	3.2
Rel. Std. Dev. (RSD)	10.6%	3.8%	13.2%	10.7%	34.6%	32.3%	4.8%	19.9%
Number	11	11	11	10	11	11	9	6
Indian Creek (2nd order)								
	Specif. Cond.(μS/cm)	**pH**	**Alkalinity (mg/L)**	**Magnesium (mg/L)**	**Sulfate (mg/L)**	**Chloride (mg/L)**	**$\delta^{18}O$ SMOW**	**^{3}H (T.U.)**
Low	59.5	6.38	26.0	1.8	1.2	5.5	-5.4	10.5
High	84.8	7.01	36.6	2.0	2.6	11.6	-4.4	11.1
Average	78.4	6.74	30.6	1.9	2.1	7.9	-5.0	10.8
Standard Deviation	7.1	0.22	3.5	0.1	0.5	2.4	0.4	0.4
Rel. Std. Dev. (RSD)	9.1%	3.2%	11.3%	4.2%	23.0%	31.0%	7.1%	3.7%
Number	11	11	11	11	11	11	8	2

Table 2 (continued)
Statistical Summary of Major Ion and Isotopic Parameters

Shallow Ground Water								
	Specif. Cond.(μS/cm)	**pH**	**Alkalinity (mg/L)**	**Magnesium (mg/L)**	**Sulfate (mg/L)**	**Chloride (mg/L)**	**$\delta^{18}O$ SMOW**	**^{3}H (T.U.)**
Low	15.2	4.89	2.7	0.4	0.2	<0.2	-6.1	12.2
High	32.2	5.29	6.1	0.5	0.9	4.3	-5.4	20.5
Average	21.0	5.17	4.0	0.5	0.6	2.9	-5.6	15.8
Standard Deviation	5.5	0.13	1.4	0.04	0.2	1.5	0.3	3.2
Rel. Std. Dev. (RSD)	25.9%	2.5%	34.6%	7.8%	38.5%	50.5%	5.0%	19.9%
Number	7	7	7	7	7	7	5	5

waters than they were a decade ago in the nearby Upper Ocmulgee River basin (Rose, 1993), consistent with radioactive decay rates.

The average tritium concentrations in base flow for the four watersheds varied only between 9.1 T.U. (Middle Oconee River) and 11.5 T.U. (first-order tributary of Indian Creek) during this study period. Two-tailed t-tests ($\alpha = 0.05$) indicate that there is no statistically significant difference between the average tritium concentration between Pole Branch Creek, Indian Creek (first-order tributary), and the Middle Oconee River near Arcade. There is no apparent relationship between tritium concentrations in base flow and watershed area. This suggests that all four watersheds process rainfall in a similar manner and that the average residence times of ground water comprising base flow in the four watersheds are also similar. The greatest temporal variability was observed for the Middle Oconee River as defined by the relative standard deviation (rsd) of 25.0% and the Indian Creek first-order tributary (rsd = 25.5%). However, this variation was apparently random and was not associated with consistent seasonal trends (Figure 7); therefore the causes of these variations are not readily identifiable. This stands in contrast to an earlier study by Rose (1993) in which tritium concentrations in stream water from the Upper Ocmulgee basin (≈50 km from the Middle Oconee River basin) were seasonal and decreased during the wetter portion of the year. During the early 1990's tritium concentrations in stream base flow were also significantly higher (18-30 T.U.) which may explain why the seasonal trend was no longer apparent.

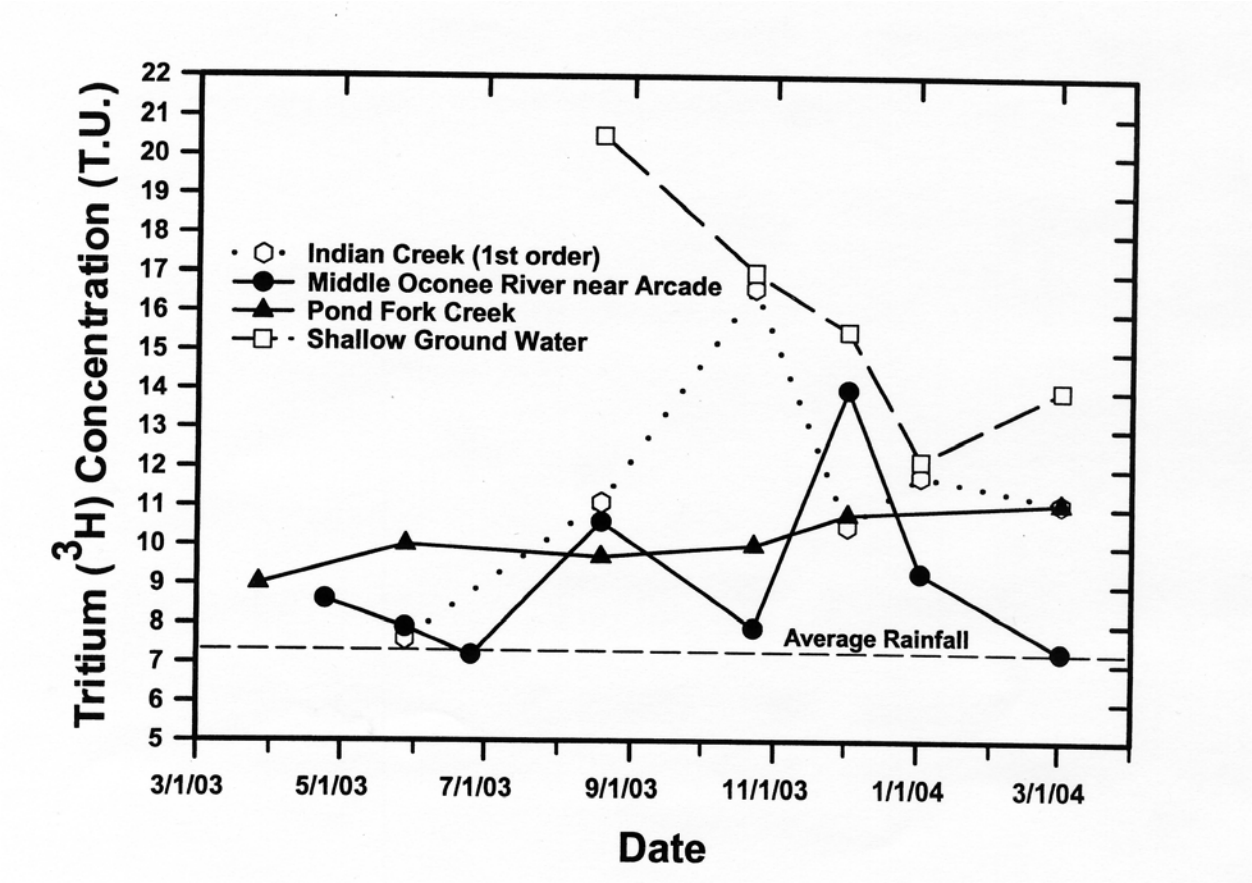

Figure 7. Environmental tritium concentrations within base flow and shallow ground water in the Middle Oconee River basin

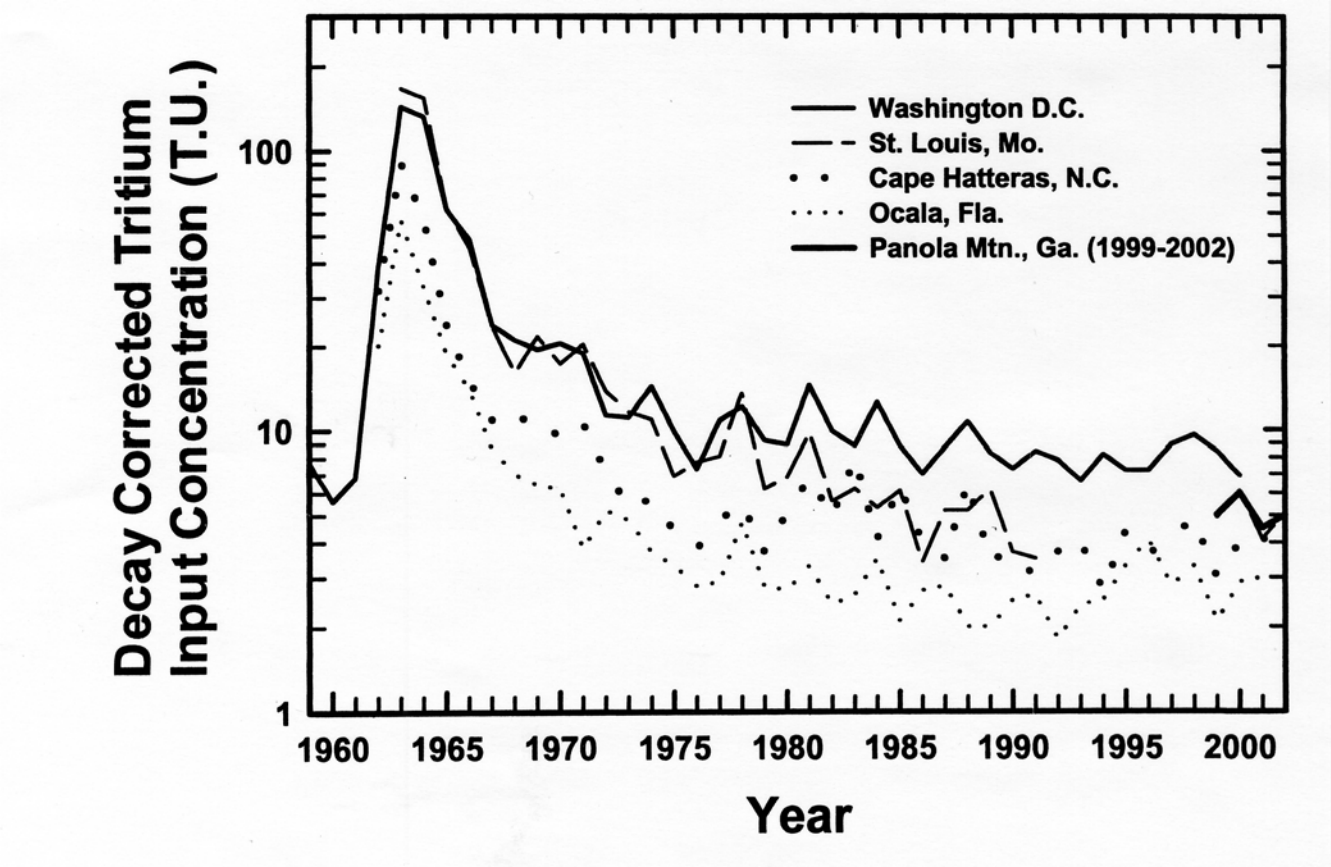

Figure 8. Decay-corrected tritium input concentrations within rainfall for the southeastern United States

Table 3
Decay Corrected Tritium Concentrations in Southeastern U.S. Rainfall
(Values are in Tritium Units [T.U.]

	Rainfall Collection Location				
Period	**Washington D.C.[1]**	**St. Louis Mo.[1]**	**Cape Hatteras[1]**	**Ocala, Fla.[1]**	**Northeastern Ga[1,2]**
2002-1993	7.9	5.0	3.9	2.8	6.1
2002-1983	8.8	5.5	4.3	2.7	No data
2002-1973	9.6	6.0	4.6	3.3	No data
2002-1963	20.0	21.0	10.1	6.6	No data

[1]International Energy Association data - compiled by Robert L. Michel, U.S. Geological Survey (written communication)

[2]Data obtained by Rose (1996)

There was a statistically significant difference (t-tests; α=0.5) between tritium values in shallow ground water (average tritium concentration = 15.8.3.2 T.U.) and the stream base flow (average tritium concentration = 10.2.2.2 T.U.). This (along with other parameters to be discussed later) indicates that the base flow cannot be equated with the shallow ground water that was monitored as part of this investigation. Decay corrected tritium input concentrations in southeastern rainfall have generally been between 5-10 T.U. for the past 10 years (Figure 8 and Table 3). In order to account for the higher values observed in shallow ground water (average tritium concentration= 15.8 T.U.) there would likely have to be a component of bomb-test water (i.e. decay-corrected rainfall from the middle 1960's) in the shallow ground water mixture.

Base flow tritium concentrations (average = 10.2 T.U.) are lower than the shallow ground and more closely resembled modern rainfall values (between 5.1 - 7.2 T.U. as measured in this study). The higher values in the ground water initially suggest that it might have a longer average residence time than base flow within the four streams in that tritium concentrations in rainfall have declined during the past 40 years from their peak bomb test values of the mid-1960's (Figure 8). This interpretation, while possibly consistent with the tritium data itself, is probably not correct in that the shallow ground water is characterized by a relatively low pH and specific conductance (see subsequent discussion of stream chemistry). In fact the low ionic loads present in shallow ground water much more closely resemble rain water than they do base flow. Therefore, it would be very problematic to imply that the shallow ground water has a lower percentage of more recent rainfall or that it has a greater residence time than the ground water that comprises base flow in the Middle Oconee River basin.

One possible explanation for these results is that the base flow consists of a mixture of post-bomb (i.e. water from the past 30 years), bomb-test, and some pre-bomb (i.e. > 40 year old)

recharge. The older pre-bomb input would have decay-corrected tritium values that are nearly zero and therefore the higher percentage of pre-bomb waters, the lower the total ^{3}H concentration of the base flow mixture. It should be emphasized that this argument is somewhat speculative and other explanations may be possible. However, it is very clear that both shallow ground and base flow are more tritiated than southeastern U.S. rainfall has been during the past two to three decades. This suggests a decade-scale residence times for both the shallow ground water and the base flow, consistent with previous interpretations of the residence time of natural waters in the Georgia Piedmont Province (Burns et al., 2003, Rose, 1996, and Rose, 1993).

Stable Oxygen Isotope Ratios ($\delta^{18}O$ relative to SMOW):

The stable oxygen isotope ratios measured in precipitation samples collected in Decatur, Georgia during the study period averaged -5.4 per mil (as a weighted value) and varied between -8.1 and -1.8 per mil (Appendix 4; Table 2). The high degree of variability between rainfall samples can be inferred from rsd value of 31.8% for the 13 samples (Appendix 4). In contrast, the $\delta^{18}O$ composition of stream base flow varied between -6.1 and -4.8 per mil during the study period (Table 2). The four-stream average base flow composition (-5.2 per mil) was similar to but slightly heavier than the average ground water value ($\delta^{18}O$ = -5.6 per mil). Both the ground water and stream base flow average values were within the analytical error of weighted rainfall (-5.4 per mil). There was no apparent relationship between $\delta^{18}O$ values (and their relative standard deviations) and stream order or watershed size. This indicates (as does the previously discussed tritium data) that rain water is processed in a similar manner in all four watersheds irrespective of their basin area. The isotopic variation observed in the four streams during the year-long study period (Figure 9) is slightly greater than the analytical error associated with these measurements

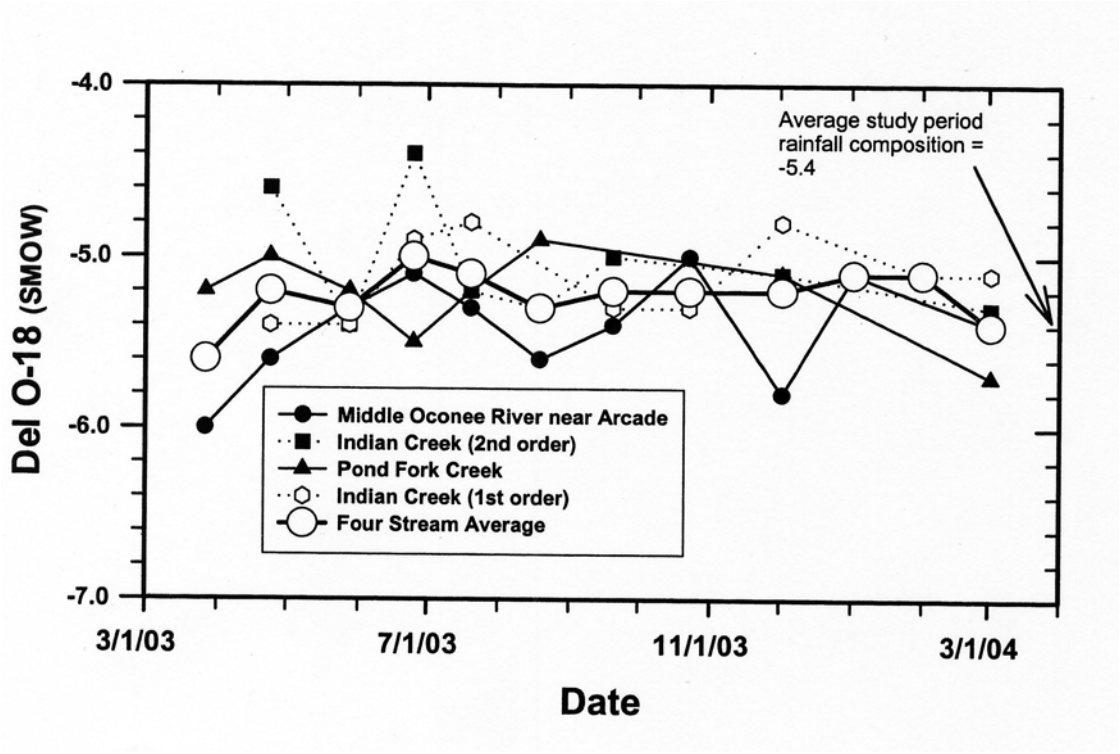

Figure 9. $\delta^{18}O$ values in base flow within the Middle Oconee River basin

(. 0.2 per mil) indicating that base flow is not, however, a completely temporally invariant, homogenous mixture. Unfortunately the hydrological significance of this isotopic variation is not precisely clear.

If rainfall is collected on a regular basis over a multi-year period, lighter isotopic ratios would be observed in winter precipitation than during the remainder of the year (Gat, 1980). Using the relationship between stable oxygen isotope compositions and monthly mean air temperatures compiled by Yurtsever (1975), winter rainfall in the southeastern U.S. is ▣5 per mil lighter than summer rainfall. Lighter isotopic ratios were not observed in stream base flow during the winter months which indicates that there was not a significant contribution of seasonal rainfall within base flow. The relative standard deviations associated with stable oxygen isotopic composition of base flow varied only between 4.8 and 7.1% for the four watersheds, very similar to the relative standard deviation of 5.0% associated with the shallow ground water. The similarity between the ground water rsd values and the base flow values suggests that seasonal isotopic variation becomes homogenized at shallow depths (i.e. < 15 meters) within the soils. The relative standard deviations for base flow and shallow ground water are very modest compared to the rsd values associated with rainfall (31.8%) and are consistent with the Aisotopic homogenization@ reported by Wenner et al. (1991) in a similar watershed in the Georgia Piedmont. The lack of seasonal variation and isotopic homogeneity is also consistent with the multi-decade residence time of ground water (both shallow ground and ground water comprising base flow) inferred from the tritium data.

Major Ion Geochemistry:

Major ion concentrations in base flow in all four basins were characteristically low as indicated by specific conductance values that ranged between 59.5 - 112.6 μS/cm and averaged 81.8 μS/cm (Table 2). These relatively low values are typical of the Georgia Piedmont which is underlain by rock comprised of relatively insoluble aluminosilicate minerals. The specific conductance of shallow ground water was considerably lower than the stream base flow and ranged between 15.2 - 32.2 μS/cm. This clearly indicates that the shallow ground water (i.e. < 17 meters) is not representative of base flow in this study area. The first-order Indian Creek stream was characterized by the highest solute loads with an average specific conductance of 92.6 μS/cm (Table 2). The relatively high solute concentrations are consistent with the land use (horse pastures) that is characteristic of most of this 3.9 km^2 basin. The relative standard deviations for specific conductance in the four streams varied between 5.1 - 10.6% and were highest for the first-order Indian Creek watershed (Table 2).

The pH of base flow remained near neutral on a year-round basis varying between 6.00 and 7.08 and averaged 6.71 within the four basins (Table 2). The shallow ground water was more acidic and ranged between 4.89 -5.29 during the study period. Magnesium concentrations, an indicator of biotite and hornblende dissolution, varied between 1.4 - 2.0 mg/L and averaged 2.0 mg/L within base flow from the four streams. Magnesium ion variation was not seasonal and relative standard deviations varied between 4.2 - 10.7% in stream base flow (Table 2), values that exceed the analytical imprecision.

Bicarbonate (as determined by alkalinity titration) is the dominant ion in these waters and concentrations ranged between 22.7 and 44.2 mg/L and averaged 30.2 mg/L. In contrast, the average magnesium ion and bicarbonate alkalinity concentrations in shallow ground water were 0.5 and 4.0 mg/L (Table 2). The relative standard deviation for bicarbonate alkalinity in base flow varied between 10.2-13.0%, also reflecting a degree of variability greater than analytical uncertainty. Alkalinity variation was somewhat seasonal and during the period between August and November, 2003 when discharge values were lowest (Figures 5 and 6), average alkalinity concentrations in base flow for the four streams increased by ≈25% (Figure 10). This seasonal variation is likely real; however, it is difficult to infer from the yearly pattern of any single stream.

Surprisingly, this seasonal variation is not co-systematic with specific conductance values in that the four-stream average specific conductance decreased during the same August-November period (Figure 11) when alkalinity concentrations increased. It is also apparent that specific conductance values for base flow did not vary as a function base flow discharge as can be inferred from the plots and related regression coefficients shown on Figure 12. Sulfate and chloride concentrations respectively ranged between 1.1 - 8.8 and 4.8 - 14.4 mg/L within stream base flow (Table 2). The upper values for these parameters likely represent some measure of contaminative input from horse pastures, fertilizer, sewage effluent and/or septic tank leakage. Seasonal relationships or relationships between chloride and sulfate concentrations and basin area are hard to infer from these data.

F-Tests for Significance of Difference with Respect to Variance:

As previously detailed (Table 2 and Appendix 5) there is at least a moderate range of temporal variation for most of the chemical and isotopic parameters for a given watershed. This is reflected in relative standard deviations that are often greater than 10%. These variations may reflect some combination of random analytical error, seasonal factors effecting water flux within a watershed and variable contaminant inputs that have occurred upstream of a given sampling location.

In order to better understand the temporal variations within these data sets, one-tailed F-tests ($\alpha = 0.05$) were utilized to determine whether there were significant differences with respect to the variance (or standard deviation) for a given parameter between watersheds. The set of parameters included magnesium, chloride, specific conductance, bicarbonate alkalinity, $\delta^{18}O$, and tritium concentrations. The results of these tests are summarized in Table 4 and they indicate that there are only a few parameters in which the variances between watersheds for a given parameter are significantly different. Most of these differences relate to the first-order tributary of Indian Creek (watershed area = 3.9 km^2) in which the variance for magnesium, alkalinity, specific conductance and a few other parameters were significantly larger than the larger watersheds. It might be expected that the smallest or least Abuffered@ of the watersheds would be more subject to temporal variation and therefore have the highest associated variances. The temporal variation might result from differential water flux through the basin and contamination inputs from the land surface. There was very little difference with respect to variance between the three larger watersheds which may indicate that similar Abuffering@ and/or mixing processes occur on a watershed scale that is greater than ▣10 km^2. This observation while relevant to the

Middle Oconee River drainage basin should not be construed as a hard-and-fast rule for all Piedmont Province watersheds.

Strontium Ion Concentrations and Isotope Ratios:

Strontium ion concentrations ranged between16.3 - 26.9 μg/L (Table 5) in base flow from the four Middle Oconee River basin streams. These values are relatively low compared to the global river average of 78 μg/L (Palmer and Edmond, 1992) and can likely be attributed to the limited input of strontium from carbonate minerals within these aluminosilicate watersheds. The base flow concentrations strontium concentrations were, however, much greater than those in rainfall (1.4 - 4.0 μg/L) and shallow ground water (5.2 - 7.1 μg/L; Table 5) indicating a strong weathering component of strontium in the stream water. There was little temporal strontium variation within base flow for a given stream as evidenced by relative standard deviations that varied between 4.1% and 12.3% and the strontium concentrations were very similar in each of the streams (Table 5). The only statistically significant differences (two tailed t-tests, $\alpha = 0.05$) between mean strontium ion concentrations were between Pond Fork Creek and the two Indian Creek tributaries and this difference was only ▣3 μg/L. This indicates that the reactions controlling the strontium ion influx were quite similar throughout the 860 km^2 study basin.

$^{87}Sr/^{86}Sr$ ratios varied between 0.7113 - 0.7176 and averaged 0.7145 within base flow in the four stream basins (Table 5). This average is more radiogenic than the global average for river water which is 0.7119 (Palmer and Edmond, 1992). The average ratio is very close to the whole-rock ratio of 0.7140 observed for the granodiorite rocks at the nearby Panola Mountain research watershed (White et al., 2001).

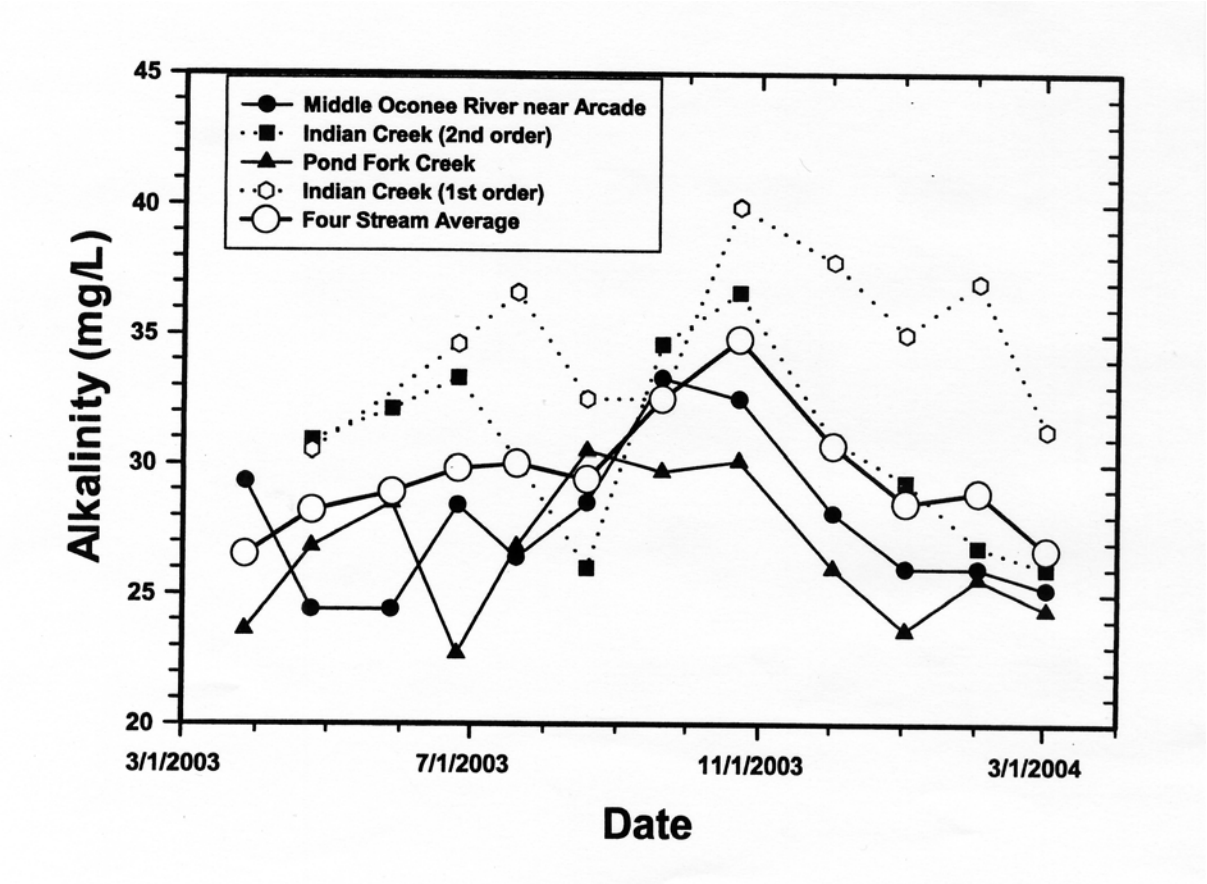

Figure 10. Alkalinity concentrations in base flow within the Middle Oconee River basin

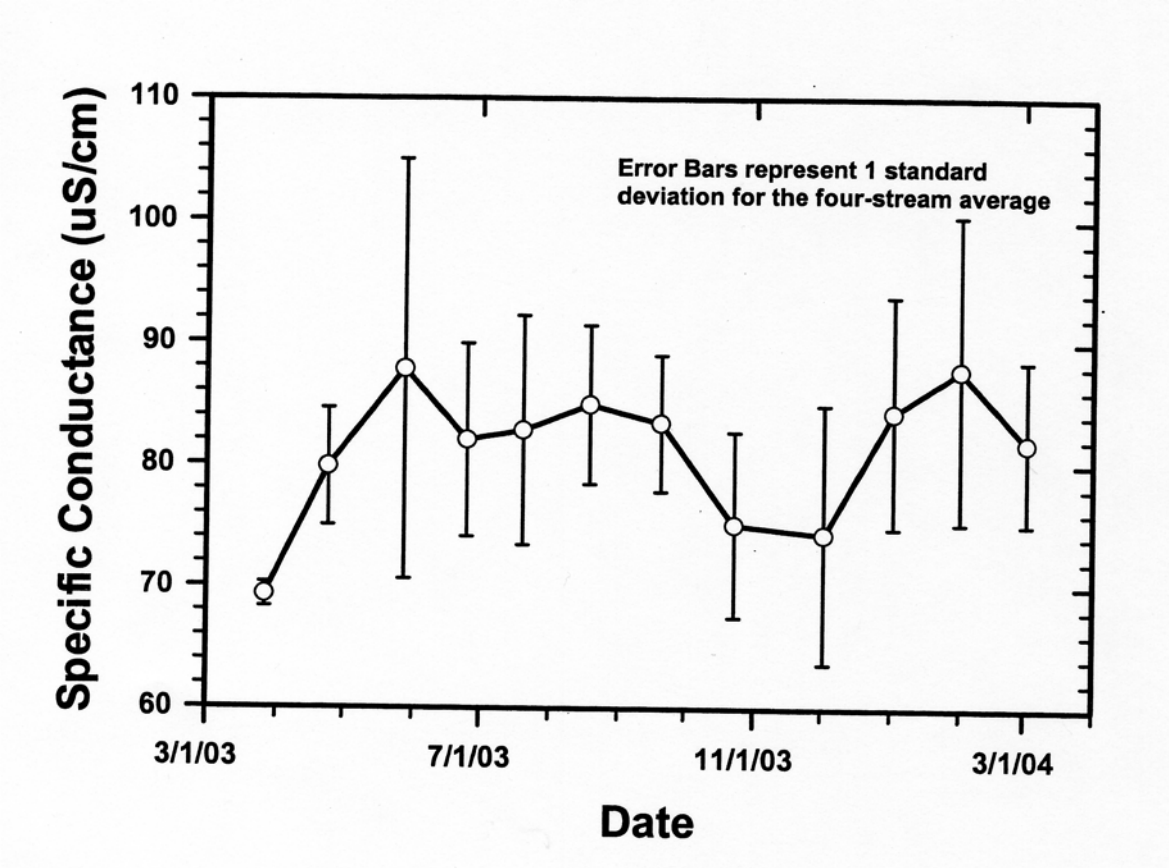

Figure 11. Average specific conductance values in base flow in the Middle Oconee River basin

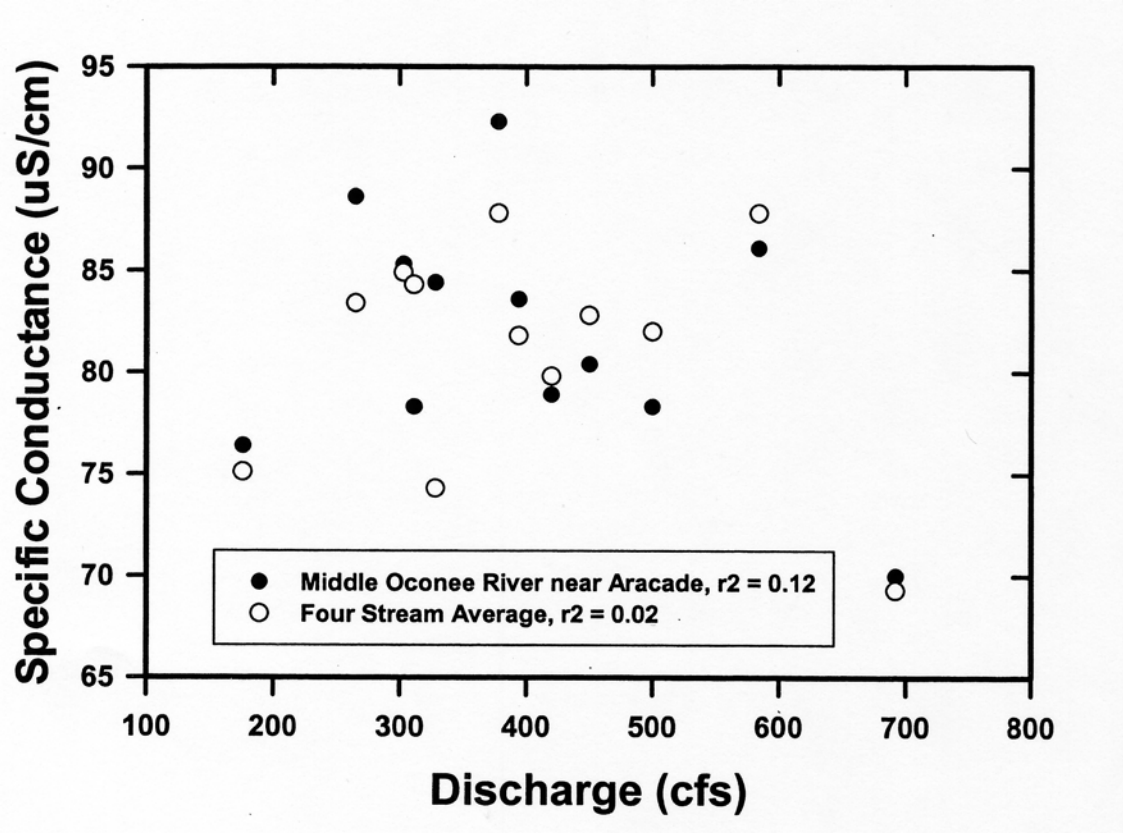

Figure 12. Relationship between specific conductance and discharge in base flow within the Middle Oconee River basin

Table 4
Summary of F-test Results for Stream Base Flow and Shallow Ground Water[1]

	Indian Creek (first order)	**Indian Creek (second order)**	**Pond Fork Creek**	**Middle Oconee River near Arcade**	**Shallow Ground Water**
Indian Creek (first order)					
Indian Creek (second order)	Magnesium, $\delta^{18}O$				
Pond Fork Creek	Magnesium, Specific[2] Conductance, Alkalinity, Tritium	Alkalinity		Tritium	Tritium
Middle Oconee River near Arcade	Magnesium	Magnesium			
Shallow Ground Water	Magnesium, Specific Conductance, Alkalinity, Chloride	Alkalinity	Magnesium	Magnesium, Bicarbonate	

[1] These are one tailed F-tests ($\alpha = 0.05$)
Parameters tested: Magnesium, Chloride, Specific Conductance, Bicarbonate Alkalinity, $\delta^{18}O$, and Tritium

[2]Explanation: The parameters in the box are those for which the standard deviation for the sampling point represented in the row is significantly ($\alpha = 0.05$) greater than the sampling point represented in the column (i.e. the standard deviation for magnesium, specific conductance, alkalinity, and tritium is greater within the sampling set for Indian Creek - first order tributary than the sampling set for Pond Fork Creek).

The relatively high ratios are consistent with the dominance of aluminosilicate minerals, particularly the Rb-bearing biotite within schists that are a dominant rock type in these watersheds. The substitution of Rb for K-feldspar may be another significant source of The mean $^{87}Sr/^{86}Sr$ ratios for all base flow were statistically significant at a very high level of confidence (two-tailed t-tests, α =0.00001) indicating that each stream is characterized by its own strontium isotopic Asignature@. The highest ratios were observed in the terminal Middle Oconee River basin ($^{87}Sr/^{86}Sr_{average}$ = 0.7172) and the lowest ratios were observed in the two small Indian Creek watersheds ($^{87}Sr/^{86}Sr_{average}$ = 0.7127 and 0.7133)

The $^{87}Sr/^{86}Sr$ ratios in base flow for all four streams were extremely consistent over the duration of the 12-month sampling period (Figure 13). The average difference between the $^{87}Sr/^{86}Sr$ ratios for the four streams (n = 35) between consecutive sampling periods was 0.000098 which is ▣40 times less than the average analytical error for this set of samples. This is not true for the ground water samples in which the average difference between the sampling periods exceeded the analytical error. The time-invariance with respect to Sr-isotope ratios is also reflected in the relative standard deviations for base flow which varied only between 0.01% - 0.02% . In comparison, the relative standard deviations for the shallow ground water and weighted rainfall were 0.07% and 0.08%, respectively. Strontium ion concentrations also varied little between sampling periods as evidenced by rsd values of <5% in three of the four streams (Table 5). In contrast, the rsd values for magnesium in stream base flow varied between 4-11% (Table 2) and magnesium was the most time-invariant major ion parameter with a total range of base flow variation between 0.2 - 0.4 mg/L. Relative standard deviations for the strontium

isotope ratios are likewise ▣50 times less than rsd values for ratios of the major ions (e.g. Mg/HCO_3) in base flow.

Strontium ion concentrations and isotope ratios have undergone a discernable evolution within the Middle Oconee River watershed. Strontium concentrations in rainfall are very low (i.e < 5 ppb) and $^{87}Sr/^{86}Sr$ ratios are also low (<0.7125, Figure 14). Strontium ion concentrations increase slightly in shallow ground water to values between 5-8 ppb); however, the isotopic ratios remain very similar to rain water. A likely source of strontium is ion exchange or desorption from the clay minerals and iron oxyhydroxides comprising the ultisols. The shallow

Table 5
Summary of Strontium Ion Concentrations and Isotope Ratios

Strontium Ion Concentrations						
	Middle Oconee River	**Pond Fork Creek**	**Indian Creek (1st order)**	**Indian Creek (2nd order)**	**Shallow Ground Water**	**Rainfall (unweighted)**
Low	16.3	20.1	22.6	23.2	5.2	1.4
High	26.9	23.3	26.3	26.2	7.3	3.3
Average	23.6	21.8	24.1	24.2	6.1	2.5
Std. Dev.	2.9	1.1	1.0	1.0	0.9	1.1
Rel. Std. Dev.	12.3%	4.9%	4.2%	4.1%	15.4%	44.8%
Number	11	8	9	8	6	5
Strontium Isotope Ratios ($^{87}Sr/^{86}Sr$)						
	Middle Oconee River	**Pond Fork Creek**	**Indian Creek (1st order)**	**Indian Creek (2nd order)**	**Shallow Ground Water**	**Rainfall (unweighted)**
Low	0.71698	0.71463	0.71329	0.71259	0.71113	0.71093
High	0.71757	0.71475	0.71343	0.71285	0.71251	0.71225
Average	0.71722	0.71470	0.71331	0.71271	0.71205	0.71174
Std. Dev.	0.00016	0.00004	0.00006	0.00009	0.00051	0.00057
Rel. Std. Dev.	0.02%	0.01%	0.01%	0.01%	0.07%	0.08%
Number	11	8	9	8	6	5

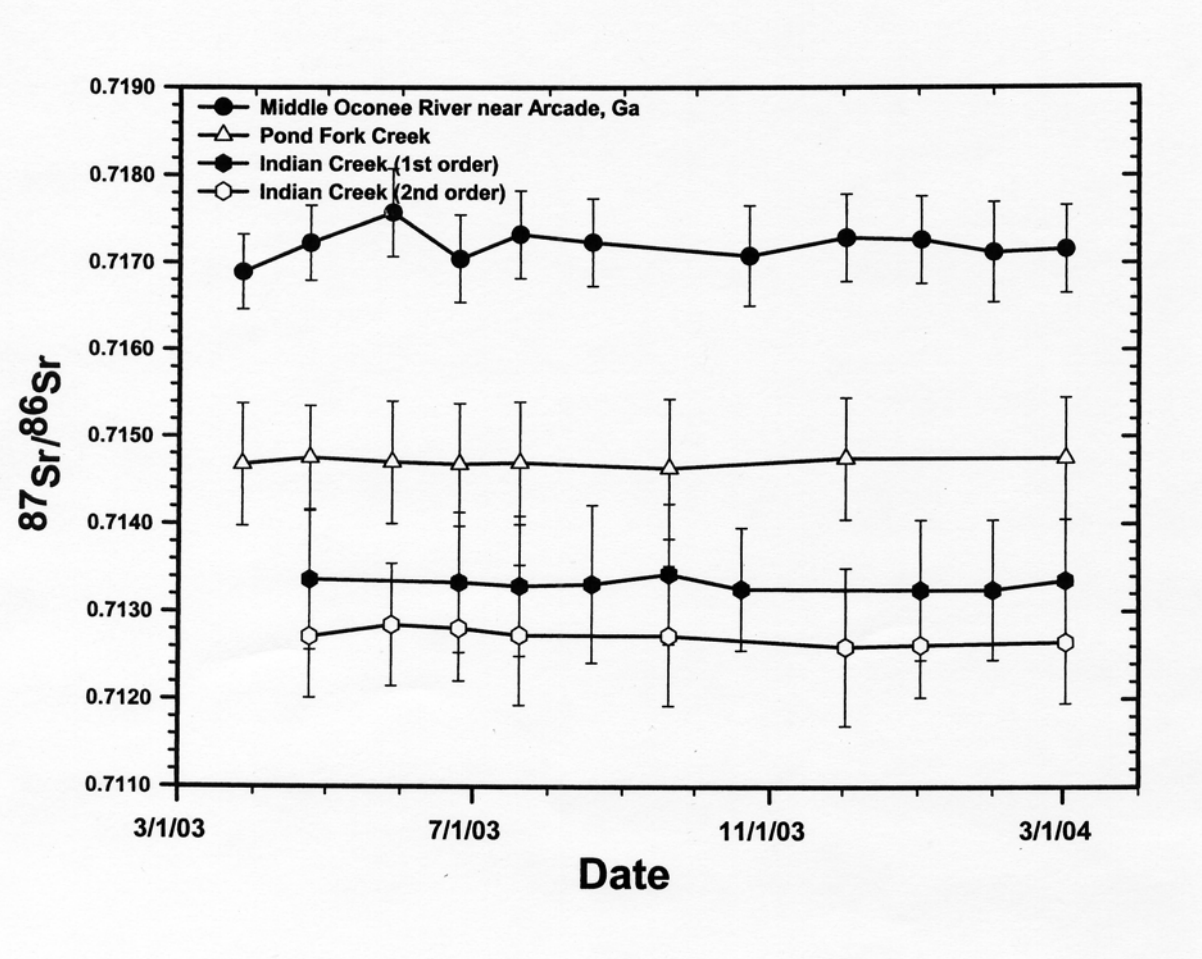

Figure 13. $^{87}Sr/^{86}Sr$ ratios in base flow within the Middle Oconee River basin

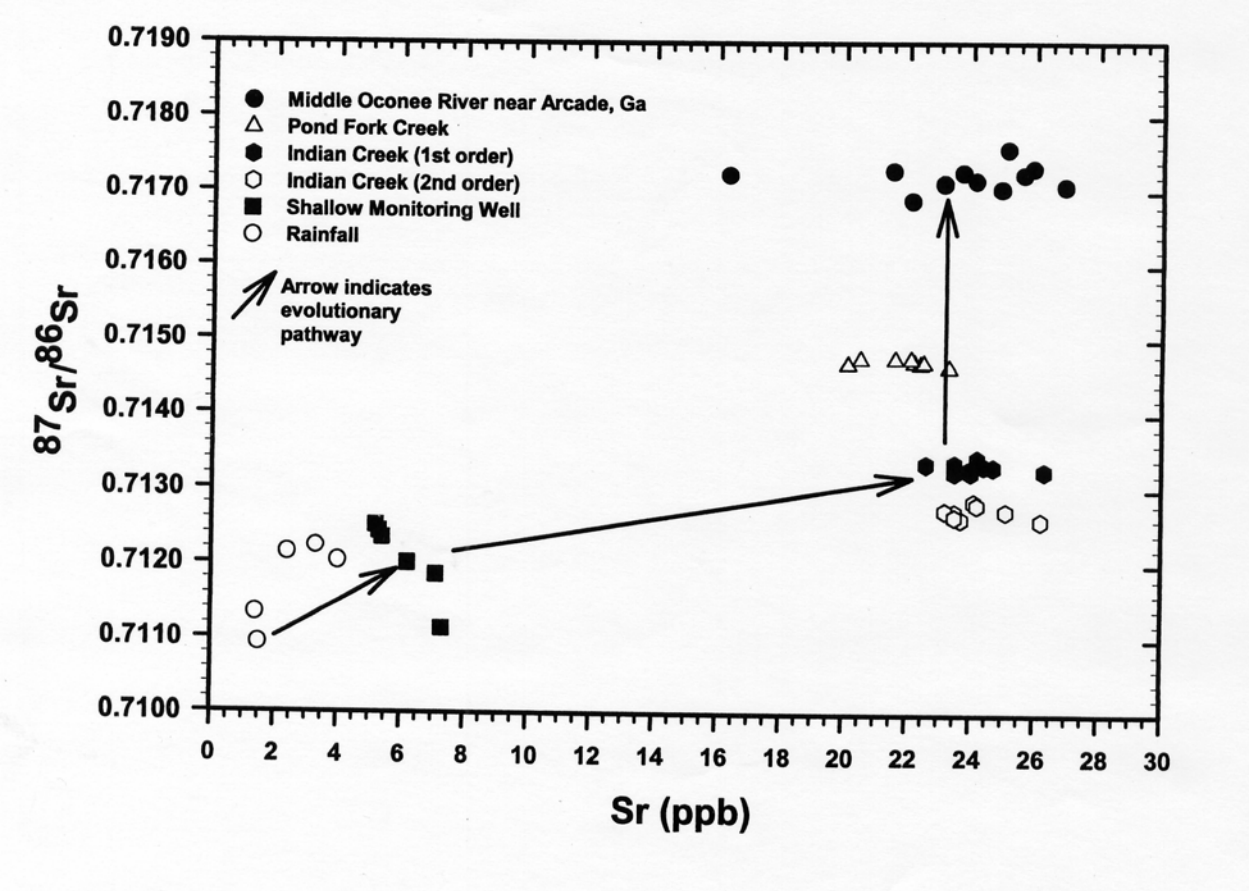

Figure 14. Evolutionary pathway for strontium isotopes in the Middle Oconee River basin

ground water is only mildly acidic (4.9<pH<5.3) and therefore strontium should be fairly stable on soil exchange sites. As weathering proceeds, strontium ion concentrations increased to approximately 25 ppb in stream base flow and each watershed retains a near-constant $^{87}Sr/^{86}Sr$ ratio, seemingly independent of water flux (discharge) and other factors that affect a range of temporal variation for other chemical parameters such as alkalinity and total solute loads. Other investigations (i.e. Land et al., 2000) have also observed that $^{87}Sr/^{86}Sr$ ratios are considerably lower within the shallow subsurface and then increase as weathering processes add increased proportions of strontium-87 to the mixture.

$^{87}Sr/^{86}Sr$ ratios were observed to increase with increasing watershed area while total strontium concentrations remain nearly constant independent of watershed area, land use, and other factors (Figure 14). Pollution from the horse-pasture in the small Indian Creek watershed does not have a discernable effect upon strontium ion concentrations. A possible explanation for this evolutionary trend with respect to increasing $^{87}Sr/^{86}Sr$ ratios might involve a Avariable source area effect@ in which larger basins acquire their solute composition from a slightly different and more expanded set of minerals than the smaller basins. It may be that base flow in the larger basins acquires a higher percentage of solutes from more recalcitrant or low-solubility minerals such as potassium feldspar which have a more radiogenic or higher $^{87}Sr/^{86}Sr$ ratio.

DISCUSSION

Seasonal Variations with Respect to Rates of Base Flow Influx:

Probably the most important aspect of base flow within the Middle Oconee River watershed for scientific consideration is that it is seasonally variable and that on average it

decreases by a factor of approximately three during the period of April through October (Figure 4) when a water deficit typically exists (Figure 3). During this study period it decreased only by a factor of two, presumably as a result of the extraordinary wet period that occurred from June - July, 2003. Seasonally variable low flow occurs throughout the Piedmont Province in the southeastern United States and has implications for water budgeting, resource planning, reservoir storage design and the maintenance of quantity and quality of water for irrigation, recreation, and wildlife conservation (Smakhtin, 2001).

One possible way to analyze this problem is to ask where does the additional water comes from during the cool months (i.e. why do base flow rates increase by a factor of ▣3 during the period between November and March?). Several hypothetical mechanisms for the additional base flow can be posed and analyzed; however, a definitive answer to this question is still elusive. The first mechanism involves the actual influx of seasonal precipitation and the outflux of this seasonal input through the watershed as base flow. This mechanism might involve increased production from the vadose zone and/or from the riparian zone near the stream itself. The second mechanism involves an increased hydraulic gradient during the November-March period, thereby increasing the ground-water discharge to the stream channel (which serves as a ground water sink). The third mechanism is similar to the first; however, it involves the outflux of previously stored water (i.e. non-seasonal or old water) to base flow during the high-flow period. Some combination of all three mechanisms is of course possible.

The first hypothesis involving the seasonal influx of new water can be evaluated using the data acquired in this study. As previously detailed, there was some variation with respect to the $\delta^{18}O$ ratios in the four Middle Oconee River watersheds analyzed in this study (Figure 9). However, most of this variation falls within the range of ▪0.5 per mil, far less than calculated

seasonal variation of 5 per mil in southeastern U.S. rainfall (Yurtsever, 1975). Furthermore, there was no seasonal trend observed in which the oxygen isotopic composition of base flow becomes progressively lighter during the winter months. This was the case for the total range of basin scales analyzed in this study.

The tritium concentrations measured in both ground water and base flow do not support new water as an important source for the additional seasonal base flow. As previously detailed, tritium concentrations observed in the shallow ground water and some of the base flow were often 5-10 T.U. higher than in recent rainfall. Furthermore, in order to account for these increased tritium concentrations there must be a significant component of base flow that was recharged during the bomb period and possibly before the bomb testing of the 1960's. In other words, the ground water that constitutes base flow has an average residence time of perhaps 20-40 years. This precludes the possibility of a significant component of very recent seasonal water within base flow. The significantly greater concentrations of dissolved solutes base flow compared to shallow ground water also indirectly indicate significantly longer residence times for the base flow. Furthermore, there are no isotopic data which indicate that the shallow ground water is comprised of seasonal recharge. Therefore, given these constraints, it is highly unlikely that the increased base flow during the relatively cool months of November-March is derived directly from the influx and outflux of seasonal precipitation; however, some small proportion of seasonal precipitation may be part of the total base flow mixture.

The second mechanism involves an increase of hydraulic gradients through the input of seasonal water which in turn increases the rate of ground water outflux in the form of base flow. This can be modeled by Darcy=s Law as follows:

$$q = K \Delta h/\Delta L \qquad [1]$$

where q is base flow discharge per unit cross-sectional area of stream bottom receiving base flow influent, K is the hydraulic conductivity of the soils and rocks comprising the ground-water flow system, and $\Delta h/\Delta L$ is the hydraulic gradient between the watershed divide (or an equivalent point in the subsurface) and the stream channel. The estimated flow path or length (ΔL) is 2,000 - 3,000 feet which is the average distance of a watershed boundary to a stream channel in the study area. The average hydraulic gradient is likely less than 0.04 which is the average topographic slope. Under these conditions, particularly considering the estimated flow length, it is not likely that hydraulic gradients can change radically enough during the high-flow period to increase the rate of discharge (q) by a factor of two or three. It should be noted that water levels observed within the monitor well varied by only ±1.5 feet during the course of the study. In short, hydraulic heads are not likely to rise by the many feet required to account for these increased rates of discharge. However, it is likely that hydraulic heads near the riparian zone increase during the November-March period, accounting for some small proportion of the increased rate of ground-water discharge.

The third mechanism involves the release of previously stored water as base flow discharge during the high-flow period. This is a documented mechanism of water influx (McDonnell, 1990) that involves a decrease in soil tensions as the percentage of saturated pore space increases during the period of the year when precipitation rates exceed evaporation rates. The new water influx in turn releases water previously retained by considerable tension around the clay-rich soil matrix. Macro-pore flow through larger channels (if such exist) would augment this process and produce higher flow rates (McDonnell, 1990). As previously discussed, most of the geochemical, $\delta^{18}O$, and tritium data support the release of previously stored or non-seasonal

water as the most important mechanism accounting for the increased rates of base flow during the high-flow period.

Environmental Tritium and Stable Oxygen Isotope Variability and Basin Scale:

One of the primary objectives of this study was to identify and interpret the relationships that emerge between isotopic and geochemical variability and basin scale. The analysis of the environmental isotopes (those present as water in precipitation) which include tritium (^{3}H) and stable oxygen ratios ($\delta^{18}O$) indicates that the processing of rainfall through Piedmont Province watersheds is *not* strongly dependent upon basin scale. The average tritium concentrations within base flow for the four watersheds during the study period only varied between 9.1 and 10.8 T.U. These concentrations were significantly higher than recent rainfall (7-8 T.U.) and lower than shallow ground water (average =15.8 T.U.). The similarity of values between the basins and the differences between rainfall and shallow ground water speak to how similar each of the basins have processed rainwater during the past several decades.

As previously stated, the temporal variability at a given sampling location can be measured in terms of relative standard deviation for the total set of samples representative of that site. Hypothetically, smaller watersheds would be expected to produce higher rsd values than their larger counterparts because there is less storage capacity to buffer those changes brought about by variable atmospheric inputs. This relationship with respect to environmental tritium concentrations is not clear cut in that the highest rsd values (25%) were observed for both the smallest watershed (Indian Creek - first order tributary; watershed area = 3.9 km^2) and the largest watershed (Middle Oconee River near Arcade, Ga.; watershed area = 860 km^2). The relative standard deviation for the set of tritium analyses for the intermediate sized watershed (Pond Fork

Creek; watershed area = 54 km^2) was considerably lower at 7.5% (Table 2). The hydrological reasons for this dissimilarity are not readily apparent.

There was no relationship between watershed area or stream order and $\delta^{18}O$ variability for the four watersheds. The rsd values for $\delta^{18}O$ ranged only between 4.8 - 7.1% and the average annual value for the study period only ranged between -5.0 and -5.4 per mil. The rsd values observed for ^3H and $\delta^{18}O$ for the limited set of shallow ground analyses were within the range of the observed stream base flow. The shallow ground water data strongly suggest that most of the seasonal variability inherent within the isotopic composition of rainfall is removed or Ahomogenized@ by mixing processes within the shallow subsurface and this process likely occurs in all watersheds with developed soil profiles (DeWalle et al., 1997 and Wenner et al., 1991). Both the tritium and stable oxygen isotope results indicate that rainfall is processed (i.e. stored and transmitted through the subsurface to stream channels) in a similar manner through Piedmont Province watersheds once the basin area exceeds just a few square kilometers. The movement of ground water through larger basins does not necessarily create greater isotopic homogenization. There exists a small measure of isotopic variability associated with all of the basins that exceeds analytical uncertainty and therefore isotopic homogenization (removal of seasonal or annual differences from ground water recharge) is not complete on any basin scale.

Major Ion Geochemical Variability and Basin Scale:

The highest solute loads were associated with the smallest basin (Indian Creek - first order tributary) where the average alkalinity concentration (35.9 mg/L) and specific conductance (92.6 μS/cm) in base flow were respectively 40% and 26% greater than within Pole Branch

Creek base flow which was characterized by the lowest base flow solute concentrations. The higher solute concentrations may well be related to impacts of the horse pastures located on the small Indian Creek watershed and the relatively low solute concentrations measured in Pole Branch Creek base flow may be related to the relatively undisturbed nature of this watershed.

The results of the previously discussed F-tests indicate that the chemical composition of base flow within the Indian Creek (first-order tributary) is significantly more variable with respect to a number of parameters (magnesium, alkalinity, specific conductance) than both shallow ground water (in which the total solute concentrations were relatively very low) and base flow from several of the larger watersheds. In short, although rainfall may be processed in more or less the same manner independent of watershed area, base flow within the smallest of the watersheds was apparently slightly more vulnerable to contamination from activities that were occurring on the land surface than the larger watersheds. Interestingly, the Indian Creek 2nd order basin (watershed area = 12.7 km^2) was characterized by lower solute concentrations and less geochemical variability than its feeder stream. Other than the smallest basin having the highest dissolved solute concentrations and the most geochemical variability, there are few (if any) other generalizations that can be made regarding the relationship between solute concentrations and basin scale. There is a degree of randomness to this in that if a larger basin was the site of some contaminating land-use activity, it would have possibly been characterized by the highest solute concentrations.

Mass balance or end-member mixing models (e.g. Burns et al., 2001) which attempt to quantify the percentage of ground water and storm runoff most often assume that the chemical composition of the ground water component (base flow) is constant. The results of this present study indicate that this is a tenuous assumption with regards to these Piedmont Province

watersheds. The first problem is that the chemistry of base flow does not at all resemble the chemistry of shallow ground water at the one site in which it was sampled. Ground water at this upslope location was chemically non-evolved and more closely resembled rainwater in terms of low pH, solute loads, and alkalinity than it did base flow. These results suggest that it is *not* likely that the ground water at any one single location or depth will be totally representative of base flow within that watershed.

The second problem with assuming that base flow can be regarded as an invariant end member is that there was significant temporal variability associated with many of the major ion parameters and this variability was greater than the analytical uncertainties. For example, the analytical uncertainty associated with the alkalinity titrations was approximately 6% while the relative standard deviation for alkalinity was 10% or greater in the base flow. Similar considerations apply for most of the other ions, including magnesium which is an ion that was very precisely measured (analytical uncertainties were ≈3-4%) while relative standard deviations for base flow were approximately twice as high. In that the only likely important source of magnesium is rock weathering, there is not one source of magnesium that produces the identical magnesium concentration in base flow throughout the year. Similar considerations apply for alkalinity which is also derived through rock weathering. There were apparently few seasonal trends with respect to base flow chemical variation other than the previously described increased bicarbonate concentrations during the dry months. This trend, however, was not clearly apparent within all the base flow and no inferences can be made with respect to basin scale.

Strontium Isotope Variability and Basin Scale:

The principal new findings of this investigation involved strontium isotope systematics within the Middle Oconee River basin and their hydrological implications for the Georgia Piedmont Province. There are two features related to $^{87}Sr/^{86}Sr$ ratios that may prove useful in

future watershed studies in this region. First, $^{87}Sr/^{86}Sr$ ratios apparently provide a unique geochemical signature or fingerprint of a given Piedmont Province basin (on all scales studied in this investigation). No other geochemical or isotopic parameter provides any similar unique results. The second feature is that, unlike most all other parameters, $^{87}Sr/^{86}Sr$ ratios remain temporally invariant within a given basin and appear to be independent of discharge, contamination inputs, and other seasonal effects. This was the case on all basin scales. In another similar watershed study (e.g. Åberg et al., 1989), strontium isotope ratios were not time-invariant and varied inversely with discharge.

Strontium isotopes above all are a signature of the types of minerals that weather within an aquifer or watershed (Bullen and Kendall, 1998 and Négrel and Lachassagne, 2000). The rocks in this watershed were similar; however, variable percentages of amphibolite (see Figure 2), mica schist, and potassium feldspar unique to a given watershed have produced $^{87}Sr/^{86}Sr$ ratios in base flow that are significantly different from one another to the fifth decimal place. The two closest and most geologically similar watersheds within the Indian Creek sub-basin were characterized by the two most similar sets of strontium isotope ratios (Figure 13). It should also be noted that the range of strontium ion concentrations (typically between 20-25 ppb) were quite similar in base flow within all four of watersheds, likely as a result of similar weathering processes effecting very similar minerals (Figure 14).

Shallow ground water was characterized by much lower strontium concentrations as well as very low alkalinity values (i.e. < 5 mg/L) and pH (< 6.0). The shallow ground water retained the relatively low $^{87}Sr/^{86}Sr$ ratios characteristic of rainfall in the study area. Rock weathering has produced little strontium in shallow ground water and perhaps the major source of strontium in these shallow waters is ion exchange. It can be inferred from the characteristically higher Sr concentrations and $^{87}Sr/^{86}Sr$ ratios that rock weathering, rather than ion exchange from shallow

soil horizons, is the dominant source of strontium in base flow. Miller et al. (1993) also determined rock weathering, rather than ion exchange accounted for the dominant source of strontium to river water in a high-elevation watershed in upstate New York.

The seasonal variations in water flux which manifest themselves in variable discharge and in possibly some geochemical variability (see previous discussion) do not appreciably affect the strontium isotope ratio within base flow. In that rainfall was characterized by relatively low $^{87}Sr/^{86}Sr$ ratios, there can not be an appreciable component of seasonal rainfall within the base flow. This conclusion is consistent with the very low concentrations of Sr in rainfall (< 4 ppb; Table 4) and the previously discussed environmental isotope ($\delta^{18}O$ and ^{3}H) results. Whatever the mineral sources of strontium are within a given watershed, the weathering reactions are apparently independent of the variable seasonal hydrological flux that occurs. Douglas et al. (2002) also observed that $^{87}Sr/^{86}Sr$ ratios were seasonally constant within the Connecticut River watershed even though there was a significant atmospheric source of strontium within these waters.

One of the interesting trends related to $^{87}Sr/^{86}Sr$ ratios is that they tend to increase with increasing basin scale although total strontium concentrations remain more or less constant (Figure 14). Bullen and Kendall (1988) noted an inverse relationship between basin scale in several basins. The trends that were observed cannot be explained solely in terms of simple mixing in that the strontium concentrations and their related $^{87}Sr/^{86}Sr$ ratio values do not fall on a mixing line (Figure 15) (Faure, 1986). Furthermore, if the strontium isotope ratios were solely controlled by the mixing of water from upstream tributaries than it would not be possible to mix waters with a lower ratio (e.g. Pole Branch Creek and Indian Creek) to produce a downstream sample that is characterized by a higher ratio (Middle Oconee River near Arcade; Figure 13).

It is uncertain as to why ratios apparently increase with stream order and watershed area; however, it is possible that as basin size increases the base flow will incorporate weathering products from a larger set of minerals. This set may include some of the more chemically resistant minerals such as K-feldspar that has a high $^{87}Sr/^{86}Sr$ ratio from the trace substitution of the ^{87}Rb which is the radiogenic parent of ^{87}Sr. The same considerations hold true with respect to muscovite which has an even higher$^{87}Sr/^{86}Sr$ ratio than K-feldspar (Bullen and Kendall (1998); however, is less chemically resistant to weathering. Interestingly, Bullen and Kendall (1988) noted an *inverse* relationship between basin scale and $^{87}Sr/^{86}Sr$ ratios in the Sleepers River Research Watershed in Vermont and attributed this to decreasing contributions from the vadose zone.

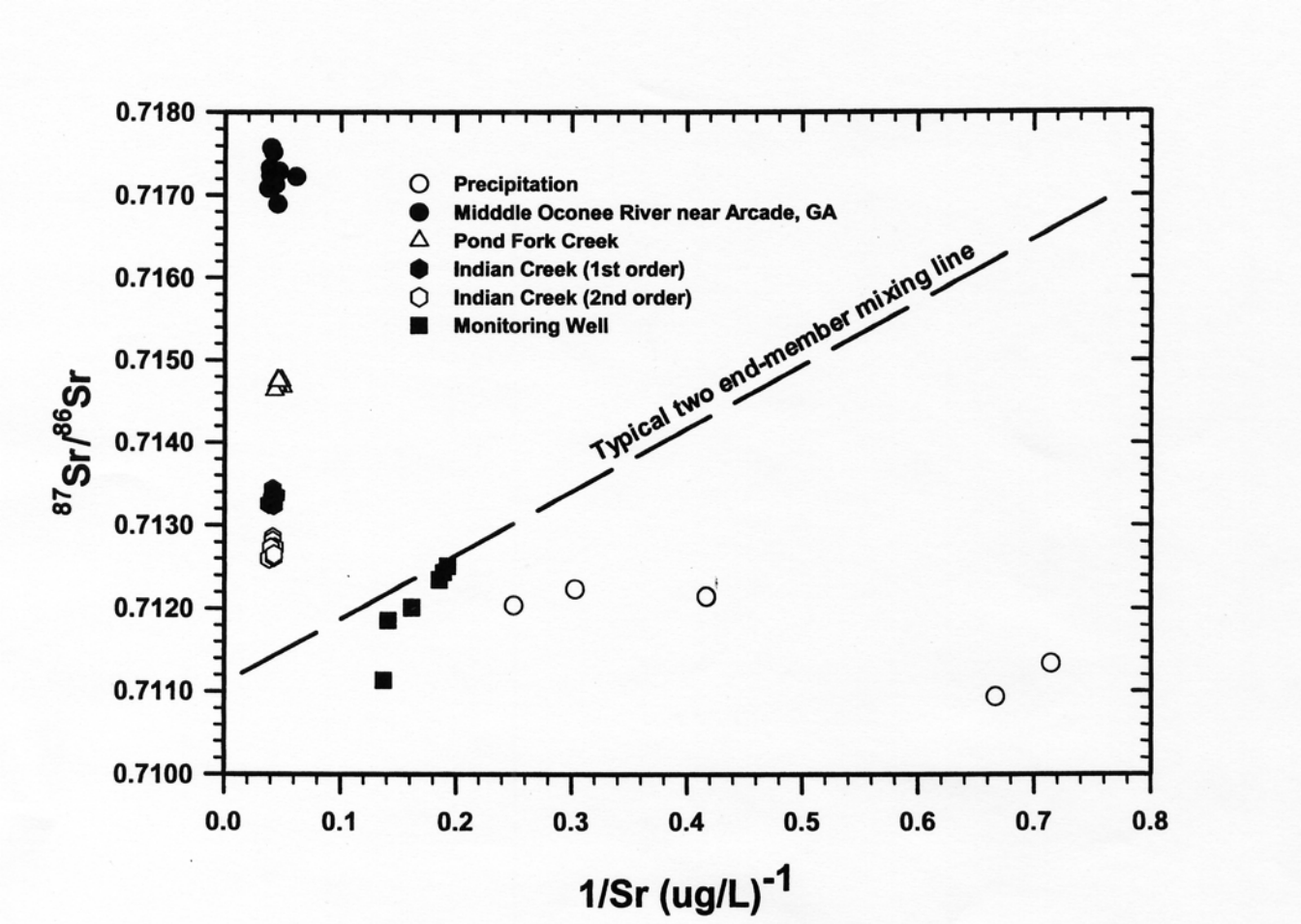

Figure 15. Relationship between strontium isotope ratios and strontium ion concentrations in base flow within the Middle Oconee River basin

Possible Uses for Strontium Isotope Systematics in Regional Watershed Studies:

The two findings of this research related to Sr isotope ratios - that they are temporally invariant in base flow at a given location and they are distinctly different between different watersheds - have important implications for how they can be used in future hydrological studies of Piedmont Province watersheds. Strontium isotopes ratios are the most constant and accurately measured of all of the water chemistry parameters that are available to the hydrologist. For purposes of illustration, the relative standard deviations with respect to the $^{87}Sr/^{86}Sr$ ratio are 250-500 times lower than alkalinity variation in base flow within the Middle Oconee River basin. This would be true for all of the major ion and environmental isotopic parameters as well. Therefore, any type of study that seeks to analyze the many problems that involve mixing dynamics should seek to utilize Sr isotope ratios in addition to other parameters.

One such problem involves end-member mixing from different horizons in the soil and subsurface (Hooper et al., 1990 and Christophersen et al., 1990). It was shown in this study that $^{87}Sr/^{86}Sr$ ratios in shallow ground water are significantly lighter than base flow and though not nearly as temporally invariant as the base flow samples, they are still relatively constant. This is likely as the result of an equilibrium that occurs between soil waters, shallow ground water and the exchange population of Sr ions present on the soil matrix. Therefore, their average composition can be possibly considered as an end-member in various mixing scenarios. Strontium isotopic ratios can provide a critical tool for studies of the mixing dynamics between tributaries within a surface water network in that each sub-watershed would likely bear its own strontium isotopic signature. Similar uses can be made in calculating water balances to lakes and reservoirs. Strontium isotope ratios may provide and adequate tool for differentiating and quantifying the amount of water that flows into a given downstream stretch of river from various upstream tributaries as well as base flow emanating from the down stream basin of interest.

Strontium isotope ratios can certainly be used to provide an excellent tracer in storm-water mixing studies in that the $^{87}Sr/^{86}Sr$ ratio of rainfall was found to be considerably lighter than that of base flow within this Piedmont Province study area.

SUMMARY AND CONCLUSIONS

Major ion geochemistry, environmental isotope (^{3}H and $\delta^{18}O$), and strontium ($^{87}Sr/^{86}Sr$) isotope ratio variation was analyzed within rainfall, shallow ground water and base flow in the 860 km^2 Middle Oconee River basin near Arcade in Jackson County, Georgia. Water samples were acquired on an approximate monthly basis during the period between March, 2003 - March, 2004. The most general objective was to analyze the chemical and isotopic variability of base flow within the study area and relate these variations to their hydrological controls. These results likely represent the first systematic utilization and interpretation of strontium isotopic variation for Piedmont Province watersheds in Georgia. The major conclusions from this study are as follows:

1) The rate of base flow varies systematically during the course of the year within the Middle Oconee River and other Piedmont Province watersheds. The rate of base flow declines by a factor of approximately 2-3 between April and October when water deficit conditions exist.

2) Environmental tritium concentrations within the shallow ground water (average = 16 T.U.) were approximately twice as great as recent rainfall (5-10 T.U.). There is no doubt that a Abomb component@ (i.e. water recharged during the period of atmospheric testing during the 1960's) is present within the shallow ground water. ^{3}H concentrations within base flow vary between ▣7-15 T.U. which as a range is higher than recent rainfall but lower than the ground water. This indicates that there is also a bomb component of recharge present within the base flow and possibly also a pre-bomb component (with no-tritium) as well. There were different

ranges of tritium concentrations observed in each of the four watersheds; however, there was no consistent nor readily interpretable relationship between tritium concentrations and basin scale.

3) Stable oxygen isotope ratios ($\delta^{18}O$) varied between ▣-5.4 and -5.0 per mil (relative to SMOW) which is very similar to the average yearly rainfall within the region. The variations observed during the sampling period were slightly greater than analytical error; however, $\delta^{18}O$ ratios did not become appreciably lighter in stream base flow or shallow ground water during the winter months indicating there is not a significantly large seasonal precipitation input to the ground water that comprises base flow.

4) Base flow within the Middle Oconee River watershed is not chemically constant during the course of the year. The variations that were observed (rsd values between ▣5 - 30%) for most of the major ion parameters are greater than analytical errors. With the exception of alkalinity concentrations, the variation is not seasonal or related to the rate of base flow discharge. The greatest variations were observed in the smallest watershed (Indian Creek - 1st order tributary) which was only 3.9 km^2. There were few differences with respect to major ion variation at a watershed scale of greater than ▣10 km^2. The hydrological significance of this major ion variability is not clear; however, it may be partially related to influx of contaminants (from horse pastures, small water treatment facilities, and leaky septic tanks) and partially related to differential inputs of water from variable source areas within a given basin. The important conclusion from this is that base flow within these watersheds can *not* be considered a chemically constant, temporally-invariant, body of water. The variation is small but significant.

5) The chemistry of the shallow ground water at depths of ▣8 meters below the water table at an upslope well-site much more closely resembled that of rainfall (e.g. specific conductance < 32 uS/cm, pH <5.3, alkalinity < 6 mg/L) than base flow. This implies that base flow is derived from deeper ground water bodies and a great deal of chemical weathering occurs

as ground water flow downslope to the stream channel. It also indicates that ground water from any given monitoring well or even a set of monitoring wells may not produce water that resembles the chemical composition of base flow.

6) Strontium ion concentrations in these waters are relatively low (typically <25 ppb) and do not vary greatly from watershed to watershed. Concentrations are approximately four times higher in base flow than in rainfall or shallow ground water indicating the predominant source of strontium in base flow is mineral weathering rather than direct atmospheric input or ion exchange reactions in the shallow subsurface.

7) $^{87}Sr/^{86}Sr$ ratios are significantly different in base flow from each of the four watersheds and the base flow was significantly more radiogenic (higher ratios) than rainfall and shallow ground water. The $^{87}Sr/^{86}Sr$ ratios were virtually temporally invariant within a given stream and therefore those hydrological processes that affect changes in base flow discharge rates and major ion chemistry do not affect the isotopic composition of strontium in these streams. The strontium isotope ratio became more radiogenic with increasing basin area perhaps as the result of increased weathering contributions of muscovite and potassium feldspar in the larger watersheds.

8) The unique strontium isotopic signature of a given watershed along with the temporal constancy of these $^{87}Sr/^{86}Sr$ ratios make for an almost ideal tracer. Therefore, strontium isotope ratios can be used to quantify or assess the mixing of ground water and storm runoff, the infiltration of vadose zone water, the contribution of ground water to stream runoff, lakes and reservoirs and other hydrological processes that occur within the Piedmont Province.

ACKNOWLEDGMENTS

I wish to thank the Georgia Water Resources Institute for funding this study. I also wish to express my extreme gratitude to Mr. Jerry Waddell and Mr. Eugene Carlson of the Jackson County Water and Sewage Authority for taking the time and effort to facilitate and permit the construction of the monitoring well used for this study. Dr. Paul Fullagar of the University of North Carolina greatly accommodated this study by providing expert strontium ratio analyses with a very quick turn around time as did the staff of the Environmental Isotope Laboratory at the University of Waterloo who provided the tritium results.

REFERENCES CITED:

Åberg, G, Jacks, G. And Hamilton, P.J. 1989. Weathering rates and $^{87}Sr/^{86}Sr$ ratios: an isotopic approach. *J. Hydrol*. 109, 65-78.

Alhadeff, S.J., Musser, J.W., Sandercock, A.C., and Dyar, T.R. 2001. *Digital Environmental Atlas of Georgia*. CD ROM.

Anderson, S.P., Dietrich, W.E., Torres, R., and Montgomery, D.R. 1997. Concentration-discharge relationships in runoff from a steep unchanneled catchment. *Water Resour. Res*. 33, 211-225.

Aubert, D., Probst, A., Stille, P., and Viville, D. 2002. Evidence of hydrological control of Sr behavior in stream water (Strengbach catchment, Vosges mountains, France). *Appl. Geochem*. v.17, 285-300.

Bailey, S.W., Hornbeck, J.W., Driscoll, C.T., Gaudette, H.E. 1996. Calcium inputs and transport in base-poor forest ecosystem as interpreted by Sr isotopes. *Water Resour. Res.* 32, 707-719.

Blum J.D., Erel, Y., and Brown, K. 1994. 87Sr/86Sr ratios of Sierra Nevada stream waters: Implications for relative mineral weathering rates. *Geochim et Cosmochim. Acta*. 58, 5019-5025.

Burns, D.A., McDonnell, J.J., Hooper, R.P., Peters, N.E., Freer, J.E., Kendall, C., and Beven K. 2001. Quantifying contributions to storm runoff through end-member mixing analysis and hydrologic measurements at the Panola Mountain Research Watershed (Georgia, USA). *Hydrol. Process*. 15, 103-1924.

Bullen, T.D. and Kendall, C. 1998. Tracing weathering reactions and water flowpaths: a multi-isotope approach. In:. *Isotope Tracers in Catchment Hydrology*. (eds. Kendall, C. and McDonnell). Elsevier Science, Amsterdam. p611-647.

Burns, D.A., Plummer, L.N., McDonnell, J.J., Busenberg, E., Casile, G.C., Kendall, C., Hooper, R.P., Freer, J.E., Peters, N.E., Beven, K., and Schlosser, P. 2003. The geochemical evolution of riparian ground water in a forested Piedmont catchment. *Ground Water* 41, p913-925.

Christophersen, N., Neal, C., Hooper, R.P., Vogt, RD, and Andersen, SCS. 1990. Modelling streamwater chemistry as a mixtgure of soilwater endmembers - a step towards second generation acidification models. *J. Hydrol*. 116, 307-320.

DeWalle, D.R., Swistock, B.R., and Sharpe, W.E. 1988. Three-component tracer model for stormflow on a small Appalachian forested catchment. J. Hydrol. 104, 301 -310.

DeWalle, D.R., Edwards, P.J., Swistock, B.R., Aravena, R. and Drimme, R.J. 1997. Seasonal isotope hydrology of three Appalachian forest catchments. *Hydrol. Process*. 11, 1895-1906.

Douglas, T.A., Chamberlin, C.P., and Blum, J.D. 2002. Land use and geologic controls on the major elemental and isotopic ($\delta^{15}N$ and $^{87}Sr/^{86}Sr$) geochemistry of the Connecticut River watershed, USA. *Chem. Geol*. v189, 19-34.

Faure, G. 1986. *Principles of Isotope Geology*. J Wiley & Sons, New York. 589p.

Freeze, R.A. 1974. Streamflow generation. *Rev. of Geophys. & Space Phys*. 12, 627-647.

Frederickson, G.C., and Criss, R.E. 1999. Isotope hydrology and residence times of the unimpounded Meramec River Basin, Missouri. *Chem. Geol*. 157, 303-317.

Gat, J.R. 1974. Local variability of the isotope composition of groundwater. In: *Isotope Techniques in Groundwater Hydrology, Vol. 2.* International Atomic Energy Agency, Vienna. 499p.

Gat, J.R. 1980. The isotopes of hydrogen and oxygen in precipitation. In: Handbook of Environmental Isotope Geochemistry, Vol. 1. (eds. P.Fritz and J.Ch. Fontes). Elsevier Scientific Company, Amsterdam, p21-48.

Genereux, D.P. and Hooper, R.P. 1998. Oxygen and hydrogen isotopes in rainfall-runoff studies. In: *Isotope Tracers in Catchment Hydrology* (eds.C. Kendall and J.J. McDonnell). Elsevier Science, Amsterdam. p319-343.

Georgia Automated Environmental Monitoring Network. 2004. Automated Environmental Site Page. http://www.griffin.peachnet.edu/

Goldstein, S.J. and Jacobsen, S.B. 1987. The Nd and Sr isotopic systematics of river water dissolved material: Implications for for the sources of Nd and Sr in seawater. *Chem. Geol*.66, 245-272.

Harris, D. McDonnell, J.J. and Rodhe. 1995. Hydrograph separation using continuous open system isotope mixing. *Water Resour. Res.* 31, 157-171.

Hewlett, J.D. and Hibbert, A.R. 1963. Moisture and energy conditions within a sloping soil mass during drainage. *J. Geophys. Res*. 68, 1081-1087.

Hewlett, J.D. and Nutter, W.L. 1970. The varying source are of streamflow from small upland basins. Montana State University Symposium on Interdisciplinary Aspects of Watershed Management.

Hogan, J.F., Blum, J.D., Siegel, D.I., Glaser, P.H. 2000. $^{87}Sr/^{86}Sr$ as a tracer of groundwater discharge and precipitation recharge in the Glacial Lake Agassiz Peatlands, northern Minnesota. *Water Resour. Res.* 36, 3701-3710.

Hornberger, G.M. and Boyer, E.W. 1995. Recent advances in watershed modeling. *Rev. Geophys. Supplement*, 949-957.

Hill, A.R. 1993. Base cation chemistry of storm runoff in a forested wetland. *Water Resour. Res*. 29, 2663-2673

Hooper, R.P., Christophersen, N., and Peters, N.E. 1990. Modelling streamwater chemistry as a mixture of soilwater end-members - an application to the Panola Mountain catchment, Georgia, U.S.A. *J. Hydrol*. 116, 321-343.

Heath, R.C. 1984. Groundwater regions of the United States. *U.S. Geol. Surv. Water Supp. Pap*. 2242.

Katsuyama M., Ohte N., and Kobashi, S. 2001. A three-component end-member analysis of streamwater hydrochemistry in a small Japanese forested headwater catchment. *Hydrol. Process*. 15, 249-260.

Katz, B.G. and Bullen T.D. 1996. The combined use of $^{87}Sr/^{86}Sr$ and carbon and water isotopes to study hydrochemical interaction between groundwater and lakewater in mantled kart. *Geochim et Cosmochim. Acta*. 60, 5075-5087.

Kendall, C., McDonell, J.J., and Gu, W. 2001. A look inside >black box= hydrograph separation models: a study at the Hydrohill catchment. *Hydrol. Process*. 15, 1877-1902.

Kennedy, V.C., Kendall, C., Zellweger, G.W. Wyerman, T.A. and Avanzino, R.J. 1986. Determination of the components of stromflow using water chemistry and environmental isotopes, Mattole River basin, California. *J. Hydrol*. 84, 107-140.

Land, M., Ingri, J., Andersson, P.S. and Öhlander, B. 2000. Ba/Sr, Ca/Sr, and $^{87}Sr/^{86}Sr$ ratioos in soil water and groundwater: implications for relative contributions to stream water discharge. *Applied Geochemistry*. 15, 311-325.

LeGrand, H.E. 1967. Ground water of the Piedmont and Blue Ridge Provinces in the southeastern states. *U.S. Geol. Surv. Circ. 538.*

Lyons, W.B., Tyler, S.W., Gaudette, H.E., and Long D.T., 1995. The use of strontium isotopes in determining groundwater mixing and brine fingering in a playa spring zone, Lake Tyrrell, Australia. *J. Hydrol*. 167, 225-239.

Maloszewski, P. and Zuber, A. 1982. Determining the turnover time of groundwater systems with the aid of environmental tracers. 1. Models and their applicability. *J. Hydrol*. 57, 207-231.

Maloszewski, P. and Zuber, A. 1992. On the calibration of and validation of mathematical models for the interpretation of tracer experiments in ground water. *Advances in Water. Resour*. 15, 47-62.

Maloszewski, P, Rauert, W., Trimborn, P., Herrmann, A., and Rau, R. 1992. Isotope hydrological study of mean transit times in an alpine basin (Wimbachtal, Germany). *J. Hydrol*. 140, 343-360.

McDonell, 1990. A rationale for old water discharge through micropores in a steep, humid catchment. *Water Resourc. Res*. 26, 2821-2832.

McDonnell, J.J., Stewart, M.K., and Owens. I.F. 1991. Effect of catchment-scale subsurface mixing on stream isotopic response. *Water Resour. Res*. 27, 3065-3073.

McDonnell, J.J., Freer, J., Hooper, R., Kendall, C., Burns, D. Beven, K., and Peters, J. 1996. New method for studying flow on hillslopes. *EOS, Transactions, American Geophysical Union*, 77, 469-472.

McGuire, K.J., DeWalle, D.R., and Gburek, W.J. 2002. Evalution of mean residence time in subsurface waters using oxygen-18 fluctuations duirng drought conditions in the mid-Appalachians. *J. Hydrol*. 261, 132-149.

Miller, E.K., Blum, J.D. and Friedland, A.J. 1993. Determination of soil exchangeable-cation loss and weathering rates using Sr isotopes. *Nature*. 362, 438-444.

Musgrove, M. and Banner, J.L. 1993. Regional ground-water mixing and the origin of saline fluids: midcontinet, United States. *Sci*. 259, 1877-1882.

Naftz, D.L., Peterman, Z.E., and Spanlger, L.E. 1997. Using δ^{87}Sr values to identify sources of salinity to a freshwater aquifer, Greater Aneth Oil Field, Utah, USA. *Chem. Geol*. 141, 195-209.

National Academy of Sciences, 1991. *Opportunities in the Hydrological Sciences*, National Academy Press, 348p.

Négrel, P. and Lachassagne, P. 2000. Geochemistry of the Maroni River (French Guiana) during the low water stage: implications for water-rock interaction and ground water characteristics.*J. Hydrol*. 237, 212-233.

Nelms, D.L., Harlow, G.E., and Hayes, D.C., 1997. Base-flow characteristics of streams in the Valley and Ridge, the Blue Ridge, and the Piedmont physiographic provinces of Virginia. U.S. Geological Survey Water-Supply Paper 2457, 48p.

Ninz, G.E. 1998. Lithogenic and cosmogenic tracers in catchment hydrology. In: *Isotope Tracers in Catchment Hydrology* (eds.C. Kendall and J.J. McDonnell). Elsevier Science, Amsterdam. 830p.

Ohrui, K. and Mitchell. M.J. 1999. Hydrological flow paths controlling stream chemistry in Japanese forested watersheds. *Hydrol. Process*. 13, 877-888.

Ophori, D. and Tóth, J. 1990. Relationships in regional groundwater discharge to streams: an analysis by numerical simulation. *J. Hydrol*. 119, 215-244.

Palmer, M.R. and Edmond, J.M. 1992. Controls over the strontium isotope composition of river water. *Geochim et Cosmochim. Acta*. 56, 2099-2111.

Plummer, G.L., 1983. Georgia Rainfall Preciptiation Patterns at 23 Places, 1734-1982. Georgia Academy of Science, Athens, GA. 119p.

Pionke, H.B., Hoover, J.R., Schnabel, R.R., Grubek, W.J., Urban, J.B., and Rogowski, A.S. 1988. Chemical-hydrological interactions in the near-stream zone. *Water Resour. Res*. 24, 1101-1110.

Piñol, J., Ávila, A., and Rodá, F. 1992. The seasonal variation of streamwater chemistry in three forested Mediterranean catchments. *J. Hydrol*. 140 119-141.

Rose, S. 1993. Environmental tritium systematics of baseflow in Piedmont Province watersheds, Georgia (USA). *J. Hydrol*. 143, 191-216.

Rose, S. 1994. Major ion variation and efflux related to discharge in a mafic Piedmont Province watershed.. *Hydrol. Process*. 8, 481-496.

Rose, S. 1995. Analysis of temporal environmental isotopic variation in ground water of the Georgia Piedmont. *Ground Water* 33, 541-652.

Rose, S. 1996. Temporal environmental isotopic variation within the Falling Creek (Georgia) watershed: implications for contributions to streamflow. *J. Hydrol*. 174, 243-261.

Rose, S. and Peters, N.E. 2001. Effects of urbanization on streamflow in the Atlanta area (Georgia, USA): a comparative hydrological approach. *Hydrol. Process*. 15, 1441-1457.

Rose, S. 2002. Comparative major ion geochemistry of Piedmont streams in the Atlanta, Georgia region: possible effects of urbanization. *Envir. Geol*. 42, 102-113.

Sklash, M.G. and Farvolden, R.N. 1979. The role of groundwater in storm runoff, *J. Hydrol*. 43, 45-65.

Sklash, M.G., Stewart, M.K., and Pearce, A.J. 1986. Storm runoff generation in humid headwater catchments, 2, A case study of hillslope and low-order stream response. *Water Resour. Res*. 22, 1273-1282.

Smakhtin, V.U. 2001. Low flow hydrology: a review. *J. Hydrol*. 240, 147-186.

Stewart, M.K., and McDonnell, J.J., 1991. Modeling base flow soil water residence times from deuterium concentrations. *Water Resour. Res*. 27, 2681-2693.

Stokes, W.R. and McFarlane, 1998. Water Resources Data Georgia Water Year 1998. *U.S. Geol. Survey Water Resources Data-Georgia*. 668pp.

Taylor, B.R. and Hamilton, H.R. 1993. Regional and temporal patterns of total solutes in the Saskatchewan River basin. *Water Resour. Bull*. 29, 221-234.

Turner, J.V., and Macpherson, D.K. 1990. Mechanisms affecting streamflow and stream water quality: an approach via stable isotope, hydrogeochemical and time series analysis. *Water Resour. Res*. 26, 3005-3019.

U.S.Geological Survey. 2004a. USGS Water Resources of Georgia. http://ga.waterdata.usgs.gov/

U.S. Geological Survey. 2004b. USGS 022174745 Middle Oconee River near Arcade, GA. http://ga.waterdata.usgs.gov/

Wadleigh, M.A., Veizer, J. and Brooks, C. 1985 Strontium and its isotopes in Canadian rivers. Fluxes and global implications. *Geochim. et Cosmochim. Acta*. 49, 1727-1736.

Wenner, D.B., Ketcham, P.D., and Dowd, J.F. 1991. Stable isotopic composition of waters in a small Piedmont watershed. Stable Isotope Geochemistry Special Publication No. 3.195-203.

White, A.F., Bullen, T.D., Schulz, M.S., Blum, A.E., Huntington, T.G., and Peters, N.E. 2001. Differential rates of feldspar weathering in granitic regions. *Geochim. et Cosmochim. Acta*. 65, 847-869.

Woods, T.L, Fullagar, P.D., Spruill, R.K., and Sutton, L.C. 2000. Strontium isotopes and major elements as tracers of ground water evolution: example from the Upper Castle Hayne Aquifer of North Carolina. *Ground Water*. 38, 762-771.

Yurstever, Y. 1975. Worldwide survey of stable isotopes in precipitation. Rep. Sect. Isotope. Hydrology International Atomic Energy Association, 40p.

Appendix 1

Precipitation Record (in inches)

From the USDA- ARS collection site at Watkinsville; Oconee Co., GA. Georgia Automated Environmental Network: http://www.griffin.peachnet.edu

	2003										2004		
Day	**Mar**	**April**	**May**	**June**	**July**	**Aug**	**Sept**	**Oct**	**Nov**	**Dec**	**Jan**	**Feb**	**Mar**
1	0.08		0.02		4.82								
2			0.32			0.01	0.5					0.66	
3				0.83		0.26				0.07			
4	0.03			0.06		0.64	0.09		0.02	0.57	0.38	0.01	
5	0.86	0.11	1.96		1.82	0.01			0.44			1.15	
6	1.17	0.05	1.26	0.47		0.01		0.06	0.01				0.13
7	0.11	0.55	0.38	1.75	0.01	0.21		0.01		0.01	0.04		
8		0.23	0.34					0.17			0.27		
9		0.07				0.28		0.01	0.04				
10		0.53			1.34				0.01	0.95			
11		0.01	0.09	0.09	0.15	0.23						0.15	
12				0.02		0.62						1.29	
13				0.95	1.49					0.25			
14	0.02		0.53	0.52						0.22		0.54	
15	0.55		0.32									0.47	
16				0.17		0.14		0.03					0.04
17	0.93	0.39	0.55	0.08					0.03	0.15	0.1		
18	0.12		0.01	0.06					0.91	0.02	0.3		
19	1.14		0.02						1.29				
20	0.58		0.24		0.02								0.09
21	0.01	0.33	2.45		0.14		0.01						0.07
22					0.46		1.42						
23					0.98		0.01			0.31		0.22	
24		0.02			0.01					0.01		0.31	
25		0.57							0.21		1.65	0.12	
26			0.02		0.07			1.43	0.13			0.29	
27	0.7			0.03	0.06		1.3		0.39		0.19	0.01	
28				0.37									
29													
30	0.15			0.24	0.02								0.59
31					1.24					0.03			0.05
Total	**6.45**	**2.86**	**8.51**	**5.64**	**12.63**	**2.41**	**3.33**	**1.71**	**3.48**	**2.59**	**2.93**	**5.22**	**0.97**

APPENDIX 2

Discharge Record for the Middle Oconee River near Arcade, GA. (USGS Gage No. 022174745)

Study Period: March, 2003 - March 2004 (Data Source: http://ga.waterdata.usgs.gov/)

All Values are in Cubic Feet per Second (cfs) and Represent Daily Maximum Values

Day	March	April	May	June	July	Aug	Sept	Oct	Nov	Dec	Jan	Feb	Mar
1	**2003**	513	392	435	5280	1280		207	220	372	321	394	408
2		498	465	415	10800	653			209	331	311	387	398
3		478	433	389	10100	511	261		211	313	317	674	415
4		470	405	431	2530	511	350	202	236	412	315	564	415
5		524	374	448	1930	902	285	202	261	429	389	419	392
6		527	419	405	1300	635	241	202	524	387	480	2070	419
7		662	441	383	1050	621	226	211	433	329		2210	398
8		589	480	387	874	473	220	227	305	309	307	955	403
9		545	493	1030	677	623	219	245	266	295	369	656	363
10		748	511	800	767	626	211	259	245	754	376	545	369
11		964	579	615	942	629	202	239	236	955	333	493	361
12		716	556	524	683	532	201	234	238	543	307	1419	335
13		564	540	1400	783	527	191		236	415	301	1350	329
14		511	490	1719	2370	463	167	196	226	933	303	833	329
15		478	480	1729	1690	408	217	199	220	850	295	659	331
16		450	556	1060	823	356	209	178	212	508	283	584	354
17	793	443	556	3300	716	483	184	178	295	470	274	521	356
18	958	470	521	3560	581	396	173	184	348	343	358	480	323
19	767	463	559	2920	513	325	167	184	2380	283	358	468	319
20	7070	426	559	1690	475	301	166	178	2290	277	297	429	311
21	7510	475	562	1040	463	354	159	175	745	261	287	426	350
22	3240	939	567	757	803	309	490	170	495	346	274	422	346
23	1330	553	567	623	823	283	1440	167	405	352	268	495	301
24	1040	422	567	556	671	268	641	167	394	595	261	426	293
25	877	970	570	535	488	263	313	173	405	564	1570	422	291
26	777	1040	589	465	426	263	246	350	350	405	1880	495	291
27	698	609	598	438	398	253	261	671	343	438	1140	519	291
28	641	495	598	578	387	238	448	424	653	348	695	498	293
29	612	438	545	584	363	238	350	274	612	329	543	441	289
30	600	415	503	478	343		232	241	419	363	473		367
31	595		465		490			224		363	422		394
Total	**29,511**	**17,395**	**15,940**	**29,694**	**50,539**	**13,724**	**8,470**	**6,561**	**14,412**	**13,872**	**14,107**	**20,254**	**10,834**

APPENDIX 3
Environmental Tritium Concentrations in Tritium Units (T.U.)
Analyses are from the Environmental Isotope Laboratory, University of Waterloo

Rainfall

	Tritium (T.U.)	Std. Dev.	Weighted Period	Repeats (T.U.)	Repeats (T.U.)
	6.9	0.8	Weighted rainfall from March to December, 2003		
	7.5	0.7	Weighted rainfall from January to March, 2004	7.2	7.8
Average	**7.2**				
Std. Dev.	**0.4**				
Rel. Std. Dev. (%)	**5.9**				
Range	**6.9-7.5**				
Number	**2**				

Middle Oconee River near Arcade, Ga.

Date	Tritium (T.U.)	Std. Dev.	Repeats (T.U.)	Repeats (T.U.)
4/24/2003	8.6	0.9		
5/28/2003	7.9	0.9		
6/25/2003	7.2	0.7		
8/19/2003	10.6	0.9		
10/23/2003	7.9	0.8	7.1	8.7
12/2/2003	14.0	1.2		
1/2/2004	9.3	0.9		
3/2/2004	7.3	0.8		
Average	**9.1**			
Std. Dev.	**2.3**			
Rel. Std. Dev. (%)	**25.0**			
Range	**7.3 - 14.0**			
Number	**8**			

Note: 1 T.U. = 1 tritium atom in 1 E18 atoms of hydrogen in water

APPENDIX 3

Environmental Tritium Concentrations in Tritium Units (T.U.)
Analyses are from the Environmental Isotope Laboratory, University of Waterloo
Indian Creek (2nd order)

Date	Tritium (T.U.)	Std. Dev.
12/2/2003	11.1	1.0
3/2/2004	10.5	0.9
Average	**10.8**	
Std. Dev.	**0.4**	
Rel. Std. Dev. (%)	**3.7**	
Range	**10.5-11.1**	
Number	**2**	

Pole Branch Creek

Date	Tritium (T.U.)	Std. Dev.
3/27/2003	9.0	0.9
5/28/2003	10.0	1.0
8/19/2003	9.7	0.9
10/23/2003	10.0	0.9
12/2/2003	10.8	1.0
3/2/2004	11.1	1.0
Average	**10.1**	
Std. Dev.	**0.8**	
Rel. Std. Dev. (%)	**7.5**	
Range	**9.0-11.1**	
Number	**6**	

APPENDIX 3
Environmental Tritium Concentrations in Tritium Units (T.U.)
Analyses are from the Environmental Isotope Laboratory, University of Waterloo
Indian Creek (1st order)

Date	Tritium (T.U.)	Std. Dev.	Repeats (T.U.)	Repeats (T.U.)
5/28/2003	7.6	0.8		
8/19/2003	11.1	1.0	10.5	11.7
10/23/2003	16.6	1.4		
12/2/2003	10.5	0.9		
1/2/2004	11.8	1.0		
3/2/2004	11.1	1.0	11.7	10.5
Average	**11.5**			
Std. Dev.	**2.9**			
Rel. Std. Dev. (%)	**25.5**			
Range	**7.6-16.6**			
Number	**6**			

Shallow Ground Water Monitoring Well

Date	TU	Std Dev	Repeats	Repeats
8/19/2003	20.5	1.5		
10/23/2003	17.0	1.4		
12/2/2003	15.5	1.3		
1/2/2004	12.2	1.0		
3/2/2004	14.0	1.1		
Average	**15.8**			
Std. Dev.	**3.2**			
Rel. Std. Dev. (%)	**19.9**			
Range	**12.2 - 20.5**			
Number	**5**			

APPENDIX 4

Stable Oxygen Isotope Ratios (in per mil relative to SMOW)
Analyses made by Geochron Laboratories

Rainfall (collected in Decatur, GA)

Collection Date	Inches Rain	Del O-18 per mil	Repeat
6/3/2003	0.5	-4.8	
6/17/2003	3.3	-5.9	
7/1/2003	3.4	-4.4	
7/23/2003	1.3	-4.5	
8/7/2023	1.5	-4.4	
9/22/2003	1.8	-4.5	
10/17/2003	0.40	-1.8	
10/26/2003	1.70	-4.7	
11/5/2003	1.30	-4.4	
11/18/2003	2.80	-7.6	
1/9/2004	1.50	-4.3	
1/29/2004	2.50	-5.8	-6.1
2/11/2004	1.60	-8.1	
Unweighted Average			**-5.0**
Unweighted Std. Dev.			**1.6**
Rel. Std. Dev. (%)			**31.8**
Number			**13**

Middle Oconee River near Arcade, Ga.

Collection Date	Del O-18 per mil
3/27/2003	-6.0
4/24/2003	-5.6
5/28/2003	-5.3
6/25/2003	-5.1
7/20/2003	-5.3
8/19/2003	-5.6
9/20/2003	-5.4
10/23/2003	-5.0
12/2/2003	-5.8
1/2/2004	-5.1
3/2/2004	-5.4
Average	**-5.4**
Std. Dev.	**0.3**
Rel. Std. Dev. (%)	**5.7%**
Number	**11**

Indian Creek (2nd order)

Collection Date	Del O-18 per mil	Repeat
4/24/2003	-4.6	
5/28/2003	-5.4	
6/25/2003	-4.4	
7/20/2003	-5.2	
8/19/2003	-5.3	
9/20/2003	-5.0	
12/2/2003	-5.1	
3/2/2004	-5.3	-5.3
Average	**-5.0**	
Std. Dev.	**0.4**	
Rel. Std. Dev. (%)	**7.1%**	
Number	**8**	

APPENDIX 4
Stable Oxygen Isotope Ratios (in per mil relative to SMOW)
Analyses made by Geochron Laboratories

Pond Fork Creek				Indian Creek (1st order)		Shallow Ground Water Monitoring Well	
Collection Date	Del O-18 per mil	Repeat	Repeat	Collection Date	Del O-18 per mil	Collection Date	Del O-18 per mil
3/27/2003	-5.2			4/24/2003	-5.4	8/19/2003	-5.7
4/24/2003	-5.0			5/28/2003	-5.4	10/23/2003	-5.4
5/28/2003	-5.2			6/25/2003	-4.9	12/2/2003	-5.5
6/25/2003	-5.5	-5.2	-5.9	7/20/2003	-4.8	2/1/2004	-5.5
		-5.7	-5.4	9/20/2003	-5.3	3/2/2004	-6.1
7/20/2003	-5.2			10/23/2003	-5.3		
8/19/2003	-4.9			12/2/2003	-4.8		
12/2/2003	-5.1			2/1/2004	-5.1		
3/2/2004	-5.7			3/2/2004	-5.1		
Average	**-5.2**			**Average**	**-5.1**	**Average**	**-5.6**
Std. Dev.	**0.3**			**Std. Dev.**	**0.3**	**Std. Dev.**	**0.3**
Rel. Std. Dev. (%)	**7.1**			**Rel. Std. Dev. (%)**	**5.0**	**Rel. Std. Dev. (%)**	**5.0**
Number	**8**			**Number**	**9**	**Number**	**5**

APPENDIX 5
Summary of Major Ion Geochemical Data
Middle Oconee River near Arcade, Georgia

Date	Temp. (oC)	Specific Conductance (uS/cm)	pH	Alkalinity (mg/L)	Calcium (mg/L)	Magnesium (mg/L)	Sodium (mg/L)	Potassium (mg/L)	Sulfate (mg/L)	Chloride (mg/L)
3/27/2003	18.4	70.0	6.00	29.3	6.7	1.8	5.4	2.4	4.8	5.2
4/24/2003	15.4	78.9	6.69	24.4	6.6	1.9	5.7	2.1	2.1	5.8
5/28/2003	18.1	86.4	6.39	24.4	8.7	2.0	5.7	1.9	8.7	5.1
6/25/2003	24.0	78.3	6.69	28.4	10.4	1.8	5.1	2.4	4.9	4.8
7/20/2003	26.1	80.4	6.83	26.4	9.5	1.8	5.2	2.5	4.7	5.0
8/19/2003	25.3	85.3	6.69	28.5	8.2	2.0	5.9	2.5	4.5	7.4
9/20/2003	22.9	88.6	6.89	33.3	8.2	2.0	6.6	2.3	5.6	7.9
10/23/2003	17.1	76.4	7.08	32.5	14.8	1.8	7.0	2.6	5.3	7.9
12/2/2003	9.1	84.4	6.86	28.1	11.1	1.8	6.2	2.3	5.6	10.4
1/2/2004	10.6	78.3	6.60	26.0	4.4	1.7	5.7	1.7	4.3	10.3
2/1/2004	6.7	92.3	7.06	26.0	4.1	2.0	6.8	1.8	8.4	11.4
3/2/2004	14.4	83.6	6.67	25.2	4.3	1.8	6.4	1.7	6.2	11.0
Low	**6.7**	**70.0**	**6.00**	**24.4**	**4.1**	**1.8**	**5.1**	**1.7**	**2.1**	**4.8**
High	**24.0**	**92.3**	**7.08**	**33.3**	**14.8**	**2.0**	**6.8**	**2.6**	**8.7**	**11.0**
Average	**17.3**	**81.9**	**6.70**	**27.7**	**8.1**	**1.9**	**6.0**	**2.2**	**5.4**	**7.7**
Std. Dev.	**6.4**	**6.1**	**0.29**	**2.9**	**3.2**	**0.1**	**0.6**	**0.3**	**1.8**	**2.5**
Rel. Std. Dev. (%)	**37.1**	**7.4**	**4.4**	**10.5**	**39.1**	**5.7**	**10.4**	**15.1**	**32.8**	**33.2**
Number	**12**	**12**	**12**	**12**	**12**	**12**	**12**	**12**	**12**	**12**

Appendix 5
Summary of Major Ion Geochemical Data
Indian Creek (2nd order stream)

Date	Temper. (oC)	Specific Conductance (uS/cm)	pH	Alkalinity (mg/L)	Calcium (mg/L)	Magnesium (mg/L)	Sodium (mg/L)	Potassium (mg/L)	Sulfate (mg/L)	Chloride (mg/L)
4/24/2003	15.2	76.6	6.51	30.9	9.0	1.9	5.4	1.9	2.1	5.6
5/28/2003	17.1	80.1	6.38	32.1	7.0	1.9	5.2	2.2	2.5	5.5
6/25/2003	21.7	81.5	6.61	33.3	6.6	1.9	5.4	2.1	1.9	5.5
7/20/2003	27.2	77.6	6.52	30.1	8.8	1.8	5.2	2.7	1.9	5.6
8/19/2003	26.0	84.3	6.67	26.0	8.2	2.0	5.5	2.1	1.3	7.1
9/20/2003	22.6	81.3	6.98	34.6	8.6	2.0	5.6	2.0	2.6	6.2
10/23/2003	18.1	73.4	6.96	36.6	9.2	1.9	6.1	2.2	1.2	8.1
12/2/2003	10.9	59.5	7.01	30.9	9.7	1.8	5.8	2.0	2.2	10.2
1/2/2004	10.8	82.5	6.90	29.3	4.3	1.8	5.8	1.4	2.2	10.7
2/1/2004	6.4	84.8	6.82	26.8	4.0	1.8	5.8	1.5	2.7	11.6
3/2/2004	14.7	80.4	6.80	26.0	3.9	1.8	6.5	1.2	2.4	10.7
Low	**6.4**	**59.5**	**6.38**	**26.0**	**3.9**	**1.8**	**5.2**	**1.2**	**1.2**	**5.5**
High	**27.2**	**84.8**	**7.01**	**36.6**	**9.0**	**2.0**	**6.1**	**2.2**	**2.6**	**11.6**
Average	**17.3**	**78.4**	**6.74**	**30.6**	**7.2**	**1.9**	**5.7**	**1.9**	**2.1**	**7.9**
Std. Dev.	**6.6**	**7.1**	**0.22**	**3.5**	**2.2**	**0.1**	**0.4**	**0.4**	**0.5**	**2.4**
Rel. Std. Dev. (%)	**38.0**	**9.1**	**3.2**	**11.3**	**30.7**	**4.2**	**6.9**	**21.9**	**23.0**	**31.0**
Number	**11**	**11**	**11**	**11**	**11**	**11**	**11**	**11**	**11**	**11**

APPENDIX 5
Summary of Major Ion Geochemical Data
Pond Fork Creek

Date	Temper. (oC)	Specific Conductance (uS/cm)	pH	Alkalinity (mg/L)	Calcium (mg/L)	Magnesium (mg/L)	Sodium (mg/L)	Potassium (mg/L)	Sulfate (mg/L)	Chloride (mg/L)
3/27/2003	19.1	68.6	6.36	23.6	6.0	1.9	4.3	1.8	2.7	4.8
4/24/2003	12.7	76.9	6.83	26.8	6.5	1.9	4.6	2.1	2.4	4.9
5/28/2003	18.7	72.5	6.82	28.5	9.2	1.8	4.5	2.4	2.1	5.1
6/25/2003	23.6	75.1	6.83	22.7	9.2	1.9	4.6	2.3	2.0	5.1
7/20/2003	27	76.4	6.92	26.8	7.1	1.8	4.8	2.4	1.8	5.3
8/19/2003	23.6	77.1	7.06	30.5	7.4	1.9	5.1	2.3	3.8	7.0
9/20/2003	23.6	76.4	6.92	29.7	7.2	1.8	5.4	2.3	1.2	7.5
10/23/2003	16.9	66.2	6.91	30.1	12.8	1.7	5.3	2.2	1.5	9.8
12/2/2003	9.9	78.3	7.15	26.0	4.2	1.7	6.0	2.0	2.1	10.1
1/2/2004	8.7	78.1	6.55	23.6	4.4	1.7	5.2	1.5	2.0	9.7
2/1/2004	8.8	72.2	6.89	25.6	3.9	1.8	4.5	1.2	2.1	9.1
3/2/2004	17.4	73.5	6.61	24.4	3.9	1.6	4.7	1.1	2.0	9.9
Low	**8.7**	**66.2**	**6.36**	**22.7**	**3.9**	**1.6**	**4.3**	**1.1**	**1.8**	**4.8**
High	**23.6**	**78.3**	**7.06**	**30.5**	**12.8**	**1.9**	**6.0**	**2.1**	**3.8**	**10.1**
Average	**17.5**	**74.3**	**6.82**	**26.5**	**6.8**	**1.8**	**4.9**	**2.0**	**2.1**	**7.3**
Std. Dev.	**6.3**	**3.8**	**0.22**	**2.7**	**2.7**	**0.1**	**0.5**	**0.5**	**0.6**	**2.3**
Rel. Std. Dev. (%)	**36.1**	**5.1**	**3.2**	**10.2**	**39.1**	**5.6**	**10.0**	**23.6**	**29.9**	**30.7**
Number	**12**	**12**	**12**	**12**	**12**	**12**	**12**	**12**	**12**	**12**

APPENDIX 5
Summary of Major Ion Geochemical Data
Indian Creek (1st order)

Date	Temper. (oC)	Specific Conductance (uS/cm)	pH	Alkalinity (mg/L)	Calcium (mg/L)	Magnesium (mg/L)	Sodium (mg/L)	Potassium (mg/L)	Sulfate (mg/L)	Chloride (mg/L)
4/24/2003	15.1	86.9	6.53	30.5	7.9	1.6	7.7	2.0	2.1	7.5
5/28/2003	16.0	112.2	5.99	47.2	9.8	NA	2.9	2.5	3.7	5.1
6/25/2003	21.2	93.2	6.58	34.6	8.0	1.6	7.7	2.3	2.0	7.4
7/20/2003	24.8	96.6	6.61	36.6	8.4	1.8	8.3	2.6	2.0	7.9
8/19/2003	24.2	92.9	7.06	32.5	8.0	1.7	7.4	2.1	1.5	9.4
9/20/2003	21.7	87.3	6.63	32.5	5.2	1.7	7.2	2.0	1.3	9.7
10/23/2003	16.9	84.5	6.67	39.9	13.8	1.4	9.4	2.5	1.1	11.6
12/2/2003	11.4	74.8	6.68	37.8	12.9	1.8	9.7	2.3	2.2	14.7
1/2/2004	12.2	98.1	6.45	35.0	3.9	1.4	8.4	1.7	2.1	14.4
2/1/2004	7.6	102.0	6.50	37.0	3.7	1.4	8.7	1.8	2.9	14.7
3/2/2004	15.1	89.7	6.50	31.3	3.6	1.4	4.1	1.5	2.6	12.8
Low	**7.6**	**86.9**	**6.53**	**30.5**	**3.6**	**1.4**	**4.1**	**1.5**	**1.1**	**5.1**
High	**24.2**	**112.2**	**7.06**	**47.2**	**13.8**	**1.8**	**9.4**	**2.6**	**3.7**	**14.4**
Average	**16.9**	**92.6**	**6.56**	**35.9**	**7.7**	**1.6**	**7.4**	**2.1**	**2.1**	**10.5**
Std. Dev.	**5.5**	**9.9**	**0.25**	**4.7**	**3.5**	**0.2**	**2.1**	**0.4**	**0.7**	**3.4**
Rel. Std. Dev. (%)	**32.5**	**10.6**	**3.8**	**13.2**	**45.2**	**10.7**	**28.4**	**16.9**	**34.6**	**32.3**
Number	**11**	**11**	**11**	**11**	**11**	**11**	**11**	**11**	**11**	**11**

APPENDIX 5
Summary of Major Ion Geochemical Data
Shallow Monitoring Well

Date	Temper. (oC)	Specific Conductance (uS/cm)	pH	Alkalinity (mg/L)	Calcium (mg/L)	Magnesium (mg/L)	Sodium (mg/L)	Potassium (mg/L)	Sulfate (mg/L)	Chloride (mg/L)
8/19/2003	18.1	20.4	5.17	3.2	1.2	0.5	1.1	2.1	0.9	2.1
9/20/2003	19.5	32.2	5.25	6.1	1.7	0.5	2.0	1.4	0.8	4.3
10/23/2003	18.7	16.7	5.29	4.0	2.4	0.5	1.1	0.6	0.6	3.1
12/2/2003	15.4	21.1	5.18	5.4	1.0	0.5	1.1	0.5	0.8	3.3
1/2/2004	16.3	21.3	4.89	3.9	0.6	0.4	1.2	0.6	0.5	3.7
2/1/2004	15.2	15.2	5.20	2.4	0.6	0.5	1.1	1.7	0.5	4.0
3/2/2004	17.5	20.4	5.23	2.7	0.5	0.5	1.0	0.2	0.2	0.0
Low	**16.3**	**15.2**	**4.89**	**2.7**	**0.5**	**0.4**	**1.0**	**0.2**	**0.2**	**0.0**
High	**19.5**	**32.2**	**5.29**	**6.1**	**2.4**	**0.5**	**2.0**	**2.1**	**0.9**	**4.3**
Average	**17.2**	**21.0**	**5.17**	**4.0**	**1.1**	**0.5**	**1.2**	**1.0**	**0.6**	**2.9**
Std. Dev.	**1.7**	**5.5**	**0.13**	**1.4**	**0.7**	**0.04**	**0.3**	**0.7**	**0.2**	**1.5**
Rel. Std. Dev. (%)	**9.6**	**25.9**	**2.5**	**34.6**	**61.0**	**7.8**	**28.1**	**70.5**	**38.5**	**50.5**
Number	**7**	**7**	**7**	**7**	**7**	**7**	**7**	**7**	**7**	**7**

APPENDIX 6
Strontium Concentrations and Isotope Ratios
Strontium Concentrations and 87/86 Isotope Ratios Analyzed at the Department of Geology, University of North Carolina

	Rainfall				Middle Oconee River near Arcade, Ga.			
Dates	**Rainfall Collected (cms)**	**Strontium Conc. (ppb)**	**Strontium 87/86 Ratio**	**Percent Std. Error**	**Date**	**Sr Conc. (ppb)**	**Strontium 87/86 Ratio**	**Percent Std. Error**
6/03 - 6/31/03	11.4	1.4	0.711336	0.0014	3/27/2003	1.4	0.716981	0.0006
7/1/03 - 9/22/03	19.3	2.4	0.712139	0.0024	4/24/2003	16.3	0.717223	0.0006
9/28/03- 10/26/03	11.2	4.0	0.712033	0.0040	5/28/2003	25.1	0.717572	0.0007
10/26/03 - 11/18/03	17.3	3.3	0.712249	0.0033	6/25/2003	24.9	0.717043	0.0007
1/1/03- 3/31/03	26.4	1.5	0.710932	0.0015	7/20/2003	25.9	0.717324	0.0007
Unweighted Average		**2.5**	**0.711738**		8/19/2003	25.6	0.717233	0.0007
Unweighted Std. Dev.		**1.1**	**0.000574**		10/23/2003	26.9	0.717081	0.0008
Unweighted Rel. Std. Dev. (%)		**44.8**	**0.08**		12/2/2003	21.5	0.717289	0.0007
					1/2/2004	23.7	0.717264	0.0007
					2/1/2004	23.1	0.717217	0.0008
					3/2/2004	24.1	0.717157	0.0007
				AVERAGE		**21.7**	**0.717217**	
				STD. DEV.		**7.3**	**0.000159**	
				REL. STD. DEV.		**33.7%**	**0.02%**	
				NUMBER		**11**	**11**	

APPENDIX 6
Strontium Concentrations and Isotope Ratios

INDIAN CREEK - 2ND ORDER

	Date	Strontium Conc. (ppb)	Strontium 87/86 Ratio	Percent Standard Error
	4/24/2003	23.5	0.712712	0.0007
	5/28/2003	24.1	0.712847	0.0007
	6/25/2003	24.2	0.712807	0.0006
	7/20/2003	23.2	0.712728	0.0008
	9/20/2003	25.1	0.712723	0.0008
	12/2/2003	26.2	0.712595	0.0009
	1/2/2004	23.7	0.712617	0.0006
	3/2/2004	23.5	0.712647	0.0007
AVERAGE		**24.2**	**0.712710**	
STD. DEV.		**1.0**	**0.000088**	
REL.STD. DEV.		**4.1%**	**0.01%**	
NUMBER		**8**	**8**	

Pond Fork Creek

	Date	Strontium Conc. (ppb)	Strontium 87/86 Ratio	Percent Standard Error
	3/27/2003	20.1	0.714677	0.0007
	4/24/2003	20.5	0.714750	0.0006
	5/28/2003	22.2	0.714701	0.0007
	6/25/2003	22.4	0.714676	0.0007
	7/20/2003	22.5	0.714695	0.0007
	9/20/2003	23.3	0.714633	0.0008
	12/2/2003	22.1	0.714693	0.0007
	3/2/2004	21.6	0.714749	0.0007
AVERAGE		**21.8**	**0.714697**	
STD. DEV.		**1.1**	**0.000039**	
REL. STD. DEV.		**4.9%**	**0.01%**	
NUMBER		**8**	**8**	

INDIAN CREEK - 1ST ORDER

	Date	Strontium Conc. (ppb)	Strontium 87/86 Ratio	Percent Standard Error
	4/24/2003	23.5	0.713363	0.0008
	6/25/2003	24.4	0.713330	0.0008
	7/20/2003	24.0	0.713290	0.0008
	8/19/2003	24.7	0.713314	0.0009
	9/20/2003	24.2	0.713429	0.0008
	10/23/2003	26.3	0.713257	0.0007
	1/2/2004	23.5	0.713244	0.0008
	2/1/2004	24.0	0.713244	0.0008
	3/2/2004	22.6	0.713353	0.0007
AVERAGE		**24.1**	**0.713314**	
STD. DEV.		**1.0**	**0.000062**	
REL. STD. DEV.		**4.2%**	**0.01%**	
NUMBER		**9**	**9**	

Shallow Ground Water Monitoring Well

	Date	Strontium Conc. (ppb)	Strontium 87/86 Ratio	Percent Standard Error
	8/19/2003	6.2	0.712009	0.0007
	9/20/2003	7.1	0.711854	0.0009
	10/23/2003	7.3	0.711134	0.0009
	1/2/2004	5.4	0.712341	0.0007
	2/1/2004	5.3	0.712429	0.0007
	3/2/2004	5.2	0.712507	0.0008
AVERAGE		**6.1**	**0.712046**	
STD. DEV.		**0.9**	**0.000513**	
REL. STD. DEV.		**15.4%**	**0.07%**	
NUMBER		**6**	**6**	

Assessment of In-Stream Processes in the Development of Sediment TMDLs for Urban Streams

Basic Information

Title:	Assessment of In-Stream Processes in the Development of Sediment TMDLs for Urban Streams
Project Number:	2003GA43B
Start Date:	3/1/2003
End Date:	2/28/2004
Funding Source:	104B
Congressional District:	5
Research Category:	Not Applicable
Focus Category:	Sediments, Non Point Pollution, Surface Water
Descriptors:	
Principal Investigators:	Terry Sturm

Publication

1. Robinson, Joshua and Terry W. Sturm, 2004. "Assessment of In-stream Processes in Urban Streams for Development of Sediment Total Maximum Daily Loads." Georgia Water Resources Institute, Georgia Tech, Atlanta, GA., 62p.
2. Robinson, Joshua, in progress. "Assessment of In-stream Processes in Urban Streams for Development of Sediment Total Maximum Daily Loads." MS Thesis, Environmental Fluid Mechanics and Water Resources, School of Civil and Environmental Engineering, Georgia Institute of Technology, Atlanta, GA.
3. Robinson, J.R., and T. W. Sturm. "Measurement of Total Sediment Flux in Urban Streams for Assessing TMDLs." to be submitted to J. AWRA.

ASSESSMENT OF IN-STREAM PROCESSES IN URBAN STREAMS FOR DEVELOPMENT OF SEDIMENT TOTAL MAXIMUM DAILY LOADS

by

Joshua L. Robinson

and

Terry W. Sturm

School of Civil and Environmental Engineering
in Cooperation With the
Georgia Water Resources Institute
Georgia Institute of Technology
Atlanta, Georgia 30332

June 2004

TABLE OF CONTENTS

ABSTRACT

The North Peachtree Creek drainage basin located in DeKalb County, Georgia, has been subject to rapid urban development over the last several decades and suffers impaired water quality as a consequence. Urbanization results in increased washload to the stream due to runoff from construction sites that are inadequately protected by erosion control measures. In addition, the runoff volume and peak discharge increase due to an increase in impervious area on the watershed. The result is a loss of equilibrium in the sediment regime of the stream characterized by increased bank erosion and lateral migration of the stream. Because the stream cannot transport the increased sediment load caused by urbanization, changes in cross-section and plan-form (meandering) occur and the stream becomes biologically impaired by sediment. Section 303(d) of the Clean Water Act requires the establishment of TMDLs (total maximum daily loads) for quantifying allowable sediment loads where excess sediment loads threaten the biological integrity of streams. However, the development of TMDLs for sediment is complex because of various in-stream processes that contribute to the problem as well as upstream sources of sediment such as erosion. This study focuses on field data collection using existing technology but in an expanded and more comprehensive manner for resolving some longstanding problems with the measurement of sediment discharge in streams. The field sampling site at Century Boulevard has been established and equipped with an Isco 6700 water quality sampler that has provided a field record of automatically sampled suspended sediment concentration (SSC) of point water samples over a wide range of storm events in terms of magnitude and time distribution. These samples have also been analyzed for turbidity and grain size distribution in particular cases. This sampling has shown that a strong relationship exists between SSC of the fine fraction of the sediment and turbidity at the sampling location ($R^2 = 0.976$). These point samples have also been coupled with intensive sampling of the stream bed and banks for comparing grain size distributions and turbidity characteristics. Depth-integrated sampling is currently being performed during storm events in order to develop an empirical relationship between total sediment discharge and the point measurements of suspended sediment concentration. These findings show that turbidity measurement can be coupled with other sediment transport measurement techniques to provide more accurate data and help identify sources of and changes in sediment input. Continuing research involving the use of depth-integrated samplers along with additional laboratory analyses will provide a more definitive procedure for coupling automatic point samplers with continuous turbidity measurement for accurate estimation of sediment loads.

CHAPTER I

INTRODUCTION

The North Peachtree Creek drainage basin located in DeKalb County, Georgia, has been subject to rapid urban development over the last several decades and suffers impaired water quality as a consequence. Urbanization produces eroded sediment in the form of washload due to runoff from construction sites that are inadequately protected by erosion control measures. Following construction, the runoff volume and peak discharge increase due to an increase in impervious area on the watershed as paved parking lots and manicured landscapes replace undeveloped natural areas. The result is permanent alteration of the hydrologic and hydraulic response of the stream accompanied by loss of equilibrium in the sediment regime. Because the stream cannot transport the increased sediment load caused by urbanization, changes in cross-section and plan-form (meandering) occur and the stream becomes biologically impaired by sediment.

Consequences of such changes in stream sediment regime include increased bank erosion and associated lateral migration of the stream, along with sediment deposition along the stream in areas of low velocity. This process results in degradation and loss of aquatic habitat and spawning areas, inhibition of photosynthesis due to turbidity in the water column, increased water treatment costs, loss of storage capacity in water supply reservoirs, and transport of contaminants associated with the fine-grained silt- and clay-sized sediment. Such impairment of water quality is addressed by Section 303(d) of the Clean Water Act, which requires the establishment of TMDLs (total maximum daily loads) for quantifying allowable pollutant loads for stream reaches in which the

biological integrity of the stream is threatened. However, the development of TMDLs for sediment is complex because of various in-stream processes that contribute to the total sediment load as well as upstream sources of sediment such as erosion. Furthermore, measuring natural sediment loads for comparison with loads in impaired watersheds is not a straightforward process. Sediment moves both from upland watershed sources and within the stream system during large storm events, and then is redeposited so that it becomes a potential source for resuspension in succeeding storm events. In urban streams, sediment loads include sediment from surface erosion at construction sites and at other locations in the watershed, as well as eroded material from the stream bed and banks.

Previous research on the relative contribution of sediment sources in Peachtree Creek revealed that in the 1970s and 1980s, when the Atlanta area was experiencing rapid urbanization, approximately 53 percent of the sediment discharge was due to erosion of the watershed, while 47 percent was due to erosion of the channel and floodplain (Weber, 2000). By the 1990s, when urbanization had decreased, 44 percent of the sediment discharge was due to erosion of the watershed and 56 percent of the sediment discharge was due to channel and floodplain erosion. In addition, the sediment discharge in the 1970s was 75,500 tons/year, it increased during the 1980s to 88,400 tons/year, and then decreased to 74,200 tons/year in the 1990s. The changes in sediment yield and the relative contribution of sediment sources were due to changes in land use in the Peachtree Creek Basin. These changes highlight the effects that construction activities had on the sediment budget of Peachtree Creek and the subsequent changes in channel geometry that occurred, and continue to occur, as Peachtree Creek adjusts to

reach equilibrium. These changes also make it difficult to identify sediment sources through field sampling alone.

For these reasons, locating sediment sources and measuring sediment loads are challenging problems that require solution for effective establishment of sediment TMDLs and sediment source controls.

Currently, the measurement of sediment loads in streams involves the use of:

(1) programmable point samplers that pump water samples (for later measurement of suspended sediment concentration) at specified time intervals from the stream with simultaneous measurement of stage;

(2) sensors for the continuous measurement of turbidity as a surrogate parameter for suspended sediment concentration;

(3) manual depth-integrating samplers that collect samples over several stream verticals to obtain the average cross-sectional suspended sediment concentration;

(4) velocity meters for establishing the stage-discharge relationship for the stream at the sampling cross section.

These techniques may be used in several combinations in order to estimate sediment discharge and the resultant sediment load, which is defined as the mass of sediment transported for a specified time interval such as a day, month, or year. In fact, the time interval is of considerable importance in developing sediment TMDLs. Average annual sediment loads can be measured by using a combination of depth-integrated sampling and discharge measurement using the flow-duration method. Storm-event sediment loads, however, may be more important in determining sediment TMDLs, especially in urban watersheds in which significant quantities of sediment are transported by large infrequent

storm events. In this case, a pumping sampler or a continuous turbidity sensor in combination with discharge measurement may be required. The problems introduced by these methods include transforming a point measurement of suspended sediment concentration to a cross-sectional average, and determining a calibration relationship between turbidity and suspended sediment concentration. The latter calibration depends on the percentage of fine sediments in the suspended sediment in the stream. The fine sediments are the primary contributors to turbidity, but the percentage of fine sediments and their resultant turbidity depend on the magnitude of the discharge and the sediment sources as well as the sediment mineralogy and presence of additional suspended matter such as organics.

This study focuses on field data collection using existing technology but in an expanded and more comprehensive manner for resolving some of the longstanding problems associated with the measurement of sediment discharge and sediment loads in streams for the purpose of establishing sediment TMDLs and sediment controls. In previous research, a field sampling site at Century Boulevard on the North Fork of Peachtree Creek has been established and equipped with an Isco 6700 automatic water quality sampler that has provided a field record of automatically sampled suspended sediment concentration (SSC) of point water samples over a wide range of storm events with respect to magnitude and time distribution. These samples have also been analyzed for turbidity and grain size distribution in particular cases. Sediment samples from the streambed and banks in the vicinity of the automatic sampler and in upstream locations have been collected and analyzed. Depth-integrated sampling is currently being performed during storm events in order to develop an empirical relationship between total

sediment discharge and the point measurements of suspended sediment concentration from the Isco sampler. This phase of the research is intended to establish the contribution of the fine fraction of suspended sediment to turbidity and to develop a methodology for separately estimating fine and coarse sediment loads during storm events. In a second phase of the research, numerical modeling will be used in combination with point measures of suspended sediment concentration to develop reliable measures of total cross-sectional sediment discharge.

This report summarizes the results obtained so far in phase one of the research. Chapter II is a review of the current literature related to measurement of suspended sediment discharge. Field sampling techniques and experimental laboratory procedures are given in Chapter III. Results and discussion are found in Chapter IV, and the final chapter provides a summary and conclusions.

CHAPTER II

LITERATURE REVIEW

2.1 Introduction

Accurate measurement of fluvial sediment transport is necessary for effectively assessing the geomorphic and environmental health of any river or stream. This data is difficult to collect, however, because suspended sediment varies greatly both spatially and temporally, and sampling methods are labor-intensive and time consuming. Surrogate measurements of stream parameters that correlate with sediment concentration are often used and may offer satisfactory results. Turbidity is one of the most notable surrogates since it can be measured continuously and with little comparative cost. Turbidity has been used to effectively assess and predict sediment concentration for such uses as stream bank erosion analysis and contaminated sediment transport monitoring.

2.2 Importance of Suspended Sediment Monitoring

Suspended sediment affects nearly every aspect of a riparian environment. During periods of high flow, sediment erodes from stream banks and is lifted from the streambed and carried downstream. Deposition of such sediment often occurs at an undesirable location such as in a reservoir or near an in-stream hydraulic structure, thereby decreasing storage volume or otherwise impeding flow. Thus, design and maintenance of such structures requires an understanding of the deposition tendencies of suspended sediment and accurate quantitative measures of sediment volumes. Sediment discharge, the measure of the amount of sediment that passes a specific point in the stream per unit time, is often calculated for this purpose. A related quantity is the dry

weight of sediment that is transported over a specified time interval, which is referred to as sediment load. Over the last two decades suspended sediment data have been used in such fields as contaminated sediment management, stream restoration, environmental quality, and geomorphic classification (Gray, 2002). The environmental concerns associated with suspended sediment are such that the U.S. Environmental Protection Agency (1998) identifies sediment as the single most widespread cause of impairment in the Nation's streams, rivers, lakes, reservoirs, ponds, and estuaries (Gray et al., 2000). Fine sediment (< 64 μm) in suspension contributes turbidity that harms biological activities. By reducing light penetration in the water column, suspended sediment impairs photosynthesis and limits spawning areas. In addition to biological impacts, sediment also acts as a vehicle for carrying harmful chemicals and trace elements downstream (Grayson et al., 1996; Faye et al., 1978). These concerns initiated the Total Maximum Daily Load (TMDL) program, set forth by the EPA. This program, established by the Clean Water Act, section 303, regulates the total amount of pollutant that a body of water can receive from all sources and still meet water quality standards. Observation of the TMDL program requires accurate measurements of suspended sediment discharge.

The TMDL program also involves allocation of pollutant to each contributing point and non-point source. Accordingly, monitoring sediment transport is very helpful in establishing the sediment's origin. Stream bank erosion and lateral migration can be examined during peak periods of sediment transport to identify causes of erosion and establish preventive measures for future erosion (Green et al., 1999). Fluvial sediment is the result of both watershed and bank erosion, and the balance is dictated by land use.

Urban areas are characterized by impervious pavement and structures and storm drainage systems that carry away most runoff. In addition, exposed land is routinely landscaped so that its absorptive capabilities are minimal. The result is a series of point discharges instead of the sheet flow that would occur naturally. This causes exaggerated peak discharges into streams during storms and resulting amplified channel erosion. Whereas urban streams experience significant stream bank erosion, agricultural areas involve mostly watershed erosion. The exposed land associated with cultivation, livestock feeding areas, grazing pastures, and fields of row crops is highly susceptible to sheet erosion during storm events. This process contributes to sediment loads in nearby streams, although such non-point discharges cause minimal channel erosion (Faye et al., 1978).

2.3 Need For Surrogate Technologies in Suspended Sediment Monitoring

Direct sampling of fluvial suspended sediment is a labor-intensive, costly procedure that is subject to several sources of error. Additionally, because suspended sediment concentration varies temporally and spatially in a stream cross-section, single point measurements are not sufficient for quantifying sediment loads. Experiments have shown that point measurements underestimate sediment loads (Horowitz et al., 1990). To account for this variability, calibrated depth- and point-integrating isokinetic samplers are employed. These samplers are used in conjunction with the Equal-Discharge Increment or Equal-Width Increment Methods to provide a representative sample. This procedure was established by the Federal Interagency Sedimentation Project (FISP), a subordinate of the Subcommittee on Sedimentation that began in 1938 (Gray, 2002). Because this

time-tested standard procedure for sampling suspended sediment produces reliable data, these data are often coupled with surrogate measurements for gauging their effectiveness. The procedure is difficult to conduct, however, as it requires sampling during periods of high stream flow, which coincide with storm events. The sampling equipment is unwieldy and archaic by modern standards, and the sampling procedures require a team of trained staff for proper implementation. In addition, the samples produced require extensive laboratory analysis, making reliable data costly to produce.

The laboratory analysis that follows field sampling is subject to error such that, in spite of carefully executed sampling procedures, the resulting data can be skewed or otherwise unrepresentative. A common error lies in the discrepancy between the two laboratory methods used for measuring sediment concentration in a sample. The Total Suspended Solids (TSS) procedure, set forth by the American Public Health Association, American Water Works Association, and the Water Pollution Control Federation (1995), was designed for analyzing wastewater effluent samples but has also been used for measuring sediment concentration in stream samples. The procedure involves filtering an aliquot of the sample under the assumption that it is representative of the entire sample. Withdrawal of the representative aliquot is often difficult, particularly when large particles that settle quickly constitute much of the sediment in the sample. This inherent bias in the TSS procedure produces unreliable results that do not accurately represent the concentration of sediment within a sample. In comparison, the Suspended Sediment Concentration (SSC) test presented by the American Society of Testing and Materials involves measuring the entire sample to obtain total sediment mass. This is accomplished through evaporation, filtration, or wet-sieve filtration, and produces reliable results that

are a true measure of the concentration of solid material in a stream sample. Because the entire sample is measured, the SSC procedure is not affected by particle size and related settling velocities of particles. In order to quantify the differences between the two methods, the U.S. Geological Survey (2000) conducted an analysis of 3,235 paired TSS and SSC data taken from many different regions in the Nation. The study found that the TSS method was essentially unreliable for analyzing natural water samples, and TSS values demonstrated particle size bias by underestimating the sediment concentration when the sand-sized material exceeded about a quarter of the total sediment dry weight. In spite of the fundamental differences between the two procedures, investigators have commonly used the terms TSS and SSC interchangeably, an erroneous practice that has produced unreliable data. The study concluded that the SSC method should be used exclusively for measuring sediment concentration in natural-water samples to prevent error in laboratory analyses (Gray et al., 2000).

2.4 Existing and Emerging Surrogate Technologies

Several surrogate measurements are commonly employed to avoid the difficult and costly procedure of sampling suspended sediment directly. Traditional surrogates such as stream discharge offer somewhat acceptable results but can suffer from large uncertainties in predicted suspended sediment concentration, especially if fine sediment is a significant proportion of the total size distribution. Emerging technologies such as laser diffraction and acoustic backscatter measurements show promise but are costly and are yet to experience widespread use.

Stream discharge as a surrogate parameter can be paired with measured sediment concentration for development of a discharge vs. suspended sediment concentration relationship, or sediment rating curve. This relationship can be used in conjunction with the stage-discharge relationship of a particular reach, allowing sediment discharge predictions to be made from water surface elevation measurements. This process is based on the idea that as stream flow increases, shear stresses on the streambed and banks also increase, causing erosion and suspension of sediment particles. Accordingly, as discharge increases, mean particle size of the suspended sediment increases in a similar fashion. Intensive calibration of a particular river section can yield acceptable results such that stage can be used to predict sediment loads and grain size distributions. Oftentimes, when precision is required or when such calibration is not practical, stream discharge is not a suitable measurement. Once the calibrations are established, however, the method is essentially free of cost. For this reason it is often used with other surrogates as a comparison or for filling in potential gaps in data sets caused by equipment failure (Green et al., 1999). Sediment rating curves using a power function that relates suspended sediment concentration and stream discharge have been used for more than 60 years. In general, this approach underestimates highs and overestimates lows (Horowitz, 2002). Thus, rating curves should be used for analyzing portions of storm events rather than entire events (Lewis, 2002).

Many technically advanced methods for monitoring sediment discharge are currently being developed or tested, and several have been used successfully on a limited basis. These devices employ measuring principles such as differential density, optical transmission, nuclear, laser diffraction, and acoustic backscatter intensity. The ideal

surrogate technology would involve a direct relationship with suspended sediment and/or particle size distribution that could be monitored and recorded automatically in a fashion representative of the entire cross-section for any river in any flow situation (Gray, 2002). Although this technology does not yet exist, two of the most promising instruments involve laser diffraction and acoustic backscatter intensity. Both apparatuses have been field tested and yielded effective results in certain situations.

Laser diffraction devices, unlike many other instruments, are unaffected by changes in grain-size or particle color and refractive index. The apparatus uses technology based on the Mie theory model for light scattering physics by generating a collimated beam and collecting the beam with a receiving lens. As a particle passes through this beam and blocks light waves, some waves enter the particle while others are diffracted around it. The angular scattering caused by the particle leaves a distinctive silhouette that appears identical to an aperture of the same diameter. This diffractive signature can be used to indicate the grain-size. As this process occurs at an in-stream gauging station, stream flow passes through the instrument such that the summation of the analysis of each particle gives the grain-size distribution and the suspended sediment concentration of the stream flow. This can be accomplished isokinetically using a recently developed low drag vehicle that encloses a laser diffraction instrument. The unit measures free-stream velocity and adjusts withdrawal using an internal flow-assistance pump. It also records sampling depth using pressure transducers (Agrawal and Pottsmith, 2002). The Grand Canyon Monitoring and Research Center tested one such instrument beginning July 19, 2001. The particular unit was designed to detect particles over a size range of 1.3 to 250 µm. Investigators made 720 point measurements with the device and

13 samples using traditional isokinetic methods integrated across the cross-section. Preliminary results indicated that the laser diffraction instrument accurately tracked the sand concentration and its variance with increasing flow. Median grain size data from the two sample sets were also in good agreement (Melis et al., 2002). The variability in measurement that laser diffraction instruments offer reinforces the advantage of continuous monitoring.

A common limitation among optical sensors is their vulnerability to biological fouling, a substantial concern in the stream environment. Acoustical measurements are not affected by fouling and can also be used for measuring suspended sediment. Acoustic instruments have been widely used for measuring in-stream flow velocity and have recently also been employed for measurement of sediment concentration using acoustic backscatter intensity. These devices apply the principles of sound scattering from small particles for estimation of suspended sediment. Calculations include adjustments for ensonified volume, source level, two-way transmission loss, and volume scattering strength, a parameter affected by particle shape, size, density, rigidity, compressibility, and acoustic wavelength. The transmission loss of the water is based on the water's acoustic frequency, salinity, temperature, and pressure. The idea behind surrogate measurements is to simplify sediment monitoring, however, so measurement of all characteristics is not practical. A reduced form of the calculations involves a simplified exponential equation that relates sediment concentration to relative backscatter. The major limitation of this technology is its inaccurate response to changes in concentration and particle size distribution, a restraint common to single-frequency instruments. An inherent mismatch of frequency versus particle size also exists.

Although the limiting effects can be minimized through extensive calibration, acoustic sensors are most sensitive to large particles and do not respond well to the frequency range that corresponds to clay-sized particle distributions. In spite of its response to certain particle sizes, acoustic backscatter technology has the advantage of providing a data profile rather than a point measurement. The measurement process is also much less intrusive to the stream environment than are many other instruments. Like all surrogate measurements, significant calibration must be conducted before accurate predictions can be made (Gartner, 2002).

A final surrogate that has been used very successfully is turbidity measurement. The relationship between suspended sediment concentration and turbidity is based on the supposition that the cloudiness of a water sample is directly related to the concentration of sediment particles suspended in the sample. Accordingly, turbidity meters quantify suspended sediment by measuring the scattering or attenuation of a beam of light through a water sample and using this measure by relating it to a particular mass of suspended material. Using turbidity measurement as a surrogate for suspended sediment concentration is a process that, like other surrogates, requires significant calibration. Site-specific regression analyses produce relationships that can be used for prediction of sediment loads. Turbidity measurement can be accomplished in several ways. Grab samples can be taken and subsequently analyzed in a laboratory for turbidity and suspended sediment concentration. This process can be used for calibrating the site such that after calibration the sediment concentration tests can be replaced with turbidity measurements (Wass and Leeks, 2002). A more advanced procedure involves *in situ* turbidity probes that continuously monitor turbidity. A data logger records the turbidity

measurements, which are converted to sediment concentration using the predetermined regression relationships. *In situ* turbidity probes require considerable maintenance since they can often be rendered ineffective by debris flowing downstream and are highly susceptible to biological fouling (Lewis, 2002). Both methods have been used extensively and, coupled with discharge measurements, can provide very accurate sediment load estimations.

There are also two major types of turbidity meters. Attenuation turbidimeters measure the loss of intensity of a light beam across a known distance of a sample. Nephelometric turbidimeters measure scattered light by detecting the beam at an angle from its origin. Turbidimeters are standardized with a substance of known turbidity, with the most common being formazine. However, in spite of standardization, the two types of instruments respond differently when measuring the turbidity caused by suspended sediment particles. Fluvial sediment is a mixture of grain sizes originating from various minerals, and this aggregation responds differently than formazine (Gippel, 1995). As a result, most turbidity measurements are instrument-specific (Pfannkuche and Schmidt, 2003).

While the use of turbidity as a surrogate for suspended sediment concentration has yielded successful results in numerous studies, it has several limitations. As mentioned previously, the relationship between turbidity and suspended sediment is very site-specific. Organic particles also contribute to turbidity in the water column and can skew suspended sediment data derived from turbidity measurements (Weigel, 1984). The predominant limitations to accurate turbidity measurement involve changes in particle shape and particle color. Each mineral that is represented in a particular stream sample

has distinctive optical properties that respond differently to a light source. Particle color can contribute to as much as ten percent error, and nephelometric turbidity is particularly vulnerable to water color since light attenuates differently through various colors, although a near infrared light source can minimize this problem (Gippel, 1995). The shape of sediment particles affects the attenuation or scattering of light through a sample as well. This combination of sediment properties reinforces the importance of developing site-specific relationships between turbidity and suspended sediment since each site has its own unique sediment characteristics. Another considerable limitation in turbidity measurement is particle size. The relationship between turbidity and suspended sediment is based on the principle that each sediment particle contributes to the overall cloudiness of a sample. Fine sediment causes high attenuation in turbidity measurements (Brasington and Richards, 2000), but when coarse sediment particles (> 64 μm) constitute a significant portion of a sample, turbidity measurement becomes difficult since these large particles settle very quickly and therefore do not contribute to turbidity readings. And, as sediment concentration measurement involves the weight of sediment within a sample volume and large particles constitute a considerable fraction of the sediment weight, omission of large particles substantially skews sediment concentration data. For this reason, application of turbidity as a surrogate is most appropriate when fine clay-sized sediment particles compose most of the sample.

2.5 Applications of Turbidity Monitoring

The development of site-specific calibration curves for use in relating turbidity and suspended sediment concentration is the most important part of successfully using

turbidity as a surrogate. Although the relationship is mostly uniform during periods of low flow, suspended sediment flux is highly variable in space and time and is difficult to quantify with single point measurements. In fact, during periods of high flow, turbidity varies for a given suspended sediment concentration. To prevent correlation error, numerous events during varying flow conditions must be incorporated in the data set. Storm events that yield the highest variation in sediment flux should be especially targeted. Turbidity data should be scrutinized to identify possible errors and periods of extended fouling should be omitted. Secondary relationships, such as between flow and suspended sediment, can serve as a check and, when turbidity data is missing, be used to form a piecewise model (Lewis, 2002).

More than two decades ago, a U.S. Geological Survey report noted that turbidity values should not be used to determine numeric values for suspended sediment concentration (Faye et al., 1978). Since then, however, turbidity has been used successfully for measuring stream bank erosion, nutrient and contaminant transport, and sediment loads. One study of the Namoi River in New South Wales, Australia measured flow and turbidity at continuous 15 minute intervals at 12 monitoring stations for predicting sediment concentrations and loads related to stream bank erosion (Green et al., 1999). Britain's Land-Ocean Interaction Study (LOIS) included establishing site-specific relationships of suspended sediment and turbidity in ten major tributaries of the River Humber. Least-squares linear regression analyses yielded correlation coefficients between 0.827 and 0.917. The success of this relationship can be partly attributed to the favorable conditions present for turbidity monitoring, namely that fine sediment constituted 96.4 percent of the total sediment. The turbidity measurements were made in

conjunction with depth-integrated sampling. The turbidity-suspended sediment relationship was well established and provided sufficient data for estimating sediment loads and sediment flux (Wass and Leeks, 1999). The German Federal Institute of Hydrology investigated the relationship between suspended particulate matter and turbidity along the Elbe River (Pfannkuche and Schmidt, 2003). This study involved a total of 1405 measurements of turbidity, suspended particulate matter, and flow taken between June 1996 and February 2001. The measurements were adversely affected by large streambed particles and water color, and measurement error was found to increase with increasing flow. The effectiveness of turbidity as a surrogate was shown in an investigation of the Kansas River and Little Arkansas River in which twenty samples were collected at eight stream gauging stations between 1998 and 2001 (Christensen et al., 2002). The Kansas River sites yielded a coefficient of determination of 0.987 between the two parameters, and the relationship between suspended sediment and turbidity in the Little Arkansas River allowed prediction of sediment loads within six percent accuracy. Although the Kansas River was affected by a series of reservoir releases during the sampling period, the median particle size for the test sites was 95 percent fines, very favorable conditions for turbidity measurement.

Contaminated sediment can also be traced using turbidity data. The Ecuadorian Meteorological Institute investigated metal contamination in the Puyango River Basin in southern Ecuador (Tarras-Wahlberg and Lane, 2003). Forty-four samples were used to develop a calibration curve of nephelometric turbidity versus suspended solids with a coefficient of determination of 0.98. This study also included investigations of the turbidity profile that concluded the difference between near-bottom samples and surface

waters only varied from six to eight percent. Grayson et al. investigated the Latrobe River in southeast Australia for suspended sediment concentration and total phosphorous using turbidity measurements during storm events (1996). The research was motivated by the poor correlation between river discharge and suspended sediment concentration and fine sediment was presumed to be key in the transport of phosphorous. Turbidity, sediment concentration, and total phosphorous data were collected during storm events of varying intensities. Although the *in situ* turbidity sensors detected that peaks in stage and sediment concentration were sometimes out of phase, the study revealed that turbidity and sediment concentration were linearly related and that turbidity probes were effective for estimating transported material with predictive capabilities generally greater than eighty percent.

2.6 Summary

Turbidity has proven to be an effective surrogate for suspended sediment concentration measurement in some cases. When compared to isokinetic suspended sediment sampling, it is cost effective and provides accuracy that is acceptable in most situations. The relationship between turbidity and suspended sediment concentration should be established through extensive sampling in order to produce dependable calibration curves. These site-specific calibrations are the most important part of the process, and when done correctly, sediment discharge estimates can be made with considerable accuracy. The method is more effective than the relationship between discharge and suspended sediment concentration (Christensen et al., 2002; Grayson et al., 1996). Turbidity like all other surrogate measurements currently employed to predict

suspended sediment concentration has various limitations, but site-specific calibration is used in an attempt to overcome the limitations. In particular, when fine sediment constitutes a significant portion of transported sediment, turbidity offers high predictability of sediment concentration. Consequently, accuracy in turbidity measurement decreases with increasing suspended sediment grain sizes. In addition, the use of continuous turbidity monitoring suffers from translating a point measurement of turbidity to a suspended sediment discharge for the entire cross section. As a result, turbidity as a surrogate is particularly problematic in streams that have a mixture of fine and coarse sediment that changes with the size of the storm and with time during the same storm. Although turbidity does not provide absolute measures, the level of predictability that turbidity measurement affords is particularly attractive when compared to the other costly or otherwise highly inaccurate methods available if the limitations just described can be overcome.

CHAPTER III

EXPERIMENTAL METHODS

3.1 Introduction

The data for this research were provided through field sampling and subsequent laboratory analysis. Field sampling was conducted at Century Boulevard in DeKalb County, Georgia, located in metro Atlanta. The North Fork Peachtree Creek at this bridge crossing, shown in Figure 3.1, is approximately 50 feet wide with a bank-full depth of approximately 8 feet. Storm event samples were collected at this location using an automatic point sampler and a depth-integrated sampler. Sediment samples were collected at multiple locations in the immediate vicinity of the sampling equipment as well as several upstream sites. Laboratory analyses subsequent to field sampling explored the concentration of sediment in a water sample, the turbidity of the sample caused by suspended sediment particles, and the particle size distribution of sediment in the sample.

a) Sampling location shown at base flow. Image taken looking downstream.

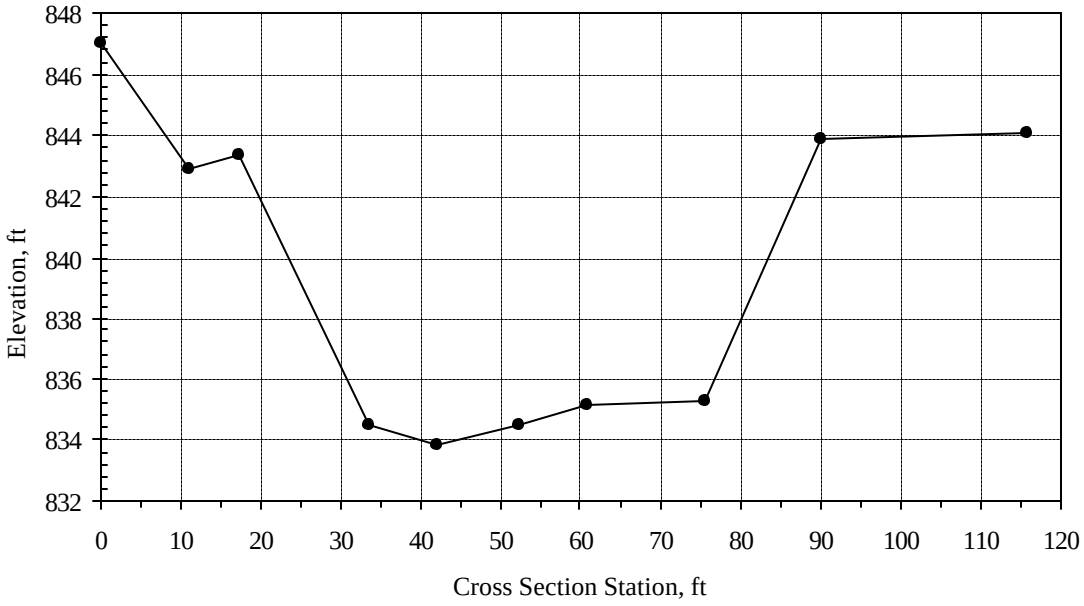

b) Surveyed cross section at sampling location looking downstream.

Figure 4.1 Sampling location: North Fork Peachtree Creek at Century Blvd.

3.2 Point Sampling

Point sampling was performed using a portable water quality sampler manufactured by Isco, Inc. (6700 series, full-size portable unit). The programmable unit, which includes a sampling pump with 24 one-liter bottles, was positioned in the floodplain. The suction line and an attached submerged strainer to withdraw water samples was located in the stream in the deepest part of the cross section on the left side looking downstream. The strainer was fixed at 1 ft above the streambed. Stage was measured directly above the strainer on the end of the suction line using an ultrasonic device attached to a bridge pier. The Isco unit continuously logged stage data at 5-minute intervals and was triggered to pump water samples by an increase in stage of 1 ft above the base level. After being activated, the sampler withdrew water samples with volumes ranging from 500-1000 mL and deposited each individual sample sequentially in one of the 24 bottles located within the sampling unit. Sampling was performed at an interval of 30 minutes and continued until the stage decreased below 1 ft or until the 24 sampling bottles were filled, providing the potential for 12 hours of sampling.

Following a storm event, the filled sample bottles were retrieved from the unit and replaced with empty bottles. An Isco 581 rapid transfer device was used to download data from the Isco unit. This information was then downloaded to a laboratory computer and written to a spreadsheet. The stage and time data were used to construct a storm hydrograph, and the time data were used to establish the timing of each sample relative to the hydrograph. The water samples subsequently underwent a variety of laboratory tests that provided information regarding the characteristics of the sediment present in the samples. In most applications, the contents of each sampling bottle were analyzed

individually; in specific cases, however, samples were combined based on their relative locations in the storm hydrograph to provide fewer samples of larger volumes.

3.3 Depth-Integrated Sampling

Depth-integrated isokinetic sampling was used to acquire water samples representative of the entire stream cross section. A US D-77 depth-integrating suspended sediment sampler was utilized for collecting such samples. The sampler was equipped with a 5/16-inch intake nozzle attached to a 3-liter sampling bottle. The sampler was deployed into North Fork Peachtree Creek from the Century Boulevard bridge crossing. This was accomplished using a specially designed apparatus constructed in the Georgia Tech hydraulics laboratory, which used a telescoping boom and winch attached to a service vehicle truck ladder rack. The selected sampling scheme involved collecting depth-integrated samples at equally spaced stream verticals in the cross section. Stations at 10-ft intervals, beginning at 10 ft from left bank, were established and marked on the concrete bridge railing. This scheme provided five equal increments and the sampler was deployed at each of the four verticals that separated the respective increments. The same transit velocity was used for all verticals and was kept uniform within each vertical. This method allowed the sample volume to be determined only by the stream velocity and the corresponding depth at each vertical. A separate sampler bottle was used at each vertical, and the representative samples resulted from combining the partial samples collected at each vertical.

3.4 Soil Sample Collection

Soil samples were taken at several upstream locations. Stream banks experiencing active erosion were first identified. Then a sample was taken above the elevation of the base flow water surface at each location. The samples were approximately 150 g in mass and were taken to the laboratory in individual resealable plastic bags. Photographs of each location were also taken to aid in identifying each sample.

3.5 Suspended Sediment Concentration (SSC) Measurement

Suspended sediment concentration (SSC) analyses were performed in accordance with standard test method ASTM D 3977-97 Test Method B. The procedure consisted of measuring the volume of the sample, and then filtering the entire sample through a glass-fiber filtration disk. The sample volume was measured by agitating the sample and transferring it to a 1000 mL graduated cylinder. The sample was then filtered through a Whatman type 934-AH glass-fiber disk with 1.5 µm pore spaces and a diameter of 22 mm. Filtration was assisted by a vacuum system. After the entire sediment-water sample was filtered through the filtration disk, the disk and remaining sediment were oven-dried and then weighed. Calculation of suspended sediment concentration of the sample in mg/L was accomplished using the measured volume of the sample and the dry mass of sediment obtained from the measured weights of the filtration disk before and after filtration.

3.6 Percent Fine Sediment Measurement

The process of measuring percent fine sediment is identical to the above procedure for measuring suspended sediment concentration with an additional step. After measuring the volume of the sample, the sample was passed through an ASTM standard number 230 sieve (63 µm mesh openings) and collected in a container beneath the sieve. The sediment remaining on the sieve was thoroughly rinsed and the rinse water was also collected in the underlying container. The remaining coarse sediment was then rinsed from the sieve into a separate container. Both containers were then filtered through separate glass-fiber disks. This enabled calculation of fines-only SSC and total SSC, both in mg/L.

3.7 Turbidity Measurement

Turbidity was measured using an HF Scientific, Inc. Micro 100 laboratory turbidimeter equipped with a pour-through apparatus that enables turbidity measurement of a water sample of any volume. When storm event samples were measured for turbidity, their concentration was scrupulously maintained by not adding any rinse water when transferring between containers. The sample was thoroughly agitated before and during the process of pouring into the turbidimeter receptacle. The turbidity value was recorded after the turbidimeter reading stabilized.

For specific cases, the turbidity of a sample was measured after the coarse sediment had been removed. This was accomplished by pouring the entire sample through an ASTM standard number 230 sieve (63 µm mesh openings) and collecting the resulting mixture of

water and fine sediment. This mixture was then poured through the turbidimeter and the value was recorded.

3.8 Particle Size Analysis

Particle size analysis was conducted in accordance with standard test method ASTM D 422-63. For storm event samples and bed sediment control samples, only the sieve analysis portion of the test was performed. For several control samples conducted with upstream soil samples, hydrometer analysis was also performed to provide a more exact and complete grain size distribution.

Sieve Analysis

Sieve analysis was performed on various sediment samples. The test requires a dry sediment sample of a known weight and a nest of sieves that encompass the range of sediment sizes in the sample. The weight of each sieve is measured and recorded before stacking the sieves in ascending order of size. The entire sediment sample is then poured into the top of the nest, the lid and pan are secured, and the nest is placed in a shaking device that jars and agitates the sieves for a length of time. Following shaking, each sieve is weighed so that the weight of sediment retained on each sieve can be determined. This data can then be plotted to provide information regarding the distribution of sediment sizes within the sample, and it leads to calculation of important sediment transport variables such as median grain size.

Hydrometer Analysis

Hydrometer analyses were performed using an ASTM 152H hydrometer conforming to the requirements enumerated in Specifications E 100. A dispersing-agent

solution of sodium hexametaphosphate and distilled water was used to minimize the presence of interparticle bonds during the hydrometer analysis. After the sample was prepared in the 1000 mL sedimentation cylinder, the hydrometer was placed in the sample and readings were taken at time intervals of 2, 5, 15, 30, 60, 250, and 1440 minutes.

CHAPTER IV

RESULTS AND ANALYSIS

4.1 Introduction

The data displayed and discussed in this section were collected from October 2003 through June 2004. During this time, point sampling was accomplished automatically during notable storm events, multiple sediment samples were taken from the stream bed and banks, and equipment for conducting depth-integrated sampling was designed, fabricated, and tested. Depth-integrated sampling is scheduled for the summer months of 2004, during which time frontal thunderstorms that contribute significant stage increase are prevalent in the Atlanta metro area.

4.2 Point Sampling

Point sampling using the Isco sampler produced a field record of automatically sampled point measurements of suspended sediment concentration. Storm events of varying intensities were sampled to provide an understanding of the sediment transport response of the stream in a variety of flow conditions. Figure 4.1 shows results from the two types of analyses of the point samples. Figure 4.1 a) displays the placement of individual suspended sediment concentration (SSC) data points on the stage hydrograph collected during a storm event of medium intensity on January 5, 2004. In contrast, Figure 4.1 b) shows a longer duration storm event on February 26, 2004 that has relatively low intensity and SSC data points that represent several sample bottles grouped together and located on the hydrograph time scale based on the average of their respective sampling times. The maximum value of SSC is nearly 1500 mg/L for the

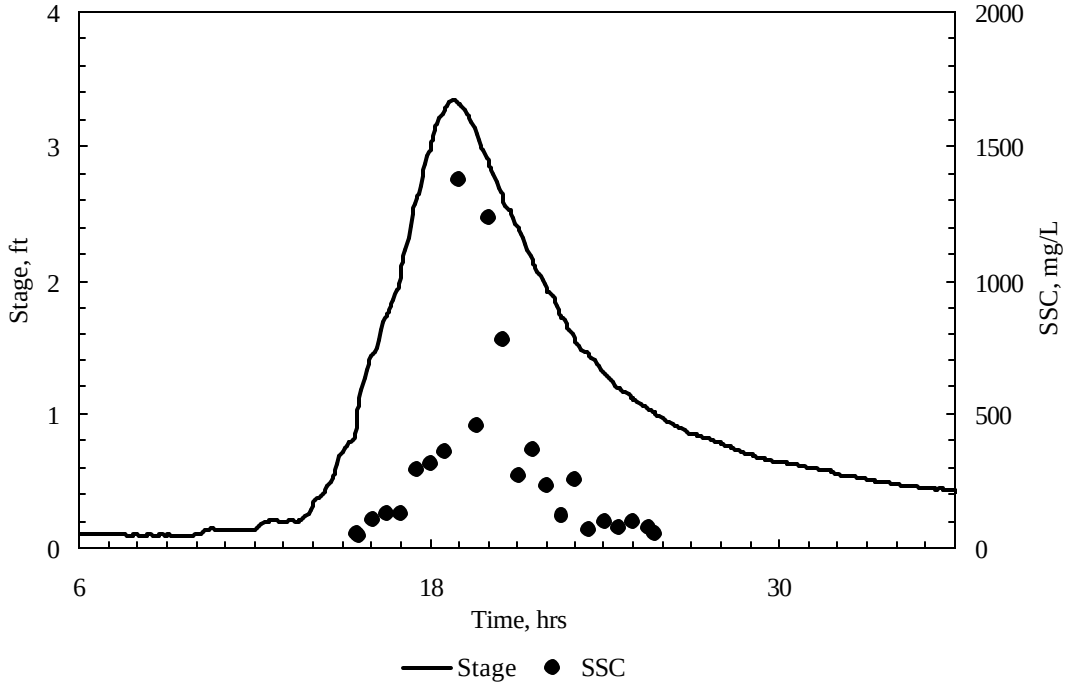

a) Stage hydrograph and SSC for 1/05/04 storm event

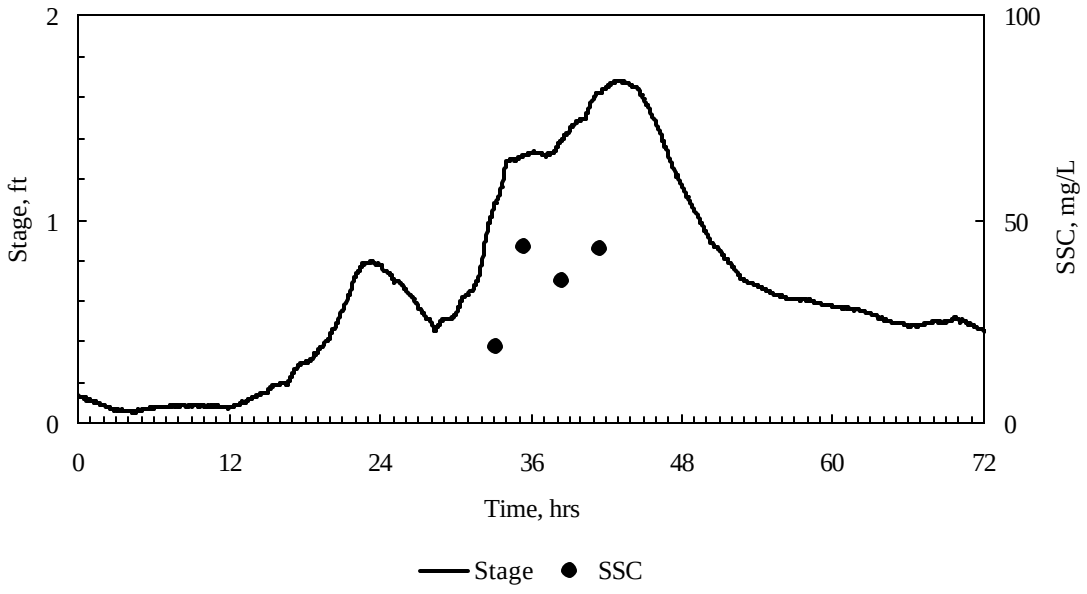

b) Stage hydrograph and grouped SSC for 2/26/04 storm event

Figure 4.1 Point sampling data for storms of varying intensities

medium-intensity storm of Figure 4.1 a), but for the minor storm of Figure 4.1 b) the values of SSC are only of the order of 100 mg/L. Bankfull stage is approximately 8 ft, so neither of these storms is very large in magnitude by comparison. The entire field record of point sampling sinceOctober 2003 is included in the Appendix.

Sediment Rating Curves

Sediment transport data are often used to produce site-specific sediment rating curves that define the relationship between stage or discharge and SSC at a sampling location. However, due to the extreme variability in stage hydrograph response to storm events and the overall flashy nature of urban streams, the sediment rating curve, shown in Figure 4.2 a), revealed that a very poor relationship exists between stage and total SSC. A sediment rating curve relating stage and SSC of fine sediment, shown in Figure 4.2 b), also produced a weak relationship. The absence of a strong relationship in either case highlights the difficulty in quantifying sediment loads through point sampling and the high degree of temporal variability of sediment concentration that occurs in urban streams.

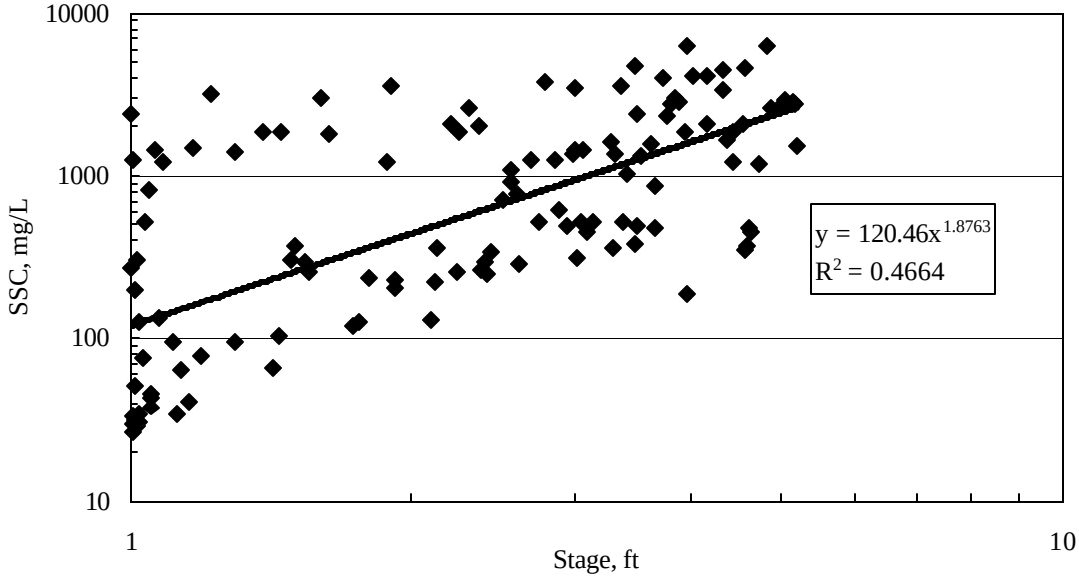

a) Log-log plot of stage and SSC data

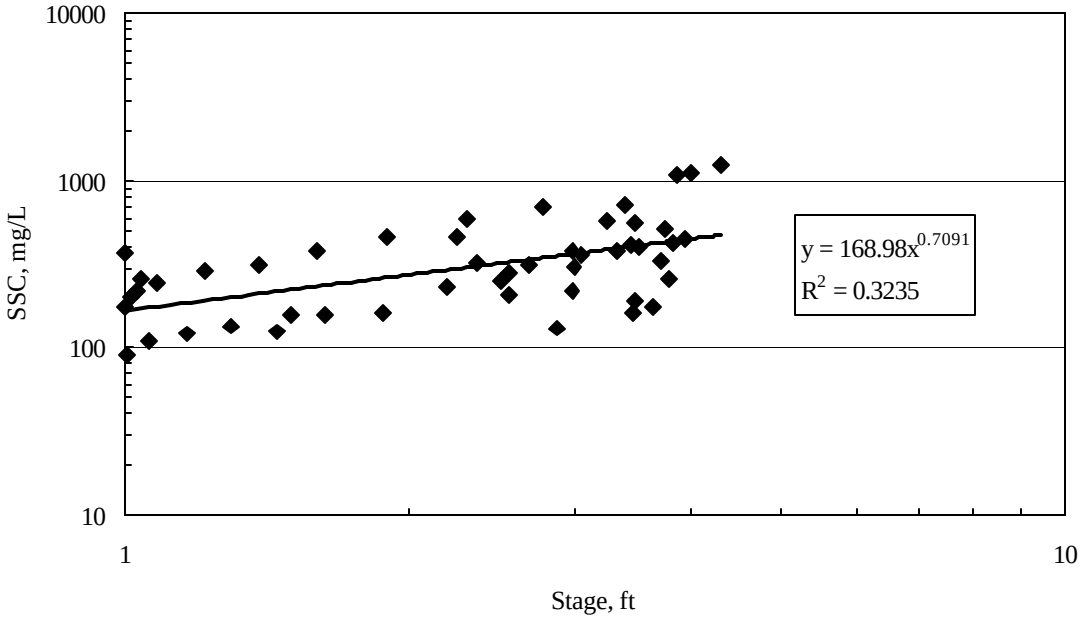

b) Log-log plot of stage and fines-only SSC data

Figure 4.2 Logarithmic plots of paired stage and SSC data

Turbidity

The point samples from several storm events were analyzed for percent fines and the turbidity of the fine sediment only. This provided a graphical relationship between fine SSC and turbidity, as shown in Figure 4.3. This favorable relationship ($R^2 = 0.976$) indicates the strong correlation that exists between fine SSC and turbidity at the sampling location.

Grain Size Distribution

Sieve analysis was performed on point samples from selected storm events to provide insight into the range of sediment sizes in transport at the sampling location. A representative sample is shown in Figure 4.4 as a cumulative distribution plotted in lognormal form.

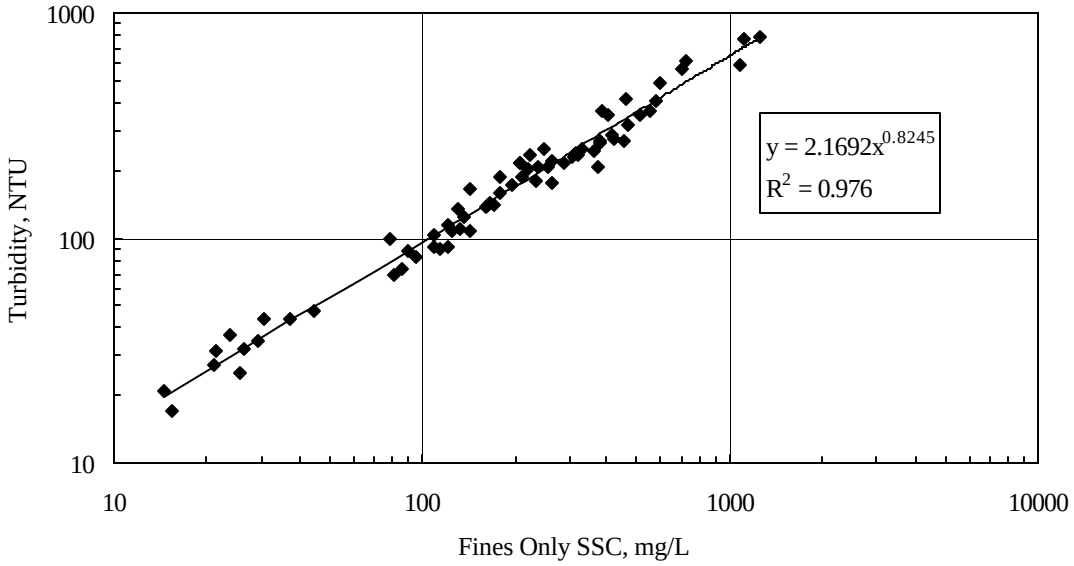

Figure 4.3 Log-log plot of fine SSC and turbidity for multiple storm events

Figure 4.4 Grain size distribution of sediment from storm event on 2/03/04.

4.3 Sediment Samples

Sediment samples were collected from several sites in the vicinity of the sampling location and at a site approximately one mile upstream where severe bank erosion is actively occurring and presumably contributes significantly to the suspended sediment transported through the sampling location.

Stream Bed Samples

The stream bed was sampled in several locations adjacent to and upstream of the automatic sampler intake nozzle so that the bed sediment could be compared with the sediment collected by the sampler during a storm event. The storm event chosen for comparison was the largest event that occurred during the sampling period and which

provided the most sediment in the point samples. This comparison, shown in Figure 4.5, reveals that although the two sediment samples are very similar, the sediment collected by the automatic sampler contains a larger percentage of fine sediment than the bed material. The median grain size of the automatically sampled sediment is approximately 60 µm smaller than the bed material. It is important to note, however, that the point samples from most storm events do not include enough sediment to perform a grain size analysis. In particular, smaller storm events include very high percentages of fine sediment. However, even samples from the selected event, which included the full range of grain sizes present in the stream, revealed the difference between the point samples and bed samples. The difference in median grain size can partially be explained by the bed armoring that occurs during high flows, along with the presence of large particles included in the bed material that are too heavy to be suspended from the bed and transported during most storm events. The difference in percent of fine sediment, however, represents additional sources of sediment that contribute to the sediment load but do not originate in the stream bed. The task of identifying these additional sources led to intensive sampling of the stream banks in areas where active erosion could be visually identified. As in bed sampling, bank samples were also taken in the immediate vicinity of the automatic sampler so that the effects of nearby sediment could also be identified.

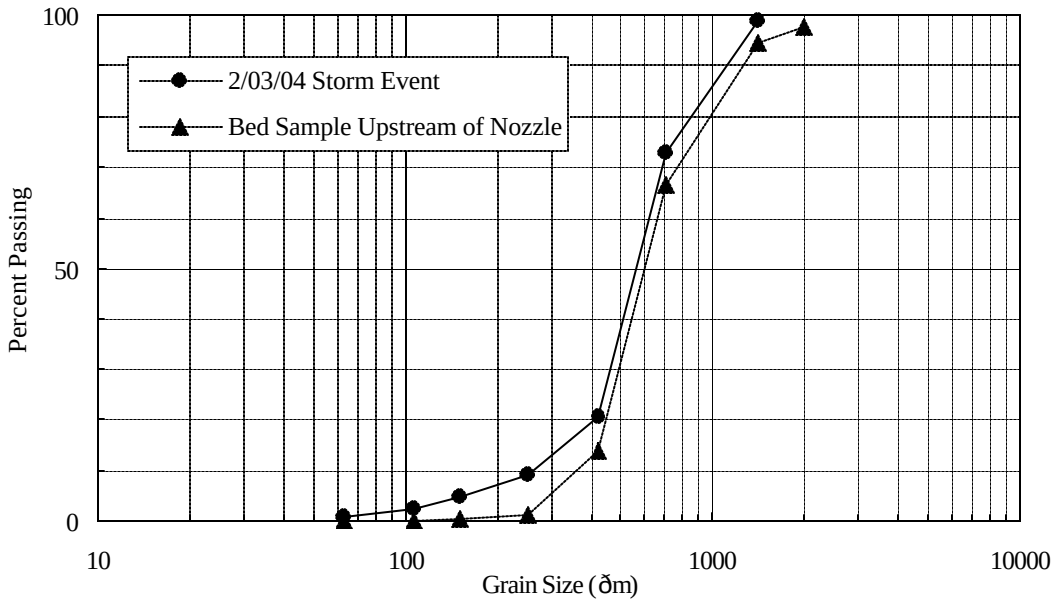

Figure 4.5 Comparison of bed sample with automatically sampled sediment

Stream Bank Samples

The stream banks were sampled approximately 100 ft upstream of the sampling site where native sediments unrelated to construction of the Century Blvd. bridge were found. The stream banks in this vicinity are stable due to the heavy vegetation in the floodplain and on the crest of the banks. However, significant bank erosion was identified approximately one mile upstream of the sampling site in a stream reach, shown in Figure 4.6, where the stream meanders sharply from its westward flow direction to a southwesterly direction. The banks in this area are vertical and are approximately 8-10 ft in height. The floodplain has been reduced in size due to the receding bank. The remains of the floodplain are perched atop the steep banks and consist of residential lawn area. The stream bed is heavily armored in this region and several deadfalls in the form of logs,

tires, and other urban litter contribute to the significant bank scouring that takes place during each event.

Figure 4.6 Bank erosion approximately one mile upstream of sampling site

4.4 Turbidity and Fine Sediment

The relationship between suspended sediment concentration of fine sediment and the turbidity it produces is a parameter measured for all sediments sampled. The record of storm event samples provides a strong relationship between fine sediment concentration and turbidity, and the bed and bank samples were used to create suspensions for which turbidity and SSC fines could be measured and correlated. This was accomplished by removing all of the coarse sediment from each sample and then using the remaining fine sediment for turbidity measurement as described previously in

Chapter III. Comparing all of the soil types sampled as shown in Figure 4.7 and Table 4.1 indicates that each sample exhibits a unique relationship between SSC fines and turbidity that can serve as the signature or fingerprint of the sediment at that location.

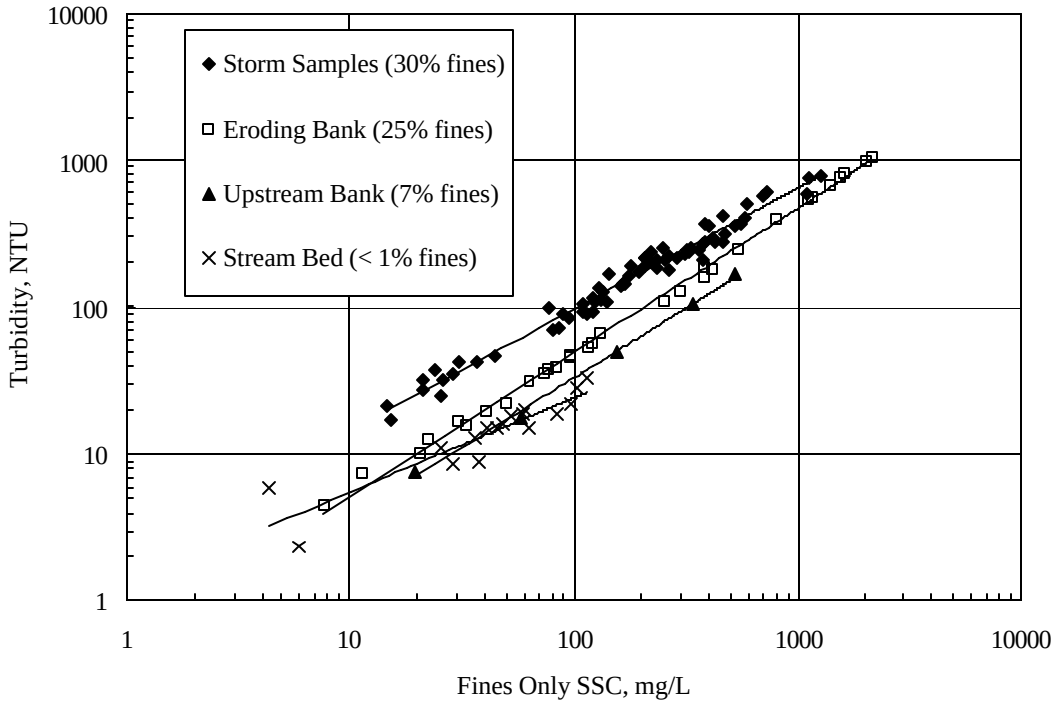

Figure 4.7 Comparison of turbidity signatures of sediment samples

Table 4.1 Comparison of turbidity signatures of sediment samples

Type of Sample	*Percent Fines*	*Regression Equation*	R^2
Storm Samples	30%	$NTU = 2.146(SSC)^{0.8251}$	0.9711
Eroding Bank	25%	$NTU = 0.545(SSC)^{0.9785}$	0.9974
Upstream Bank	7%	$NTU = 0.42(SSC)^{0.948}$	0.9972
Stream Bed	< 1%	$NTU = 1.279(SSC)^{0.6387}$	0.832

The initial motivation for exploring the relationship between SSC fines and turbidity was the attempt to locate the relative contributions of bed and bank sediment to the sediment found in the automatic sampler. Comparing the turbidity fingerprint of the fine sediment contained in the storm samples with that of the fine sediment sampled from the stream bed in Figure 4.7 shows that the two sediments are very dissimilar and thus proves that the bed sediment only constitutes a negligible fraction of the fine sediment in the automatic samples. Yet, as Figure 4.7 demonstrates, none of the bank samples match exactly the fine sediment found in the automatic samples. However, the eroding bank sediment is most similar, particularly in the upper portion of the relationship. The similarity between the automatically sampled sediment and the eroding bank sediment is indicative of eroding banks in the upstream channel contributing to the suspended sediment load.

The correlation between the percent of fine sediment in a sediment sample and the turbidity that it contributes is a separate relationship that was examined. Comparison of the sediment samples in Figure 4.7 and Table 4.1 indicates that the turbidity of a sample is highly dependent upon the percent of fine sediment that the entire sediment sample contains. Regression of each data set in Figure 4.7 reveals that an increasing percentage of fine sediment in a total sediment sample corresponds to increasing turbidity for a given fine sediment concentration created from that sediment. Said in a different way, a sediment with a high percentage of fine sediment in the total sample contributes more turbidity for a given fine sediment concentration than does the same concentration created using a sediment with a lesser percentage of fine sediment. The samples shown

in Figure 4.7 include their respective percent fines shown as an average value of all samples collected at a given location.

The increasing turbidity at a given fines concentration with increasing percent of fine sediment is related to the median grain size of the sample. An increasing percentage of fine sediment correlates to a decreasing median grain size for the entire sample. Additionally, the median grain size of the fine sediment in the sample that remains after removing the coarse sediment decreases as.the median grain size of the entire sample decreases. Furthermore, the median grain size of a sediment is related to the number of individual sediment particles that constitute a measured weight of that sediment. And, since turbidity measures the attenuation or scattering of light through liquid, and because many very small particles contribute more turbidity than a few large particles, sediment with a relatively small median grain size contributes more turbidity for a given concentration than does a sediment with a larger median grain size.

This principle may also explain the discrepancy between turbidity signatures of the record of storm samples and the eroding bank samples. Because the percent fines of the storm samples is higher than the bank samples, the turbidity signature should be different. However, this does not mean that the eroding bank sediment is not the main source of fine sediment found in the storm samples. Once the sediment is scoured from the stream banks upstream, it is subject to the sediment transport capabilities of the stream reach. The stream velocity during storm flows is not sufficient to maintain the entire range of grain sizes in suspension, and the sediment transport capacity of the stream reach requires that deposition of some of this sediment occurs. And since the eroded sediment must travel a significant distance before it reaches the sampling location,

much of the coarser sediment particles are deposited and do not reach the sampling location. When the automatic sampler withdraws water from the stream, the fine sediment it collects includes very fine sediment particles from the eroding bank, and the coarse sediment consists mostly of coarse sand particles from the stream bed. In addition, Figure 4.7 shows that the turbidity signature of the storm samples and the turbidity signature of the eroding bank samples grow more similar with higher concentrations. The upper end of the relationship represents large storm events in which most of the sediment eroded upstream reached the sampling location without a larger percentage settling.

4.5 Turbidity and SSC

Although the relationship between turbidity and suspended fine sediment is well established, the need for accurate sediment discharge measurement requires that the entire range of sediment sizes be accounted for. Furthermore, when turbidity is used as a surrogate for monitoring suspended sediment transport, the relationship between turbidity and SSC must be established. As discussed in Chapter II, however, the relationship between turbidity and SSC includes error that in some cases can preclude the use of turbidity as an accurate surrogate measurement.

Previous research performed in 1999 at the sampling location provided a record of automatically sampled storm event samples that were measured for total suspended solids and turbidity using the same laboratory equipment as described in Chapter III. As discussed in Chapter II, measurement of total suspended solids, or TSS, involves removing a subsample from the total sample and measuring its characteristics under the

assumption that it is representative of the entire sample. The relationship between TSS and turbidity is shown in Figure 4.8, along with the relationship between fine SSC and turbidity at the sampling location obtained in the present study. At low sediment concentrations, the two data sets are very similar and actually overlap. This region represents data that were collected at low stages where coarse sediment was absent or minimal in the storm samples. At high sediment concentrations, however, the two relationships diverge. This region represents large storm events during which coarse sediment is suspended and is highly concentrated in the storm samples. Additionally, the difference in the two relationships represents the effects of the coarse sediment on turbidity measurement.

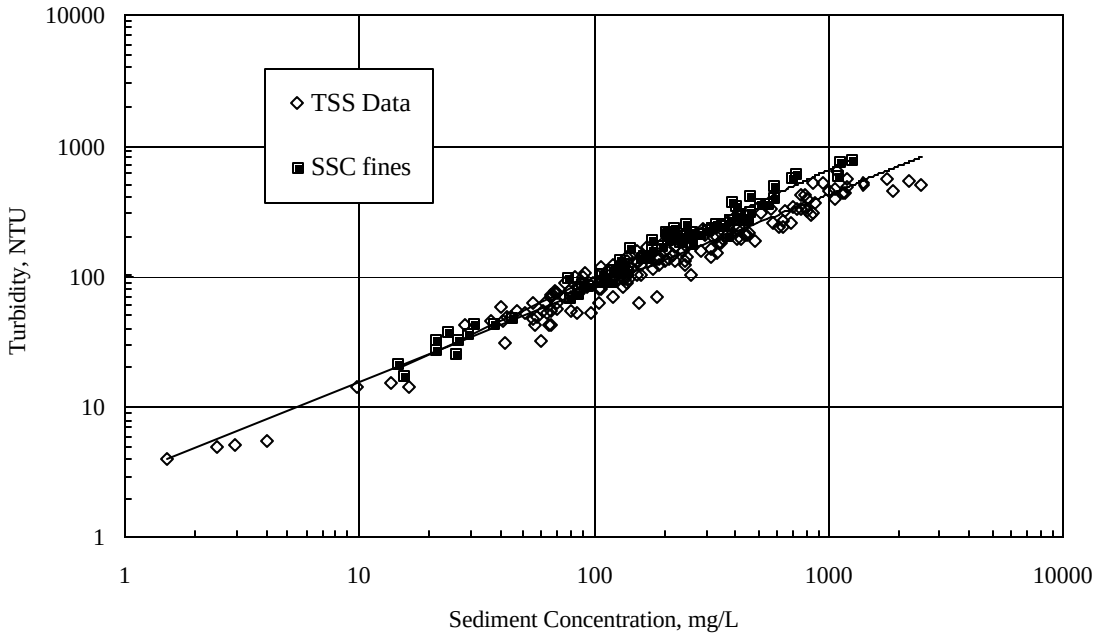

Figure 4.8 Comparison of fine SSC and TSS data.

Data from the sediment samples collected at the eroding upstream bank also show the effects of coarse sediment on turbidity measurement. Figure 4.9 shows the relationship between turbidity and total SSC obtained from the total sample, turbidity and fine SSC measured separately for the separated fine fraction, and a third data set representing the turbidity caused by each total SSC measurement multiplied by the percent fine sediment in the total sample. The third data set does not represent separate measured values, but multiplying total SSC by the percent fine sediment in the sample is a way to isolate the effects of the coarse sediment on turbidity measurement of the entire sample. Figure 4.9 then shows that the amount of additional turbidity contributed by the coarse sediment is small.

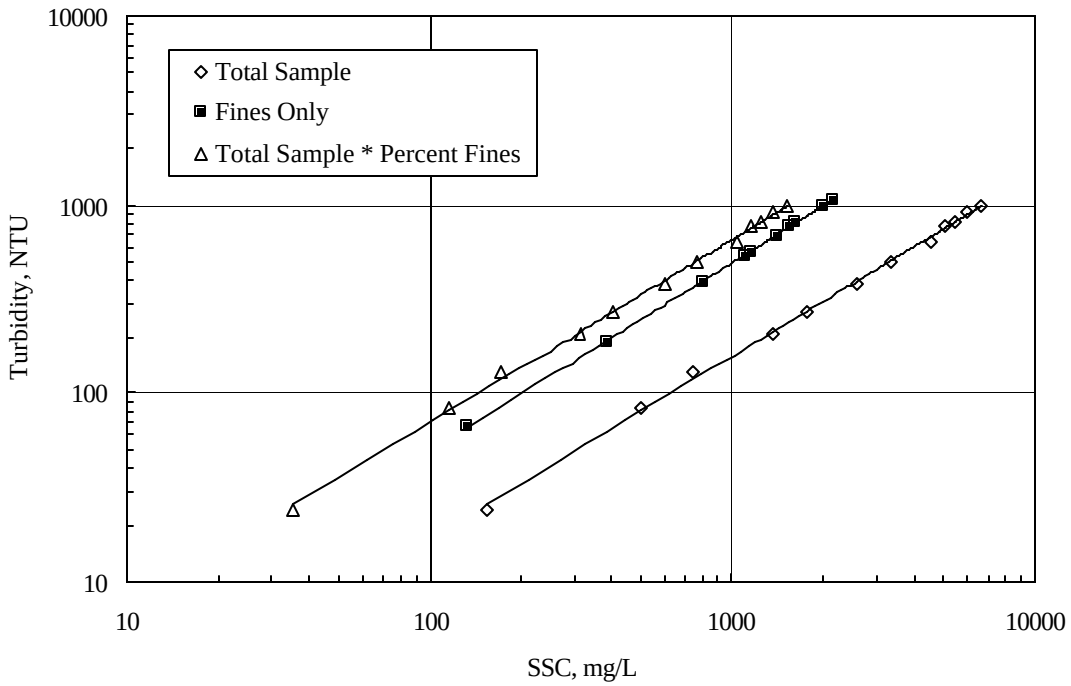

Figure 4.9 Effects of grain size on turbidity measurement.

4.6 Depth-Integrated Sampling

The depth-integrated sampling scheduled for the summer months of 2004 will provide insight into the spatial distribution of sediment in the sampling location stream cross section. This data will be coupled with the point measurements of SSC collected by the automatic sampler to determine the relationship between the point measurements and the concentration of sediment in the entire cross section. The point measurement of SSC will also be coupled with the Rouse suspended sediment distribution calculations (Sturm, 2001) for the coarse sediment fraction along with the shear stress distribution to obtain discharge of the coarse fraction.

4.7 Summary

By combining automated point sampling and depth-integrated sampling, a more accurate method for predicting coarse sediment loads will be developed as discussed above. In addition, a methodology will be developed that takes advantage of the strong correlation that exists between turbidity and fine SSC for predicting transport of fine sediment, including their sources and sinks. Since fine SSC determined from turbidity measurements can be assumed uniform over the entire cross section, measurement of both fine and coarse sediment can be accomplished at different times during the storm as the proportion of fine and coarse sediment changes. This approach will provide a more accurate method for establishing sediment TMDLs in urban streams but will not be limited by sediment size or sampler location as are feasible current methods. As a result, many of the limitations involved in measuring and enforcing sediment TMDLs will be overcome.

CHAPTER V

CONCLUSIONS

The effects of urbanization on urban streams are well documented and the quality of these streams has come under scrutiny by numerous government agencies in recent years. Of major importance in assessing and improving the quality of such streams is a thorough understanding of its sediment transport characteristics, including sediment sources and accurate quantification of sediment loads. The Total Maximum Daily Load (TMDL) program seeks to accomplish these tasks but suffers from lack of accurate, feasible data collection methods.

5.1 Project Summary

This study has employed existing technology to address many of the longstanding problems with collecting sediment transport data in an effort to develop a new methodology for gathering accurate and inexpensive data for establishing and maintaining sediment TMDLs.

Automated point sampling has provided a field record of point measurements of suspended sediment concentration (SSC). This sampling has shown that a strong relationship exists between SSC of the fine fraction of the sediment and turbidity at the sampling location (R^2 = 0.976). These point samples have also been coupled with intensive sampling of the stream bed and banks for comparing grain size distributions and turbidity characteristics. This has provided insight into the effects of sediment sizes on turbidity measurement and is being used to develop a method of identifying and

quantifying suspended fine sediment. This methodology will also be useful in tracking sediment sources and increasing accountability for developers to employ effective erosion control measures. The outcome of the this work will be particularly beneficial in applications where fine sediment impairment is a concern due to its contribution to the transport of attached contaminants, silting of spawning areas, and inhibition of photosynthesis and aesthetic quality.

5.2 Continuing Research

Depth-integrated sampling is currently being performed and will provide suspended sediment concentration data for the entire stream cross section at the sampling location. The depth-integrated sampling data will also be combined with field record of point measurements of SSC, calculation of the Rouse distribution of suspended sediment, and calculation of shear stress distribution for correlating point measurements with the cross sectional distribution of suspended sediment.

5.2 Expected Research Outcomes

Combining point sampling and depth-integrated sampling will yield a more accurate method for predicting coarse sediment loads. In addition, a methodology that takes advantage of the strong correlation that exists between turbidity and fine SSC for predicting transport of fine sediment, including their sources and sinks, will be developed. These two related research goals will produce a method that will capable of measuring both fine and coarse sediment at different times during storm events. Temporal changes in sediment transport present a major hurdle that can be overcome by

measuring both fine and coarse sediment as the proportion of fine and coarse sediment changes during a storm hydrograph. This approach will provide a more accurate method for establishing sediment TMDLs in urban streams but will not be limited by sediment size or sampler location as are current methods. As a result, many of the limitations involved in measuring and enforcing sediment TMDLs will be overcome.

LIST OF REFERENCES

Agrawal, Y.C., and Pottsmith, H.C. (2002). "New isokinetic version of LISST technology targets needs of the Federal Subcommittee on Sedimentation." *Proc. Turbidity and Other Sediment Surrogates Workshop*, Reno, Nevada.

ASTM (American Society for Testing and Materials) (2000). "Standard test methods for determining sediment concentration values in water samples," D 3977-97, Vol. 11.02, Water (II), 395-400.

ASTM (American Society for Testing and Materials) (2000). "Standard test method for particle-size analysis of soils." D 422-63

Brasington, J., and Richards, K. (2000). "Turbidity and suspended sediment dynamics in the Nepal Middle Hills." *Hydrological Processes*, Vol. 14, pp. 1448-1463.

Christensen, V.G., Rasmussen, P.P., Ziegler, A.C. (2002). "Comparison of estimated sediment loads using continuous turbidity measurements and regression analysis." *Proc. Turbidity and Other Sediment Surrogates Workshop*, Reno, Nevada.

Faye, R. E., Carey, W. P., Stamer, J. K., and Kleckner, R. L. (1980). "Erosion, sediment discharge, and channel morphology in the upper Chattahoochee river basin, Georgia." Geological Survey *Professional Paper* 1107, U. S. Govt. Printing Office, Washington, D.C.

Gartner, J.W. (2002). "Estimation of suspended solids concentrations based on acoustic backscatter intensity: theoretical background." *Proc. Turbidity and Other Sediment Surrogates Workshop*, Reno, Nevada.

Gippel, C.J. (1995). "Potential of turbidity monitoring for measuring the transport of suspended solids in streams." *Hydrological Processes*, Vol. 9, pp. 83-97.

Gray, J. R., Glysson, G. D., Turcios, L. M., and Schwarz, G. E. (2000). "Comparability of suspended-sediment concentration and total suspended solids data." *Water Resources Investigation Report* 00-4191, Reston, Virginia

Gray, J. R. (2002). "The need for surrogate technologies to monitor fluvial-sediment transport." *Proc. Turbidity and Other Sediment Surrogates Workshop*, Reno, Nevada.

Grayson, R.B., Finlayson, B.L., Gippel, C.J., and Hart, B.T. (1996). "The potential of field turbidity measurements for the computation of total phosphorous and suspended solids loads." *Journal of Environmental Management*, Vol. 47, pp. 257-267.

Green, T.R., Beavis, S.G., Dietrich, C.R., and Jakeman, A.J. (1999). "Relating stream-bank erosion to in-stream transport of suspended sediment." *Hydrological Processes*, Vol. 13, pp. 777-787.

Horowitz, A.J., Rinella, F.A., Lamothe, P., Miller, T.L., Edwards, T.K., Roche, R.L., and Rickert, D.A. (1990). "Variations in suspended sediment and associated trace element concentrations in selected riverine cross sections." *Environmental Science Technology*, Vol. 24, pp. 1313-1320.

Horowitz, A.J. (2002). "The use of rating curves to predict suspended sediment concentration: A matter of temporal resolution." *Proc. Turbidity and Other Sediment Surrogates Workshop*, Reno, Nevada.

Lewis, J. (2002). "Estimation of suspended sediment flux in streams using continuous turbidity and flow data coupled with laboratory concentrations." *Proc. Turbidity and Other Sediment Surrogates Workshop*, Reno, Nevada.

Melis, T.S., Topping, D.J., Rubin, D.M. (2002). "Testing laser-based sensor for continuous in-situ monitoring of suspended sediment in the Colorado River, Grand Canyon, Arizona." *Proc. Turbidity and Other Sediment Surrogates Workshop*, Reno, Nevada.

Pfannkuche, J. and Schmidt, A. (2003). "Determination of suspended particulate matter concentration from turbidity measurements: particle size effects and calibration procedures." *Hydrological Processes*, Vol. 17, pp. 1951-1963.

Sturm, T.W. (2001). *Open Channel Hydraulics.* Textbook Series in Water Resources and Environmental Engineering, McGraw-Hill, New York.

Tarras-Wahlberg, N.H., and Lane, S.N. (2003). "Suspended sediment yield and metal contamination in a river catchment affected by El Nino events and gold mining activities: the Puyango river basin, southern Ecuador." *Hydrological Processes*, Vol. 17, pp. 3101-3123.

Wass, P.D., and Leeks, G.J.L. (1999). "Suspended sediment fluxes in the Humber catchment, UK." *Hydrological Processes*, Vol. 13, pp. 935-953.

Weber, D. (2000). *Relative Contribution of Sediment from Upland and Channel Erosion*, M.S. Thesis, School of Civil and Environmental Engineering, Georgia Tech, Atlanta, GA.

Weigel, J.F. (1984). "Turbidity and suspended sediment in the Jordan River, Salt Lake County, Utah." *Water-Resources Investigations Report 84-4019*.

APPENDIX

FIELD RECORD OF STORM EVENT POINT SAMPLING

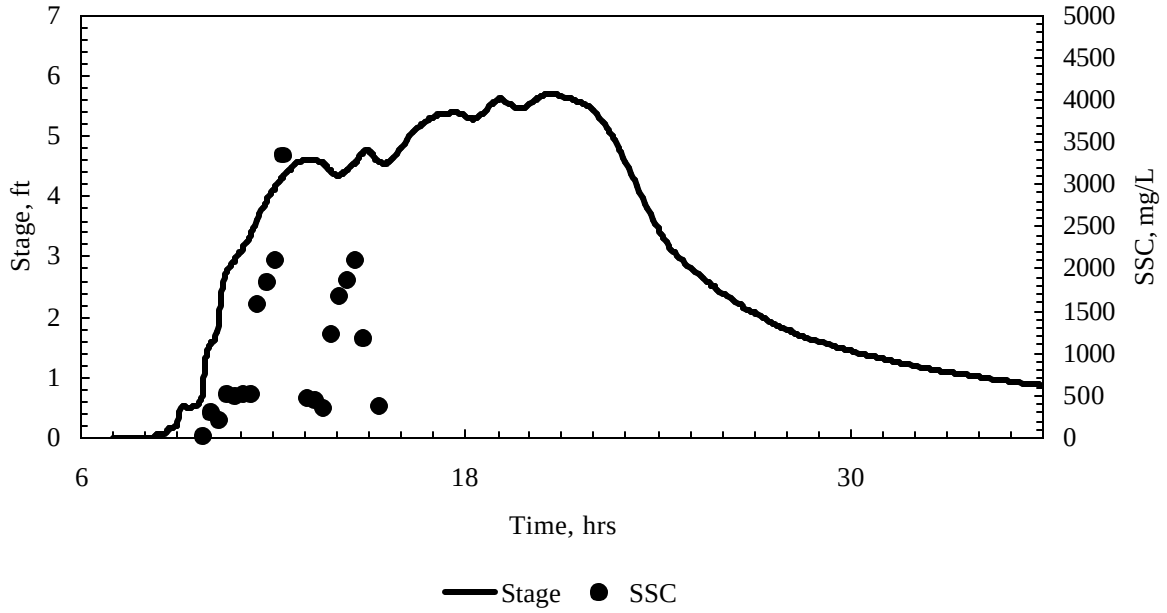

Hydrograph and SSC from 10/26/03 storm event

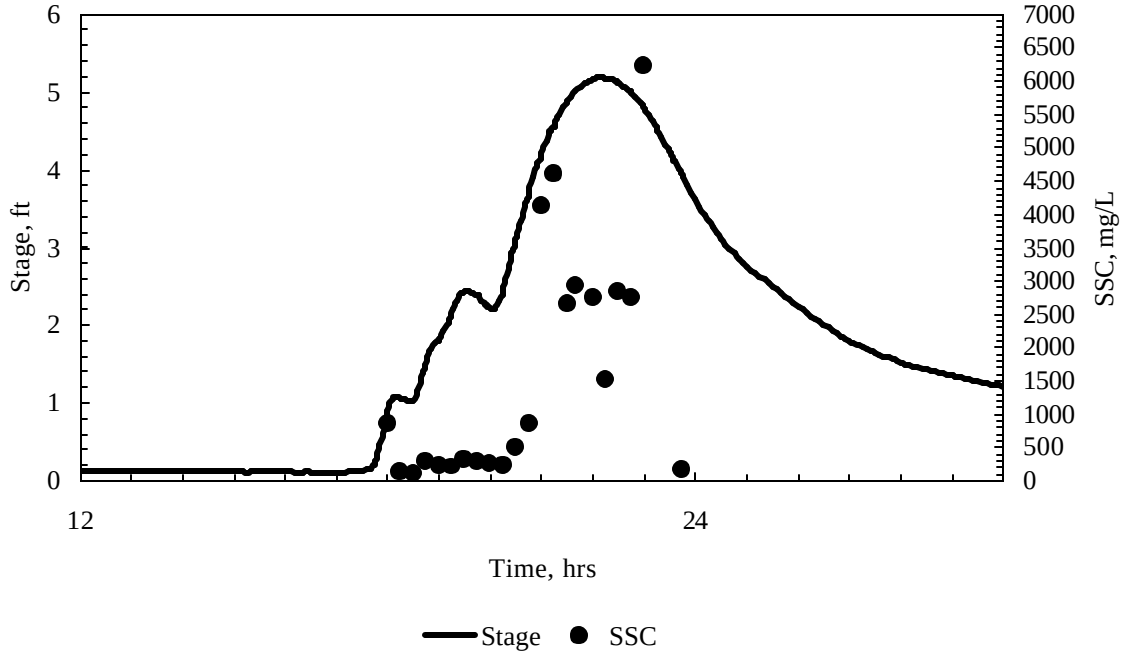

Hydrograph and SSC from 11/05/03 storm event

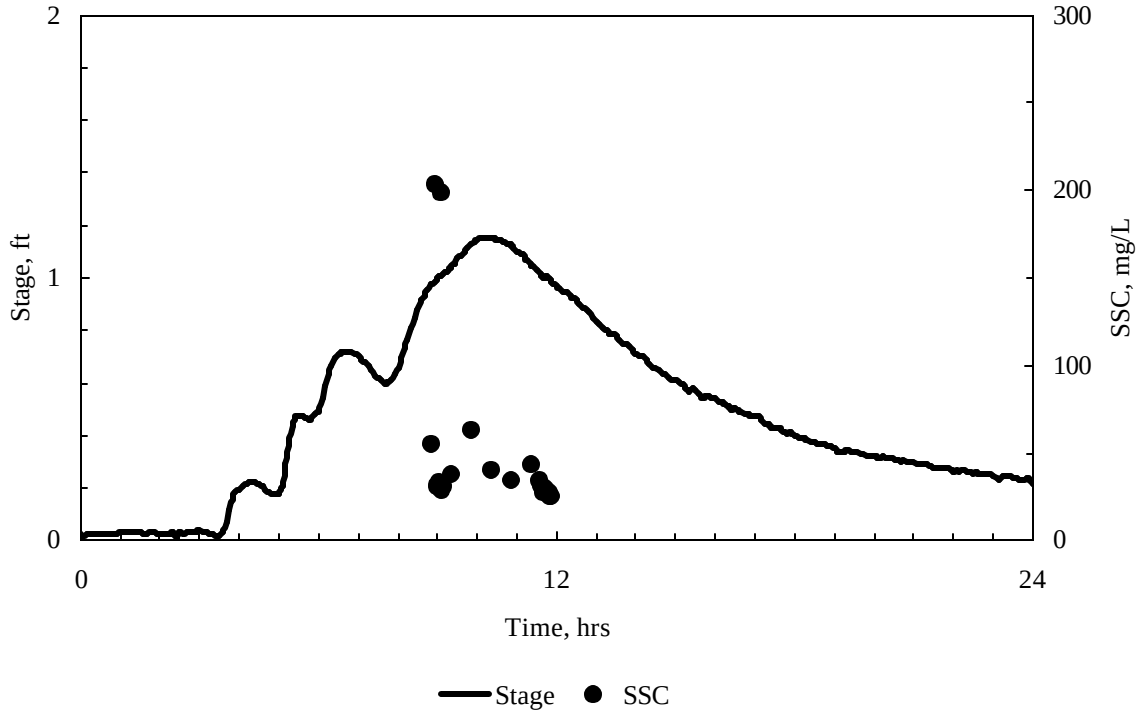

Hydrograph and SSC from 11/17/03 storm event

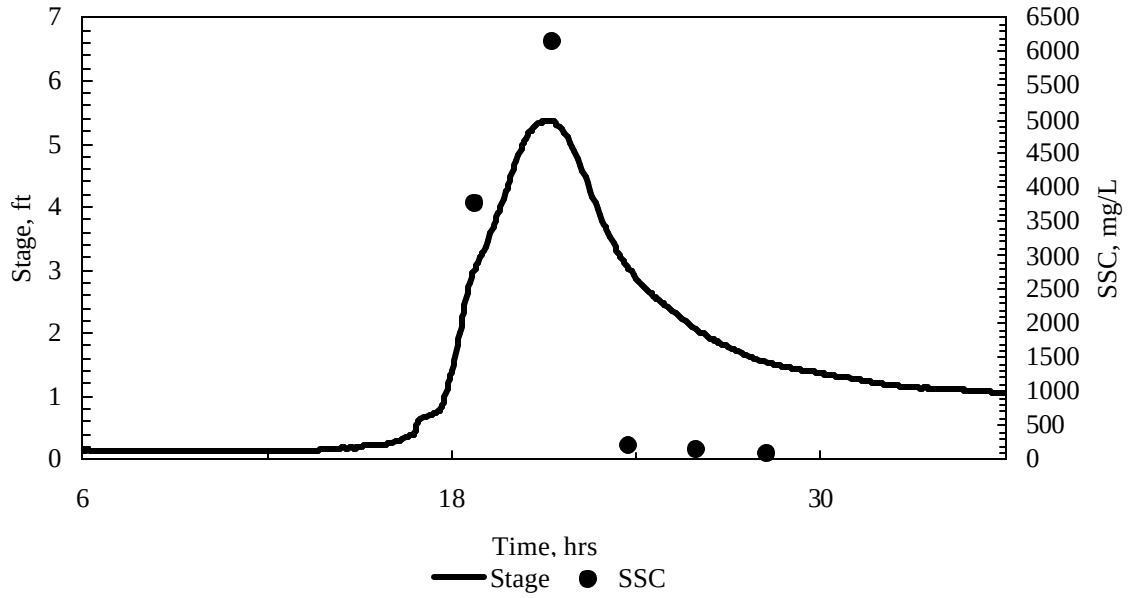

Hydrograph and grouped SSC from 2/03/04 storm event

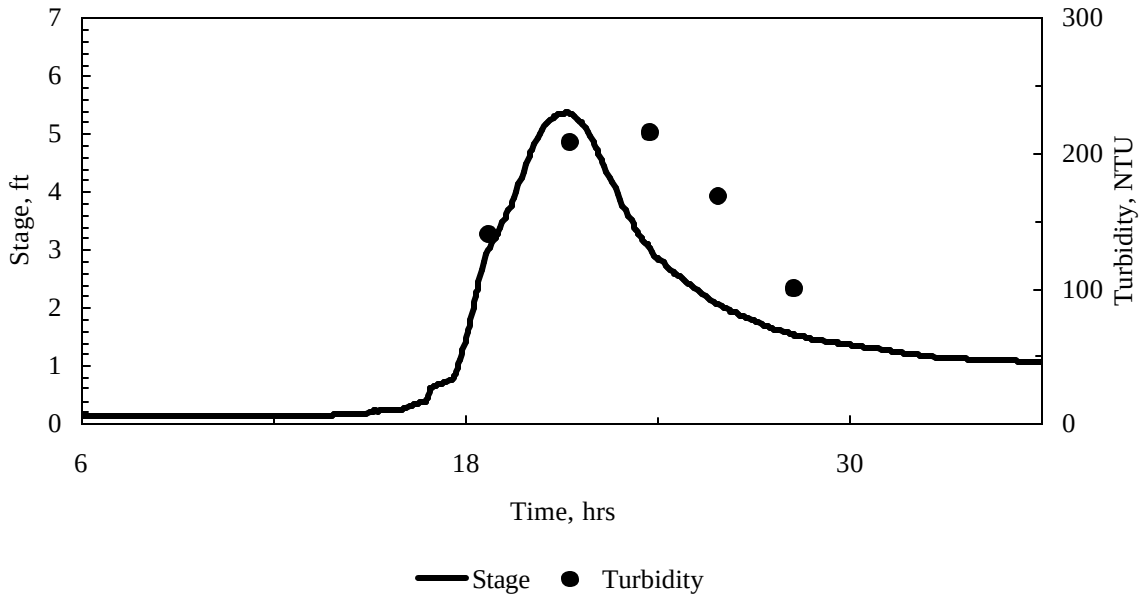

Hydrograph and grouped turbidity from 2/03/04 storm event

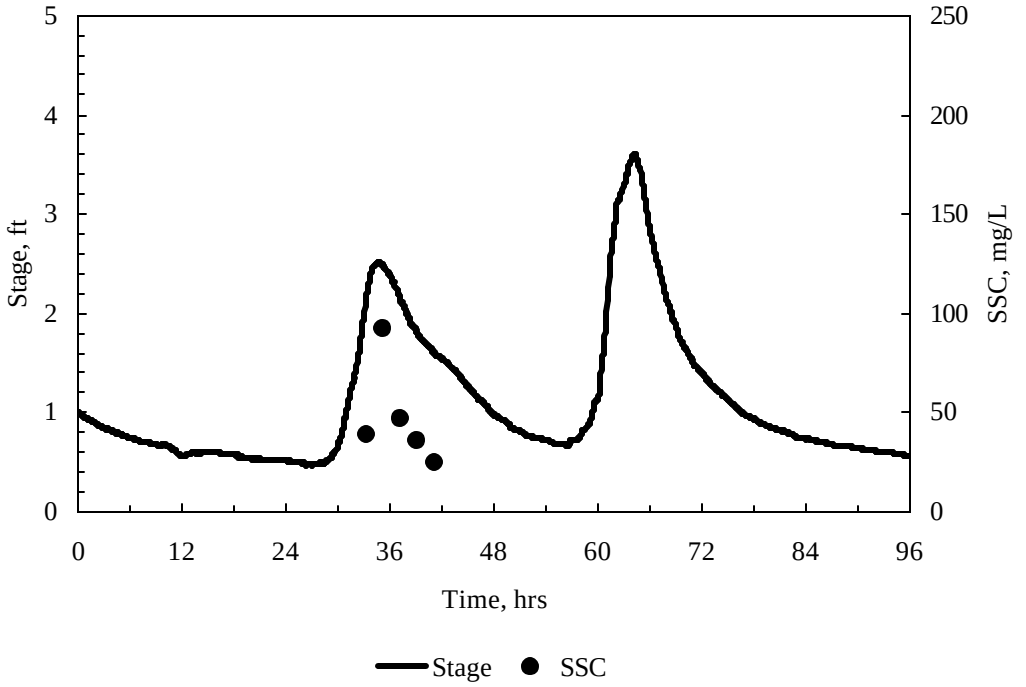

Hydrograph and grouped SSC from 2/14/04 storm event

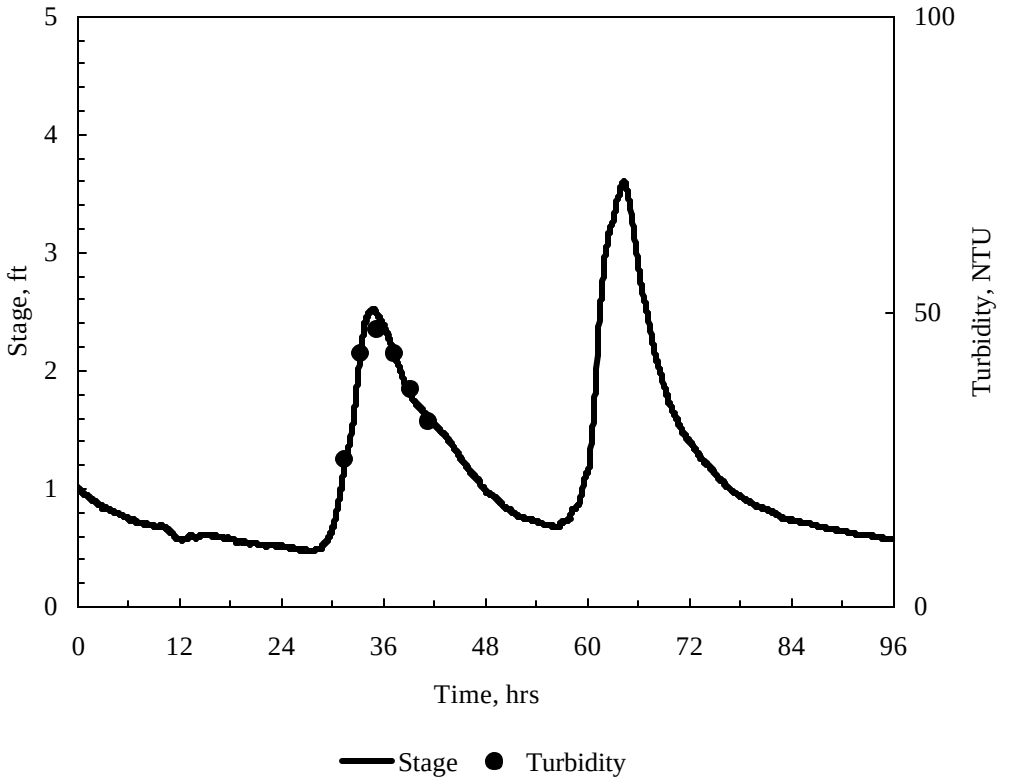

Hydrograph and grouped turbidity from 2/14/04 storm event

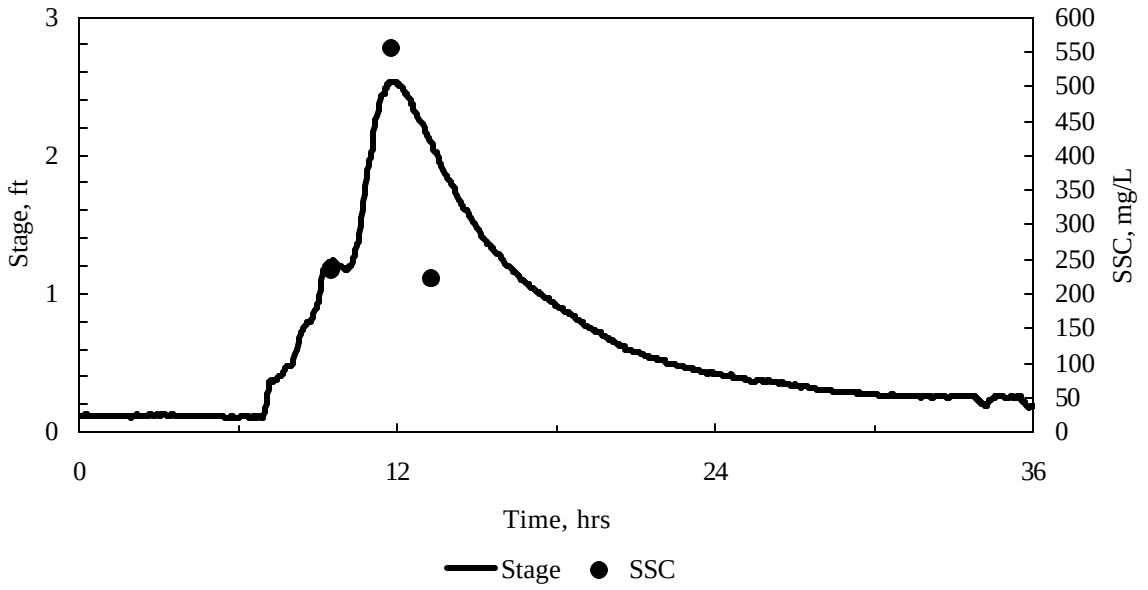

Hydrograph and grouped SSC from 3/06/04 storm event

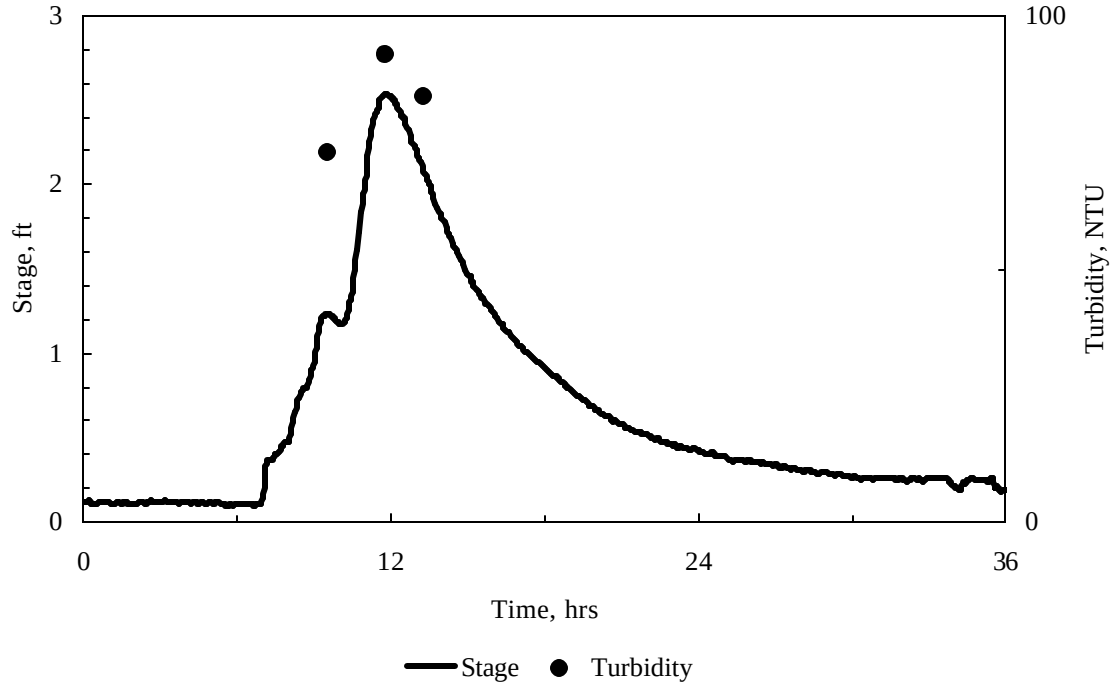

Hydrograph and grouped turbidity from 3/06/04 storm event

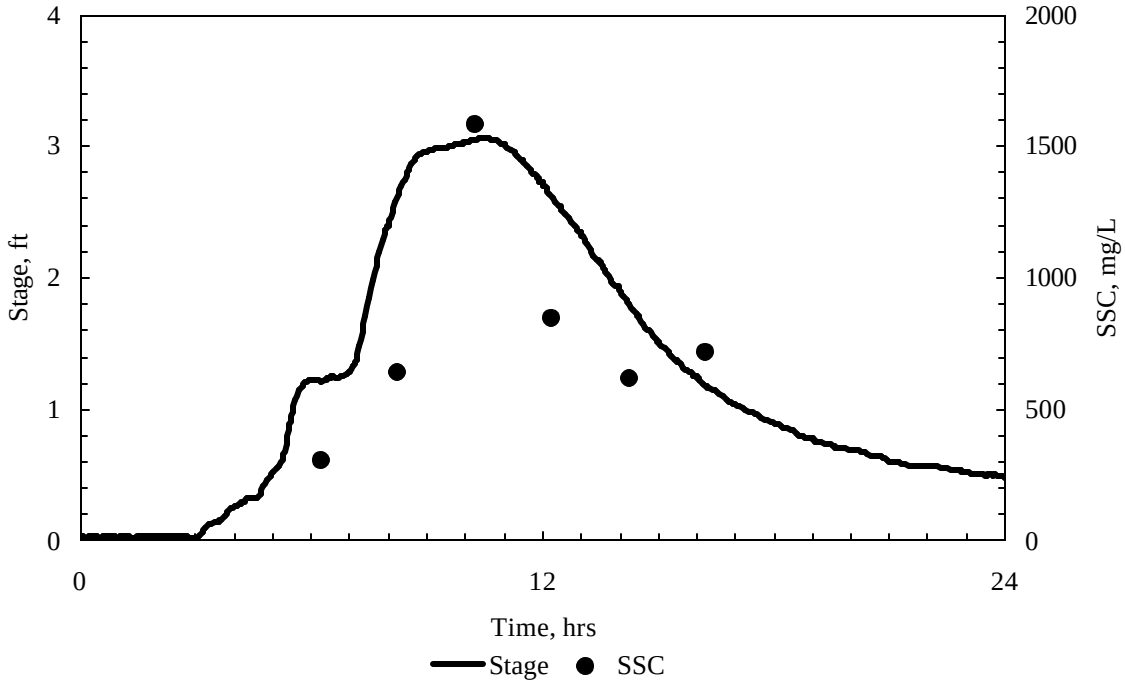

Hydrograph and grouped SSC from 3/30/04 storm event

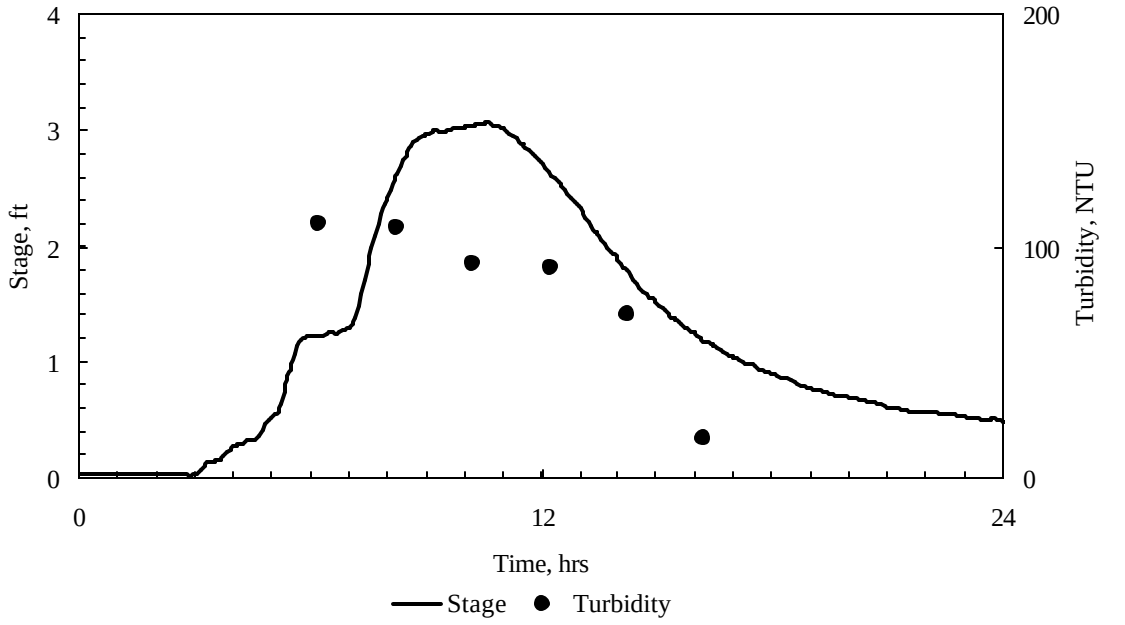

Hydrograph and grouped turbidity from 3/30/04 storm event

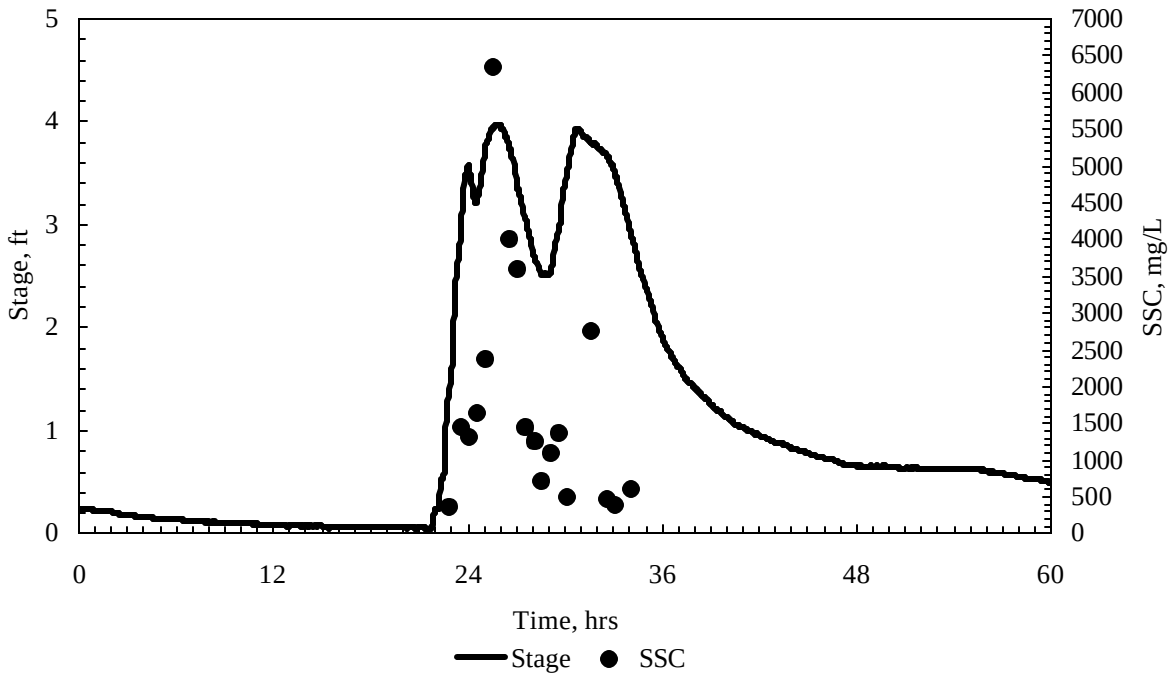

Hydrograph and SSC from 4/13/04 storm event

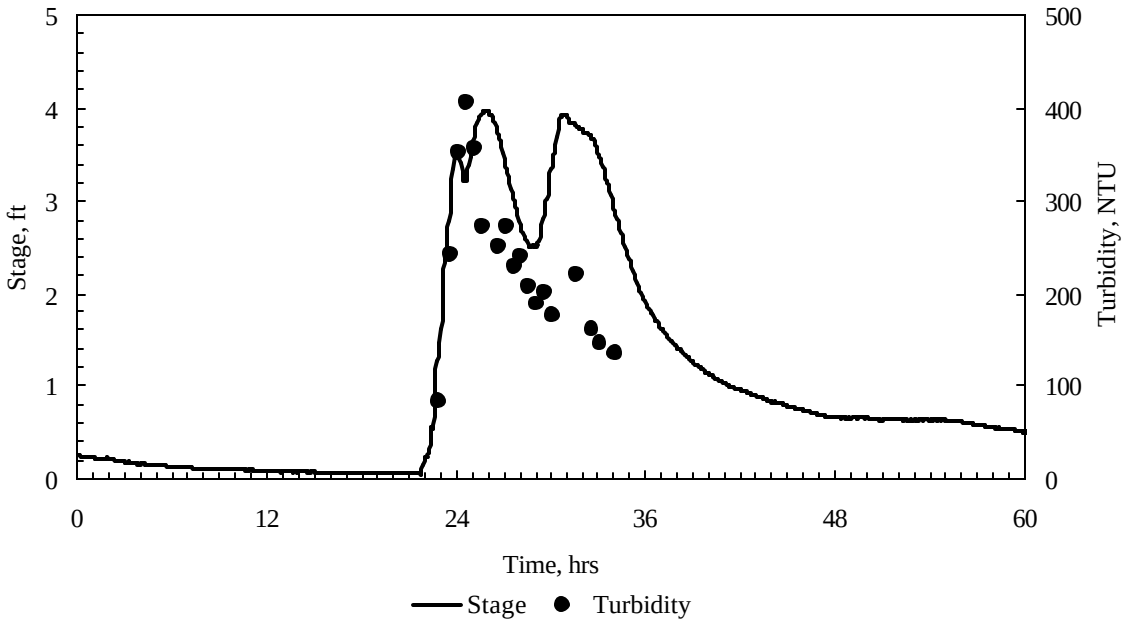

Hydrograph and turbidity from 4/13/04 storm event

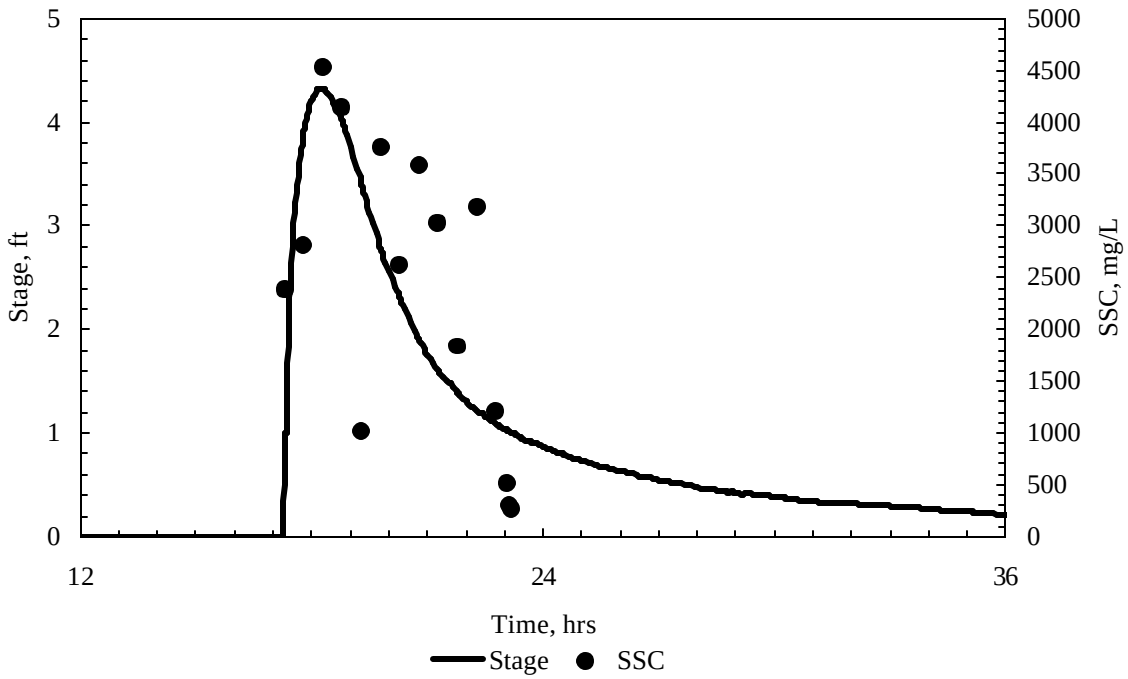

Hydrograph and SSC from 5/22/04 storm event

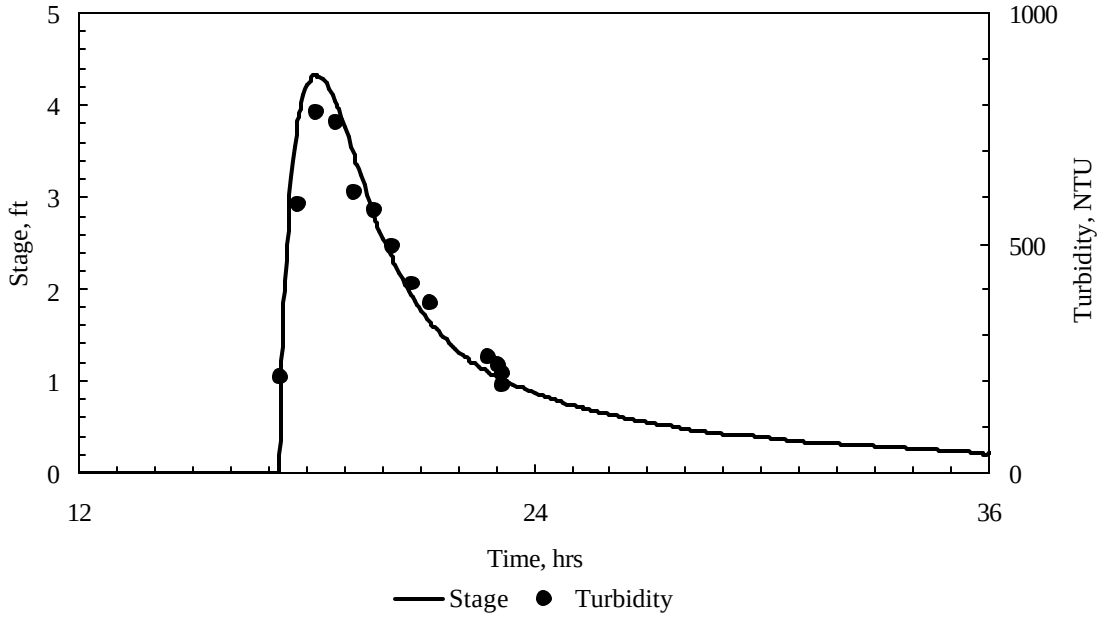

Hydrograph and turbidity from 5/22/04 storm event

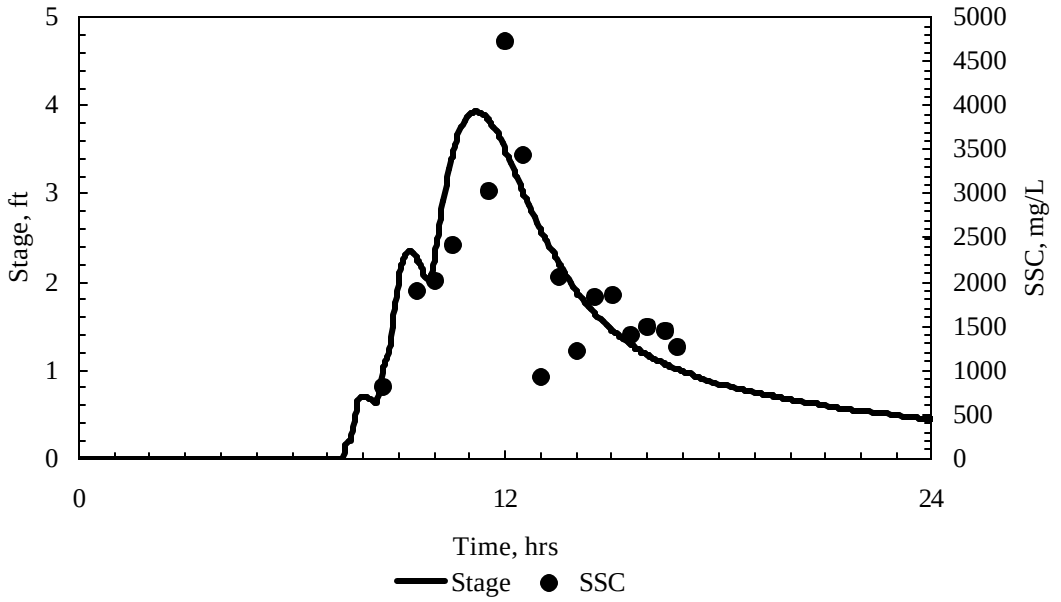

Hydrograph and SSC from 5/31/04 storm event

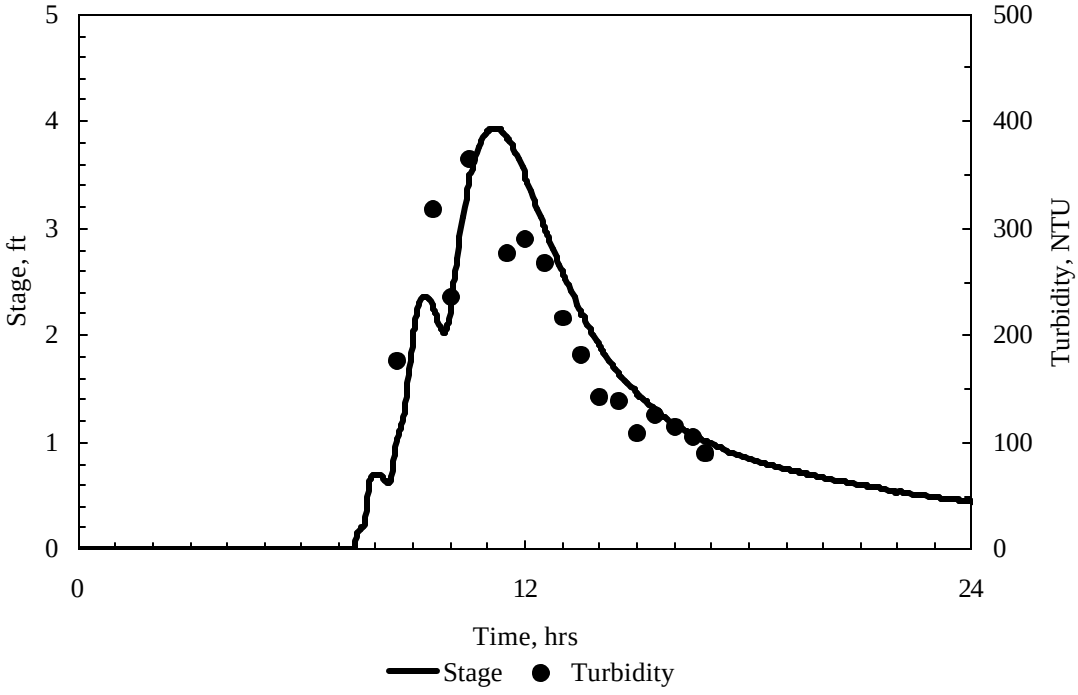

Hydrograph and turbidity from 5/31/04 storm event

Mid Infrared Water Quality Sensors for the detection of organic pollutants

Basic Information

Title:	Mid Infrared Water Quality Sensors for the detection of organic pollutants
Project Number:	2002GA30G
Start Date:	9/1/2002
End Date:	9/1/2004
Funding Source:	104G
Congressional District:	5th District John Lewis
Research Category:	Not Applicable
Focus Category:	Water Quality, Surface Water, Toxic Substances
Descriptors:	
Principal Investigators:	Boris Mizaikoff

Publication

1. Mizaikoff, Boris, 2003, "Mid Infrared Water Quality Sensors for the Detection of Organic Pollutants," Georgia Water Resources Institute, Georgia Tech, Atlanta, GA., 15p.
2. Mizaikoff, Boris, 2004, "Mid Infrared Water Quality Sensors for the Detection of Organic Pollutants," Georgia Water Resources Institute, Georgia Tech, Atlanta, GA., 25p.
3. Vogt, F, H. Steiner, K. Booksh, and B. Mizaikoff, 2004. Chemometric Correction of Drift Effects in Optical Spectra. Appl. Spectrosc. Vol. 58, 683-692.
4. Karlowatz, M., M. Kraft, and B. Mizaikoff, 2004. Simultaneous Quantitative Determination of Benzene, Toluene and Xylenes in Water With Mid-Infrared Evanescent Field Spectroscopy. Anal. Chem. Vol. 76, 2643-2648.
5. Janotta, M., F. Vogt, H. Voraberger, W. Waldhauser, J. M. Lackner, C. Stotter, M. Beutl, and B. Mizaikoff, 2004. Direct Analysis of Oxidizing Agents in Aqueous Solution with Attenuated Total Reflectance Mid-Infrared Spectroscopy and DLC Protected Waveguides. Anal. Chem. Vol. 76, 384-391.
6. Janotta, M., M. Karlowatz, F. Vogt, and B. Mizaikoff, 2003. Sol-gel Based Mid-Infrared Evanescent Wave Sensors for Detection of Organophosphate Pesticides in Aqueous Solution. Anal. Chim. Acta. Vol. 496, 339-348.
7. Janotta, M., A. Katzir, and B. Mizaikoff, 2003. Sol-gel Coated Mid-Infrared Fiberoptic Sensors. Appl. Spectrosc. Vol. 57, 823-828.
8. B. Mizaikoff, 2003. Mid-Infrared Fiberoptic Sensors. Anal. Chem. Vol. 75, 258A-267A.
9. B. Mizaikoff, 2003. Infrared Optical Sensors for Water Quality Monitoring. Water Sci. Technol. Vol.

47, 35-42.
10. Janotta, M., D. Rudolph, A. Kueng, C. Kranz, H.-S. Voraberger, W. Waldhauser, and B. Mizaikoff, 2004. Analysis of Corrosion Processes at DLC Protected ZnSe Waveguide Surfaces. Langmuir, accepted.
11. Janotta, Markus, 2004. "Chemical surface modifications for improved mid-infrared evanescent field sensing systems." Ph.D. Dissertation, School of Chemistry and Biochemistry, Georgia Institute of Technology, Atlanta, GA. 181 pages.

PROF. DR. BORIS MIZAIKOFF

Georgia Institute of Technology, School of Chemistry and Biochemistry, Applied Sensors Laboratory
Atlanta, Georgia 30332-0400, U.S.A.
Phone: (404) 894 4030, Fax: (404) 894 7452, Email: boris.mizaikoff@chemistry.gatech.edu
http://asl.chemistry.gatech.edu

Project: 2002GA30G

(U.S.G.S., WATER RESOURCES RESEARCH GRANT PROPOSAL)

Mid Infrared Water Quality Sensors for the Detection of Organic Pollutants

Technical Report, Year 2

Research Activities September 01, 2003 – June 30, 2004

Boris Mizaikoff (PI)

Atlanta, July 5, 2004

1 TITLE:

MID-INFRARED WATER QUALITY SENSORS FOR THE DETECTION OF ORGANIC POLLUTANTS

2 PROBLEM AND RESEARCH OBJECTIVE

Increasing pollution of water resources has stimulated the development of sensor systems capable of screening organic pollutants in the aquatic environment. Especially in urban areas, increasing concentration of volatile organic compounds in surface and ground water threaten primary sources of drinking water. Hence, there is a substantial demand for in-situ, continuously operating and reliable analysis methods emphasizing selective determination of abundant pollutants, such as chlorinated hydrocarbons (CHCs), pesticides or the broad class of endocrine disrupting compounds (EDCs).

The main goal of this research project is the optimization, application and validation of infrared chemical sensor systems for the determination of organic pollutants such as chlorinated hydrocarbons, pesticides or endocrine disrupting compounds in the Rottenwood Creek stream, an urban stream located in the metro Atlanta area. This stream is affected by residential, commercial and industrial land use. Synthetic sensing interfaces ('biomimetics') based on sol-gels and imprinted polymers emphasizing selective analyte recognition will be combined with existing infrared sensor systems already established by our research group. Following optimization of the instrument in the laboratory and validation with real-world samples, measurements at Rottenwood Creek are envisaged as representative example of an urbanized water resource.

In addition, our research group had the opportunity to test the developed IR chemical sensor systems for detection and quantification of chlorobenzene (CB) in the groundwater of Bitterfeld (Saxonia/Anhalt, Germany), a major remediation site.

3 METHODOLOGY

The methodology of this study is divided into three workpackages (**WPs**), which are described in the following sections:

• WP 1: Development of novel chemical recognition layers ("biomimetics") for optical waveguides based on sol-gels and molecularly imprinted polymers.

Sol-gel Chemistry

Sol-gel based chemical recognition elements have been integrated with mid-infrared (mid-IR) waveguides serving both, as enrichment membrane and as protective layer. Two different kinds of IR transparent waveguides have been applied for developing intrinsic *evanescent field sensing systems*: ZnSe ATR crystals and silver halide fibers. Utilizing attenuated total reflection (ATR) techniques the environmentally relevant group of organophosphates has been targeted and reported in the first year of this project. It should be mentioned that the study on sol-gel coated IR fiberoptic sensors has been honored with the ***Meggers Award 2004*** by the *Society of Applied Spectroscopy*, annually distinguishing the best paper published in *Applied Spectroscopy*.

Molecularly Imprinted Polymers

First experiments have been performed to create highly selective separation materials for the endocrine disrupting compound (EDC) 17β-estradiol in the first year of the project. In the second year, HPLC columns packed with either molecularly imprinted stationary phase material or control (non-imprinted) material have been prepared revealing superior separation performance even of enantiomers. Furthermore, a MIP based assay for selective determination of 17β-estradiol has been developed. Next, solid phase extraction (SPE) cartridges of the synthetic receptor material will be prepared and applied to real world samples.

• WP 2: Optimization and testing of a fiber optic evanescent wave sensor prototype for measuring organic pollutants in the aquatic environment.

IR Chemical Sensor Testing at Field Conditions

A prototype mid-infrared sensor system for the determination of volatile organic pollutants in ground and surface waters was developed and tested in the first year of this project. Mixtures of benzene, toluene and xylene isomers (BTX) at concentrations down to the low ppb region were successfully qualitatively and quantitatively investigated. Xylene has been determined in spiked pond water demonstrating real world applicability.

An extensive field measurement campaign in Bitterfeld/Germany enabled to test the IR chemical sensor system in a real world environment for remediation monitoring (chlorobenzene in groundwater).

Advanced Multicomponent Data Evaluation

All quantitative data evaluation techniques applied to spectroscopy are based on the assumption that the baseline is stable in time. If this prerequisite is violated, major concentration errors can result since drifts are evaluated along with true spectroscopic features. In this study two improved principal component regression (PCR) methods are presented in order to handle drift effects. The proposed drift correction methods take advantage of baseline drifts being rather broad compared to the absorption features. The only assumption made is that drift effects can be modeled sufficiently by polynomials of user selectable order. One correction method modifies principal components (PCs) such that drifts of polynomial shape are orthogonal to the calibration model and therefore cannot influence the concentration result. The second method extends the calibration model by synthetic so-called pseudo principal components (pPCs), which are used together with and in the same way as the real PCs. Synthetic and experimental data sets have been used for demonstrating the superiority of these novel PCR approaches compared to conventional PCR.

• WP 3: Alternative sensing concept for water analysis using an IR hollow waveguide gas sensing module combined with a supported capillary membrane sampler.

A gas sensor for application in water analysis was developed by combination of a mid-infrared (MIR) hollow waveguide with a Fourier transform infrared (FT-IR) spectrometer and coupling of the hollow waveguide gas sensor module to a supported capillary membrane sampler (SCMS) for continuous liquid-gas extraction. Different hollow waveguides have been characterized in this study for developing an optimized optical configuration. Analysis of industrially relevant compound has been performed, investigating chlorinated hydrocarbons (CHCs), such as dichloromethane and chloroform, representing highly volatile analytes and 1,4-dioxane as

example for target compounds with low volatility. The suitability of this spectroscopic IR sensing system for industrial applications is demonstrated under simulated real world conditions with limits of detection in the ppb (v/v) and ppm (v/v) concentration range for CHCs and 1,4-dioxane, respectively.

4 PRINCIPLE FINDINGS AND SIGNIFICANCE

4.1 Molecularly Imprinted Polymers

4.1.1 Introduction

Phenolic steroid hormones such as 17β-estradiol, 17α-estradiol and estrone (Figure 2) are suspected of having adverse effects on the endocrine system in wildlife and humans. The existing of these compounds in aquatic environments has been reported recently [1,2]. Therefore there is considerable interest in developing cost-effective analytical methods for determining these compounds in environmental samples at low concentration levels [2,3]. Nowadays, noncovalent molecular imprinted polymers (MIPs) have been increasingly developed as mimics of natural molecular receptors [4,5].

In MIP development studies, appropriate particle sizes for particular studies such as chromatographic application or binding assays are desired. For chromatographic evaluation (e.g. HPLC) or solid phase extraction (SPE), MIP particles with size between 10 to 25 μm are normally used. In binding assays or biomimetic recognition polymeric layers on chemical sensing surface, smaller particles (<1 μm) are necessary. Classical MIPs are prepared by bulk polymerization methods, using a porogenic solvent to create a block co-polymer [6]. The particles with desired size are obtained by grinding and sieving, which is a labor intensive and wasteful process because a lot of fine particles were produced and cannot be used. The method yields particles with rather limited control over particle size and shape.

Many attempts have been made to produce monodisperse molecularly imprinted polymer particles with methods such as suspension [7], dispersion [8], and aqueous two-step swelling polymerization [9]. Unfortunately, these techniques suffer from the need for water or highly polar organic solvents during the polymerization procedures, which may weaken the specific interactions between functional monomers and template in many noncovalent imprinted mixtures. The solubility of template and functional monomer in these techniques would be a problem for the specific recognition. First, template would be lost if it dissolves in water. Second, copolymerization between the functional monomer and cross-linker may not be obtained if acidic monomers with good solubility in water are used. In addition, the addition of large amount of disperse solvent will reduce the number and strength of the specific interactions.

4.1.2 Experimental

Preparation of the polymers: Molecular imprinted microspheres were prepared using precipitation polymerization. The first microspheres (MIP1) were prepared with 17β-estradiol (1 mmol), methacrylic acid (8 mmol), ethylene glycol dimethacrylate (6.66 mmol), and azobis (isobutyronitrile) (2.3 wt % relative to the monomer) in a mixture of acetone and acetonitrile (40ml, 1/3 v/v) in a glass vial. The second microspheres (MIP2) were prepared with 17β-estradiol (0.375 mmol), methacrylic acid (3 mmol), divinylbenzene 80 (15 mmol), and azobis (isobutyronitrile) (5 wt % relative to the monomer) in a mixture of toluene and acetonitrile (60 ml, 1/3 v/v) in a round glass flask. The solutions were degassed in an ultrasonic bath for 5 min,

purged with argon for 5 min, and sealed immediately. Polymerization was carried out at 65 ^{o}C (MIP1) or 70^{o}C (MIP2) for 24 h. Continual magnetic stirring during polymerization was performed for preparing MIP2. The obtained microspheres were separated from the reaction medium by filtration or centrifugation, successively washed three times with methanol/acetic acid (100ml, 85/15 v/v), methanol and acetonitrile respectively, and dried at 40 ^{o}C overnight. As a control, the non-imprinted microspheres (CTL1 and CTL2) were prepared and treated in exactly the same way, except that no template was added to the pre-polymerization solution. The beads were placed on silicon slides and sputter coated with 15nm of gold using a Denton DV-502A thermal evaporator. Scanning electron micrographs were obtained by using a LEO 1530 FEG scanning electron SEM at 25 kV. Optical micrographs were obtained by placing beads on glass slides with an Olympus Bx41 optical microscope.

Radioligand binding assays: For saturation studies, the microspheres (MIP1 and CTL1) were suspended in acetonitrile and appropriate volumes were incubated with 417 fmol radioligand [6,7-^{3}H(N)]estradiol in acetonitrile. The final volume was adjusted to 1ml. The samples were incubated overnight and separated by centrifugation. 500μL supernatant was added to a scintillation liquid (10ml, Ecoscint O). The radioactivity was measured by liquid scintillation counter (Packard). For competitive assays, the microspheres (MIP1 and CTL1) were suspended in acetonitrile and appropriate volumes were added into 1.5 mL polypropylene centrifuge tubes, followed by a fixed amount of [6,7-^{3}H(N)]estradiol and varying amounts of 17β-estradiol or 17α-estradiol and acetonitrile to give a total volume of 1mL. The samples were incubated overnight. The amount of bound radioligand was measured in the same way as the saturation studies described above.

Chromatographic analysis: The microspheres (MIP2 and CTL2) were suspended in acetone and packed into 150×4.6 mm stainless steel HPLC columns with an Alltech 1666 slurry packer using acetone as the packing solvent. Chromatographic analysis was performed using an HPLC system (Dionex P580 pump, UVD 340S Detector).

4.1.3 Results

For producing high quality imprinted beads, a general applicable approach is required, avoiding the use of dispersants such as water or polar solvents. Precipitation polymerization has proven to be a useful way to produce poly (divinylbenzene) [10] or poly(chloromethylstyrene-co-divinylbenzene) [11] microspheres with sizes between 2-5 μm. In the present work, we have developed a simple and attractive method which can produce imprinted beads with controlled sizes for different applications by a one-step precipitation polymerization.

By using different cross-linkers and porogenic solvents, two kinds of imprinted microspheres were obtained. MIP1 (Figure 3 A,C) was prepared by using methacrylic acid (MAA) as functional monomer and ethylene glycol dimethacrylate (EGDMA) as cross-linker, less cross-linker being used compared to bulk polymerization [12]. One attractive feature of the obtained microspheres (MIP1) is that the polymer particles (around 400nm) are easy to disperse and suspend in solution, which is ideal for binding assays. In order to obtain microspheres with size suitable for HPLC application, a series of control beads were prepared to understand the influence of monomer ratio and polymerization temperature to the size and morphology of polymer particles. Similar size and morphology was obtained when the monomer ratio was less than 11vol% of the prepolymerization solution (Figure 4 A,B). The particles began to coagulate together instead of forming bigger particles when more EGDMA was used (Figure 4 C,D). This

indicates that the size of the microspheres could not be controlled by simply varying the concentration of cross-linker used in the prepolymerization mixture. A different cross-linker is needed to prepare microspheres suitable for HPLC application. Figure 4 E and F show that the polymer particle size increased when polymerization temperature increases to 70°C. For preparation of MIP2 and CTL2, divinylbenzene, which has been proved to be a good cross-linker to produce poly (divinylbenzene) microspheres with sizes between 2-5 μm, was chose as cross-linker and 70°C was used as polymerization temperature. A solvent mixture of toluene:acetonitrile (1:3, v/v) was used as porogen to minimize the interference of a polar solvent to hydrogen bonding and increase the porosity of the microspheres. The resulting Microspheres of about 3μm in diameter have near perfect spherical shapes and narrow disperse size distribution (MIP2, Figure 2 B,D).

To confirm that the imprinting effect of obtained polymer beads are really comparable to those obtained by bulk polymerization methods, the imprinted microspheres were evaluated by radioligand binding assays and HPLC, respectively. Binding assays were carried out in acetonitrile by using [^{3}H] estradiol as a radioligand to evaluate the capacity of the imprinted microspheres (MIP1) and the corresponding control microspheres (CTL1) (Figure 5 A). Figure 4B shows the competition of [^{3}H] estradiol binding to the imprinted microspheres by unlabeled 17β-estradiol and its optical isomer 17α-estradiol. Obviously, the imprinted microspheres not only bind more [^{3}H] estradiol than that of control microspheres but also the binding is effectively inhibited by addition of the unlabeled 17β-estradiol, not by the addition of 17α-estradiol. The displacement of labeled 17β-estradiol in Figure 5 B may be used as calibration curve to determine the concentration of 17β-estradiol from biological or environmental samples.

The size and sphere shape of MIP2 and CTL2 was ideal for use in chromatographical applications. The recognition ability of MIP2 to 17β-estradiol was confirmed by HPLC evaluation. The separation of 17β-estradiol, 17α-estradiol and estrone was achieved by using MIP2 as stationary phase in HPLC (Figure 6 A, solid line). The control experiments were done by using CTL2 (Figure 6 A, dash line) and a standard Kromasil 100 C_{18} column (Figure 6 B, dot line) under identical chromatographic conditions. To further confirm that the separation is based on the imprinting effect, similar measurements were performed using acetonitrile containing 10% acetate buffer at a pH of 8.5 (Figure 6 A, dash dot line) as mobile phase. In this case, estrone, 17α-estradiol and 17β-estradiol were not separated and shorter retention times were obtained for 17α-estradiol and 17β-estradiol while the retention time of estrone remained almost the same. Polar solvents and functional monomers compete for specific interactions with the template. The addition of a polar solvent such as water in the mobile phase or prepolymerization solution would therefore disable specific interactions such as hydrogen bonding. Disappearing of the specific recognition in Figure 6 A (dashed dotted line) indicates that the specific recognition does result from the hydrogen bonding interaction between estradiol and methacrylic acid.

In summary, a precipitation polymerization method has been developed to prepare 17β-estradiol-imprinted microspheres. The size and morphology of the imprinted microspheres can be controlled by using different polymerization conditions including cross-linker, monomer ratio and polymerization temperature. Successfully imprinted microspheres with ideal sizes ranging from 400nm to 3μm were used in chromatographical applications or radioligand binding assays.

In a next step, thus prepared synthetic receptors will be applied in a solid phase extraction (SPE) format and tested with real world samples in collaboration with U.S.G.S. Atlanta.

4.2 IR Chemical Sensor Testing at Field Conditions

4.2.1 Continuous analysis of xylene in pond water

4.2.1.1 Introduction

Attenuated total reflection mid-infrared (ATR-IR) spectroscopy using ZnSe ATR crystals is applied for simultaneous detection and quantification of the environmentally relevant analytes benzene, toluene, and the three xylene isomers (BTX). The analytes are enriched into a thin ethylene/propylene co-polymer membrane coated onto the surface of the internal reflection waveguide, which is exposed to the aqueous sample. Results have been shown in the first year of this project. Detection limits lower than 20 ppb (v/v) have been achieved for all xylene isomers and of approx. 80 ppb (v/v) for benzene and 50 ppb (v/v) for toluene, respectively.

In continuation of this work applicability to real world samples has been tested. Continuous measurement series of various concentrations of o-xylene added to urban pond water utilizing the developed sensor system based on attenuated total reflection mid-infrared (ATR-IR) spectroscopy have been performed. The analyte is enriched into a thin polymer membrane coated onto the surface of an internal total reflection waveguide, which is exposed to the aqueous sample. Direct detection of analytes permeating into the polymer coating is performed utilizing evanescent field spectroscopy in the fingerprint region (> 10 μm) of the mid-infrared (MIR) spectrum (3-20 μm) without additional sample preparation. Data evaluation was performed by integration of the characteristic absorption peak of o-xylene at 740 cm^{-1}. The presented data clearly demonstrates the potential of polymer coated evanescent field sensors for real-world applications in water quality monitoring.

4.2.1.2 Experimental

The coating procedure adheres to the description in year 1 of this project with following modification: 210 μL of the hot coating solution were applied resulting in a film thickness of approx. 3.3 μm determined via differential weighing.

A 1 % (v/v) solution of o-xylene in methanol was prepared and diluted with pond water to 20, 50, and 80 ppm (v/v) of analyte concentration. Additional methanol was added to keep the amount of methanol constant at 1 % (v/v). The sample solutions have been freshly prepared prior to each measurement ensuring minimal losses due to evaporation.

Data was recorded in the spectral range of 400 cm^{-1} to 1600 cm^{-1} using a Bruker Equinox 55 Fourier transform infrared (FT-IR) spectrometer (Bruker Optics, Billerica, MA) equipped with a liquid N_2 cooled mercury-cadmium-telluride (MCT) detector (Infrared Associates, Stuart, FL). A total of 100 scans were averaged for each spectrum with a spectral resolution of 4 cm^{-1}. For this continuous study spectra were recorded every minute for a period of approx. 8 hours. For ATR measurements a horizontal ATR accessory (Specac, Smyrna, GA) utilizing trapezoidal ZnSe ATR elements (72*10*6mm, 45º; Macrooptica Ltd., Moscow, Russia) and a stainless steel flow-cell (custom made, Volume: 2 ml, free contact area to ATR crystal: 7.2 cm^2) were used. Solutions were pulled through the flow-cell via an Alitea C8-Midi peristaltic pump (Watson-Marlow Alitea, Wilmington, MA) at a constant flow rate of 4.5 mL/min.

4.2.1.3 Results

After equilibration with water as described in the main manuscript the sensor was exposed to neat pond water samples for several hours. No significant further changes of the absorption spectra could be observed. Following, the sensor was exposed to pond water samples spiked with

o-xylene and an increasing absorption feature at 740 cm^{-1} (aromatic C–H out of plane vibration of o-xylene) could be observed after a measurement time of one minute already.

Figure 7 shows the continuous measurement of o-xylene in pond water over a period of 8 hours for a repetitive concentration trace of 3 different levels (50, 80, and 20 ppm v/v). Concentrations have been changed every 30 to 35 minutes. The trace at 740 cm^{-1} clearly shows that o-xylene partitioning never reaches equilibrium conditions for the selected observation window. However, it is evident that the response time of the sensor to changing concentrations of the sample solution is < 1 min, which is an essential aspect for rapid on-line data evaluation and e.g. threshold monitoring. Appropriate multivariate data evaluation techniques, which should enable prediction of the equilibration concentration of analytes for a calibrated system after very short enrichment times are currently developed in our research group.

Slightly increasing peak area values from one repetition to the next along with a minute positive off-set after regenerating the sensor with neat pond water (see minute 300 to 420) indicate that the broad water absorption band in the spectral region between 1000 cm^{-1} and the cut-off frequency of the detector (around 600 cm^{-1}) was still slightly increasing throughout the measurement. Recently, our research group has developed a multivariate method for automated recognition and correction of baseline drifts, which will be discussed below in more detail. As most chemical sensing systems are affected by baseline drifts due to ageing, degradation, and swelling of the molecular recognition interface, this generic solution enables the application of membrane based sensing devices in real-world environments.

4.2.2 Field measurement campaign in Bitterfeld/Germany

4.2.2.1 Introduction

For the first time attenuated total reflection mid-infrared (ATR-IR) spectroscopy is applied for detection and quantification of chlorobenzene (CB) in the groundwater of Bitterfeld (Saxonia/Anhalt,Germany). The analytes are enriched into a thin ethylene / propylene co-polymer (E/P-co) membrane coated onto the surface of an internal reflection waveguide, which is exposed to the groundwater. Direct detection of the analyte permeating into the polymer coating is performed utilizing evanescent field spectroscopy in the fingerprint regime (> 10 µm) of the mid-infrared (MIR) spectral range (3-20 µm) without additional sample preparation. Data evaluation was performed by integration of the respective absorption peak of the C-H out of plane vibration band of CB (740cm^{-1}). The concentration of CB in the highly contaminated groundwater was determined in a time period of 5 consecutive days to be 28.8 mg/L with relative deviation of less then 4%. This result is in high agreement with parallel performed head-space gas chromatography (HS-GC) measurements (27.92 mg/L). The performance of the sensor system was assessed with a set of different experiments such as tests for long-term stability all concluding in satisfactory results. The straightforward experimental setup and the achieved results for this environmentally relevant volatile pollutant in the low mg/L concentration range reveal substantial potential of MIR evanescent field sensors for on-line *in-situ* environmental analysis.

4.2.2.2 Experimental

Sensor Calibration: Data was recorded in a spectral range of 600 cm^{-1} to 1400 cm^{-1} using a Bruker Equinox 55 FT-IR spectrometer (Bruker Optics Inc., Billerica, MA) equipped with a liquid N_2 cooled mercury-cadmium-telluride (MCT) detector (Infrared Associates, Stuart, FL). Flow speed: 4.5 mL/min.

Field Measurements: Data was recorded in a spectral range of 600 cm^{-1} to 1400 cm^{-1} using a Bruker Vector 22 FT-IR spectrometer (Bruker Optik GmbH, Ettlingen, Germany) equipped with a liquid N_2 cooled mercury-cadmium-telluride (MCT) detector (Infrared Associates, Stuart, FL).

Parameters Applicable to Both Scenarios: A total of 100 scans were averaged for each spectrum with a spectral resolution of 4 cm^{-1}. For ATR measurements, a horizontal ATR accessory (Specac, Smyrna, GA) in combination with trapezoidal ZnSe ATR elements (72*10*6mm, 45º; Macrooptica Ltd., Moscow, Russia) and an aluminum flow-cell (custom made, Volume: 2 mL, free contact area to ATR crystal: ~7.2 cm^2) were used. An Alitea C8-Midi peristaltic pump (Watson-Marlow Alitea, Wilmington, MA) was used to ensure continuous flow of the analyte solutions through the ATR cell. In order to minimize adsorption and diffusion losses stainless steel tubing was exclusively used to deliver analyte solutions to the flow cell.

Preparation of the Extractive Polymer Membrane: A 1 % (w/v) coating solution of E/P-co was prepared by dissolving 0.5 g of granular polymer under reflux in 50 ml n-hexane. Prior to coating, a new ATR crystal was thoroughly rinsed with methanol. About 210 µL of clear, hot solution were applied to the surface of the ATR crystal using an Eppendorf pipette. The crystal was kept at room temperature for at least 2 h ensuring evaporation of most of the solvent. Subsequently, the polymer coating was exposed to hot air treatment with a hot air gun at 150 °C for 5 min to remove remaining traces of solvent and then kept tempered at 80°C in an oven overnight. The thickness of the layer was determined by differential weighing to be 3.2 µm.

HS-GC Validation Measurements: The HS GC reference analysis was done on a HP6890 series II GC equipped with flame ionization detection (FID). An Agilent 7694 headspace autosampler was coupled to the HS-GC system. A Chrompack CP-Sil 6B capillary column (30 m x 0.250 mm, 50 µm stationary phase) was used with nitrogen as carrier and make up gas. Samples were softly shaken and extracted at 60°C for 60 min in the autosampler and subsequently injected using a split/splitless injector kept at 250 °C. The temperature program started at 45°C for 5 min followed by a ramp to 200 °C at 20°C/min and finished holding a temperature of 200 °C for 3 min. The detector was kept at a temperature of 280 °C.

4.2.2.3 Results

Among all VOCs chlorobenzene (CB) is the main pollutant in the groundwater aquifer around the SAFIRA site by several orders of magnitude. According to previously published data on the composition and concentrations of the pollutant cocktail in the groundwater of the Bitterfeld region calibration for CB of the sensor system was conducted in the concentration range from 10 mg/L to 80 mg/L at the ASL laboratory at Georgia Tech. Field measurements were conducted applying a (smaller) Bruker Vektor 22 FT-IR spectrometer. The high agreement of the results obtained under field conditions and the laboratory measurements demonstrate the transferability of the calibration data.

Prior to the calibration measurements the coated sensor element was submersed in water and equilibrated over night. Following, the calibration set consisting of 10 mg/L, 20 mg/L, 30 mg/L, 50 mg/L and 80 mg/L of CB in water was measured regenerating the E/P-co layer after each calibrant. From the MIR absorption spectra of CB, the band with the highest intensity (aromatic C-H out of plane vibration around 740 cm^{-1}) was selected for data evaluation via peak integration.

Figure 8 (left) shows the significant part of the CB absorption spectrum for 5 different concentrations of CB in water after partitioning into the E/P-co layer for 24 minutes.

Data evaluation in this case could be performed by simple band integration, as there is only one compound present in the solution. Calibrations have been performed before and after the measurement campaign with approx. 4 weeks of time lapse in between the first and the last calibration set. Figure 8 (right) shows a linear calibration derived from band integration for 3 repetitive (1 measured before and 2 after the measurement campaign) runs of the calibration set.

The acceptable linearity and the small standard deviation proof that the sensor provides superior stability despite being submersed in a highly polluted sample during the measurement campaign, the mechanical stress of being transported and several drying/wetting cycles.

The SAFIRA site offers an automated sampling system. A partial flow of groundwater is permanently pumped from various depths in the shafts through an array of glass bottles, which are placed in a cooled storage chamber in the adjacent analytical laboratory and from there back to the reactors for remediation procedures. The same flow configuration is available for water exiting the reactors after the remediation processes. Thus, samples can be conveniently collected from the glass bottles in the laboratory environment rather than descending instrumentation into the shafts. For this first test of an ATR based sensor system for groundwater monitoring it was decided to perform repetitive measurements of water from one shaft for several days in order to verify accuracy and stability of the developed sensor system at field conditions. Concentration levels in the groundwater flow in the Bitterfeld region can be considered constant for the measurement period of several days. Considering the composition of the groundwater, chlorobenzene is the main pollutant by almost 2 orders of magnitude.

After sensor equilibration with distilled water over night, a stable baseline without noticeable spectral changes due to water diffusion was obtained. Subsequently, groundwater was pumped through the flow cell and spectra were recorded every 2 min until equilibrium was reached. Figure 9 (left) shows exemplary spectra of a groundwater sample from shaft 5 and a calibration solution of 50 mg/L CB in water. Besides a concentration related difference in band intensities and the bands related to E/P-co swelling (approx. 780 cm^{-1} – 800 cm^{-1}), both spectra appear to be identical. Hence, we can deduct that all contaminants except chlorobenzene are below the threshold level of detection for this sensor system. The aromatic C-H out of plane vibration of CB around 740 cm^{-1} was selected for data evaluation via peak integration.

Figure 9 (right) shows the enrichment behavior of CB into the E/P-co layer by plotting the peak area (740 cm^{-1} band) over time (flow rate: 4 mL/min).

To verify the accuracy of the ATR measurements, the peak areas of the absorption feature at 740 cm^{-1} of all 5 measurement periods have been evaluated with a linear regression function and the values have been compared to the HS-GC validation measurement (see table below).

	Run 1	*Run 2*	*Run 3*	*Run 4*	*Run 5*
measured conc. CB (mg/L)	**28.71**	**27.54**	**31.05**	**28.01**	**29.05**
HS-GC (mg/L)	27.92	27.92	27.92	27.92	27.92
differnce mg/L	0.79	0.38	3.13	0.09	1.13
error %	2.82	1.36	11.21	0.31	4.03

With an average deviation of only 1.10 mg/L (3.94%) to the validation measurement the ATR sensor system provided surprisingly accurate results. Additionally, these results verify that it is valid to calibrate such a sensor systems at laboratory conditions, still yielding reliable accurate

results at field conditions. In this first study the cocktail of pollutants present in the groundwater (although at lower concentrations than CB), the difference in pH level and the measurements at cooled conditions (groundwater samples was at least several degrees Celsius colder than the laboratory calibration samples) did not significantly affect the sensor system performance.

4.2.2.4 Summary of field measurement campaign Bitterfeld

The first measurement campaign deploying a polymer coated IR-ATR sensor system at field conditions has successfully been performed for the determination of chlorobenzene in the groundwater aquifer of a remediation site. Performance of the sensor was accurate and stable over a period of time of several weeks, a time period which included calibration and on-site measurements. As a major point it can be stated that quantitative evaluation of the on-line measurements was in excellent agreement with results from HS-GC validation. Consequently, in spite of the deviating experimental parameters and the sample matrix during the controlled sensor calibration in a laboratory environment and the on-site measurements the performance of the sensor was not affected significantly. Furthermore the enrichment of CB into the EP/Co membrane was completely reversible in both measurement scenarios. The already pronounced effect of changing flow conditions on the enrichment kinetics has experimentally been confirmed and points out one factor of so far unexploited sensor optimization for future sensor setups. The sensor system performed well for individual measurements, in continuous monitoring operation and during the simulation of a chemical spill event. The minimum measurement repetition time for a complete enrichment and sensor regeneration cycle for the available setup was determined to be approx. 30 min, however, could be improved with higher sample flow rates and the introduction of an improved flow cell geometry. Dynamic sensor behavior has been shown to be < 2 min for increasing and decreasing pollutant concentration in the analyzed sample. This is a timescale sufficient for remediation processes and many monitoring processes.

It has been shown that polymer coated ATR-FTIR spectroscopic sensor systems have the capability of performing on-site groundwater monitoring with high accuracy and reliability. Given further development especially in the region of automated data evaluation techniques it can be expected that such sensors systems will find applications in environmental and process monitoring.

4.3 Advanced Multicomponent Data Evaluation

4.3.1 Introduction

All quantitative data evaluation techniques applied to spectroscopy are based on the assumption that the baseline is stable in time. If this prerequisite is violated, major concentration errors can result since drifts are evaluated along with true spectroscopic features. In this study two improved principal component regression (PCR) methods are presented in order to handle drift effects. The proposed drift correction methods take advantage of baseline drifts being rather broad compared to the absorption features. The only assumption made is that drift effects can be modeled sufficiently by polynomials of user selectable order.

One correction method modifies principal components (PCs) such that drifts of polynomial shape are orthogonal to the calibration model and therefore cannot influence the concentration result. The second method extends the calibration model by synthetic so-called pseudo principal components (pPCs), which are used together with and in the same way as the real PCs. While the principal components model the true spectral features the pPCs describe drifts simultaneously

and independently. Hence, drifts are explicitly included into the calibration and cannot cause erroneous concentration results. It is demonstrated that both correction methods are equivalently powerful as the conventional PCR in absence of drifts and superior if drifts are present. If computation resources are limited, the first drift correction algorithm is advantageous because less computation expense is needed. The second approach provides additional information as drifts are explicitly extracted. These can then be used for further analyses for instance to improve the experimental setup. Synthetic and experimental data sets have been used for demonstrating the superiority of these novel PCR approaches compared to the conventional PCR.

Details on the developed algorithms and on synthetic data sets are omitted here and can be found in the corresponding publication.

4.3.2 Results

The results discussed in this section only refer to real world data obtained with the developed IR chemical sensor system.

A data set obtained with a polymer coated ATR sensor coupled to a FT-IR spectrometer was used for assessing the algorithms performance on experimental data. The calibration of the FT-IR spectrometer was done under laboratory conditions using samples containing 0.5 ppm, 1 ppm, 2 ppm, 3 ppm, 4 ppm, and 6 ppm TeCE dissolved in water (Figure 10, top). From each calibration sample two calibration spectra were obtained and included into the calibration. Four relevant PCs $\mathbf{P}$ were extracted from these twelve calibration samples. Fourth order polynomials were fitted to the PCs $\mathbf{P}$ and then subtracted from the PCs resulting in polyPCs $\mathbf{P}_{\text{poly}}$. Since PC #4 could be modeled by a fourth order polynomial rather well, polyPC #4 consisted of noise only and was not used for the evaluation. For the pPCR algorithm $\mathbf{P}$ was augmented by five pPCs.

After this calibration the sensor head was deployed into the aquifer and acquired spectra for 20 hours at real world conditions in time intervals of a few minutes. During the first five hours water samples were taken right next to the sensor head and analyzed by headspace gas chromatography (HSGC). Since this measurement series took much longer than the calibration, the measurement spectra are affected by substantially more drifts (Figure 10, bottom – compare the different y-axis scaling in both graphs). There are two possible origins of the drifts: Temperature influence and the uptake of water into the polymer coating of the sensor head. Since water has an absorption band located below 900 cm^{-1} (librational or L_2 band), water uptake causes major drifts adjacent to the TeCE absorption band located around 910 cm^{-1}.

First of all, it was investigated whether the four conventional PCs obtained from laboratory measurements are able to model selected real world, drift affected spectra. For this purpose selected measurement spectra were reconstructed from the PCs $\mathbf{P}$ and the corresponding scores $\hat{\mathbf{t}}$ **Error! Reference source not found.**. The drifts contained in the calibration spectra enable the algorithm to model the main features of the drift affected measurement spectra. However, since the drift is much stronger during the measurement compared to the calibration, large scores for the less important, noise containing PCs #3 and #4 were obtained. This is of detrimental effect as large scores largely amplify noise contained in these PCs. This is evident in the reconstructed spectra, which are much noisier than the originally measured spectra. Hence, the final concentration results are affected by increased uncertainties. The same measurement spectra were reconstructed by using the pPCs $\mathbf{P}_{\text{pPC}}$ and $\hat{\mathbf{t}}_{\text{pPC}}$. In this case, the drift is modeled mainly by the pPCs, the noisy PCs # 3 and #4 are only needed for describing minute true spectroscopic

features of the analyte leading to a clear improvement of the obtained data: the reconstructed spectra are much smoother and more similar to the measured data. Consequently, the residual spectra are much smaller and the concentration results more precise. For all cases a flat baseline was found for the true TeCE spectra.

The entire monitoring series conducted over 20 hours was evaluated with all three PCR algorithms: conventional PCR, pPCR, and polyPCR. At t = 0 min TeCE was introduced into the aquifer approximately 10 meters upstream of the sensor head. On account of the gradient of the aquifer, the TeCE "plume" traveled towards the sensor head and passed it slowly. Hence, the TeCE concentration is expected to increase after some time, reach a maximum, and drop to zero again after the TeCE plume has passed. During the first five hours samples were collected next to the sensor head and analyzed by headspace gas chromatography (HSGC) as a validation reference. In Figure 11, the time evolution of the TeCE concentration is plotted for all three evaluation methods. The polyPCR and pPCR result in almost the same concentration values. Both methods are in very good agreement with the HSGC reference method. The results obtained with the conventional PCR are worse than the polyPCR and pPCR concentration values: The deviations from the reference HSGC were larger and zero concentrations were not obtained at the end of the measurement series (see arrows in the top graph of Figure 11). From comparing the HSGC concentration results with the spectroscopically determined values mean errors of all three chemometric algorithms were calculated. For conventional PCR a mean error of 0.24 mg/L was obtained, for polyPCR 0.09 mg/L, and for pPCR 0.11 mg/L. Due to the novel drift correction method presented in this study the mean error could be decreased by more than 50 percent. Although the improvements are smaller than those determined for the synthetic spectra they are still considerable and important, especially in the lower concentration range.

4.3.3 Summary

Baseline drifts affecting optical spectra after calibration result in major concentration errors despite the application of chemometric algorithms. In order to provide correct concentration values, two different methods for avoiding drift induced errors have been developed. One approach ('polyPCR') modifies conventional PCs in a way that drifts of polynomial shape cannot affect subsequent calculations. The other algorithm ('pPCR') synthetically extends the calibration model in order to model drifts independently of but simultaneously to the spectral features of analytes. polyPCR demands less computational effort than pPCR as it is part of the calibration which is done just once. This is of importance for applications with limited computation resources such as miniaturized chemical sensors. pPCR explicitly extracts the drift spectrum as additional information, which can then be used for analyzing the origin of drifts. By means of this additional information experimental setups can be improved, or it can be used for analyzing systematic errors and testing repeatability.

Both algorithms have been assessed by simulated and experimental spectra. Firstly, it was demonstrated that in the drift free case both correction algorithms determine results, which are equivalent to conventional PCR. For disturbed synthetic spectra, the conventional PCR failed completely while the novel correction methods obtained results, which were basically of similar accuracy as the results in the drift free case.

The investigated experimental data set was obtained by mid-infrared ATR spectroscopy of aqueous tertachloroethylene samples recorded in an aquifer system. Since small drifts were also contained in the laboratory calibration spectra, these drift features were included into the

conventional principal components facilitating the modeling of baseline drifts. It was confirmed by means of headspace gas chromatography reference measurements that the novel correction methods are able to provide improved concentration results. Due to the correction methods the mean errors could be decreased by more than 50 percent compared to conventional PCR.

Both drift desensitized algorithms were found to perform equally well for preventing concentration errors due to drifts. Finally, both methods ensure that results obtained in the drift free case are equivalent to results calculated by conventional PCR.

4.4 IR hollow waveguide gas sensing

4.4.1 Introduction

Sensors and sensor systems are continuously demanded for a variety of applications in industry, medicine and environmental sciences [13,14]. Among the variety of sensing schemes, optical transducers are of particular interest and can be mainly divided into two groups: (i) spectroscopic methods utilizing e.g. near-infrared (NIR) or mid-infrared (MIR) radiation enabling quantitative measurements and direct identification of analytes and (ii) so-called optrodes, which detect individual physical properties usually of a single species [15-17].

An optical sensor is presented in this study, combining an FT-IR spectrometer, a gas sensing hollow fiber module and an extracting probe enabling continuous liquid-gas transition of volatile and semi-volatile compounds. Interaction of electromagnetic radiation with matter over a wide range of frequencies has evolved from an exclusive domain of conventional spectroscopy into the interdisciplinary field of optical sensor technology: [18-21] incident light irradiates the sample and molecule-specific attenuation of the initial radiation is correlated to the concentration of the sample. During conventional absorption measurements, the sample is usually located inside the sample chamber of the spectrometer and investigated within a well-defined optical path length. The aim of an optical sensor is to extend this measurement principle by coupling radiation from the spectrometer to a waveguide, providing the opportunity of remote interaction with the sample [22]. Hollow waveguides utilized in the developed sensor system simultaneously act as both waveguide and miniaturized gas cell. Multiple internal reflections common to so-called ‘leaky guides’ [23] enhance the effective optical path length.

A hollow waveguide is generally defined as a light pipe made of dielectric materials or metals with a coaxial bore enabling radiation propagation by reflection at the inside walls [24]. Therefore, transmission losses are determined by the reflectance of the waveguide walls. Metal or metal-coated glass pipes do not transmit light very efficiently, since a small percentage of light energy is absorbed at each reflection at the metal surface. Leaky guides used in this work show increased reflectance due to an optical interference film coated onto the inside wall of the structural tube. Likewise, similar internally coated metal waveguides, such as Ge coated [25] or ZnS coated silver [26] hollow fibers show high reflectance.

AgI coated silver waveguides provide excellent light transmission in the mid-infrared (MIR) spectral range [27-29] with losses as low as 0.1 db/m at 10.6 µm. Nickel tubes coated inside with Ge show higher transmission losses.[14] Internally ZnS coated Ag hollow waveguides are an excellent alternative for IR gas sensing, except for limitations when sensing corrosives gases [30]. Sapphire waveguides have been thoroughly investigated by Harrington et al. [31,32], however, their use for gas sensing is limited due to comparatively higher transmission losses. In the course of this study, silver coated silica fibers have exclusively been used [33].

Hollow waveguides have already been proven as useful tool in spectroscopy, since liquids or gases can be sampled in the hollow core, which simultaneously acts as an efficient lightguide for remote IR gas sensing [34-36], as liquid-core waveguide for ATR sensing [37,38], and for UV/VIS gas analysis [39]. Operating in the MIR range provides access to inherently high molecular specificity due to fundamental vibrational modes of organic compounds, which allows clear distinction and quantification of classes of compounds and individual molecular species [40-42].

In order to extend this principle for measurement of volatile compounds in the liquid phase, a membrane-sampling device (supported capillary membrane sampler, SCMS) has been coupled to the hollow waveguide FT-IR (HWG-FT-IR) spectrometer module. This sensor system demonstrates reliable quantitative detection of organic compounds in water with linear response over a wide concentration range. Chlorinated hydrocarbons are demonstrated having short response and measurement times around approx. 6 min. Multicomponent analysis has been demonstrated for the quantification of BTX (benzene, toluene, xylenes) mixtures.43 Furthermore, the extraction procedure can be optimized for a variety of organic compounds and has been shown to efficiently operate even for semi-volatile organic compounds, such 1,4-dioxane, although requiring extended detection times. However, for many process analytical problems, facile and continuous detection for quality control issues is more important than rapid signal response, as frequently off-line analytical techniques, such as HPLC or GC requiring sampling and sample preparation, have to be applied. The SCMS probe enables separation of trace concentrations of semi-volatile organic compounds within a complex aqueous matrix by permeation of molecules from the aqueous phase through a thin-walled polymer tube into an inert carrier gas. The permeation process takes place at the walls of the tube, which is coiled around a stainless steel support. Permeation through the membrane is achieved by direct contact with the analyte solution and is influenced by individual permeability of the sample molecules through the polymer membrane, the temperature of the solution and the flow rate of the carrier gas inside the polymer tube. The carrier gas continuously transports extracted compounds to the hollow waveguide gas sensor module, while IR radiation is simultaneously interacting with the sample in the hollow core of the fiber.

4.4.2 Experimental

Sensor setup: (see Figure 12) A short straight section of HWG coupled to the SCMS probe via a set of steel stainless 1/16” tubing is externally aligned with a Vector 22 FT-IR spectrometer (Bruker Optik GmbH, Ettlingen, Germany). The ends of the hollow waveguide are positioned with x,y,z-positioners (Newport, Irvine/CA, USA). Both tips of the fiber are capped with custom made connection modules, each equipped with an anti-reflection coated zinc selenide (ZnSe) window (12 mm diameter, Macro Optica Ltd., Moscow, Russia) enabling simultaneous focusing of radiation into the waveguide, while the gaseous sample is constantly transported through the hollow core of the fiber. The cylindrically shaped body of the connection module is fabricated from aluminum with an outer diameter of 2 cm, which fits into standard x,y,z positioners. Ferrules reversibly sealing the hollow waveguide into the connection module are fabricated from Teflon. ZnSe windows are sealed to the cell with indium sealing rings. The dead volume of the connection module is < 3 mm^3, a detailed scheme is given elsewhere.

Signals have been detected with various liquid nitrogen cooled mercury-cadmium-telluride (MCT) detectors (Infrared Associates, Stuart/FL, U.S.A.), all equipped with a 4 mm^2 detection element. Off-axis parabolic mirrors (OAPM, f = 4.6 cm, Janos Technology Inc.,

Townshend/Vermont, USA) were used for collecting and focusing the radiation onto the detector element at the distal end of the hollow waveguide. The radiation from the FT-IR spectrometer, equipped with a silicon carbide (SiC) globar light source, was focused into the HWG sensor module via a zinc selenide (ZnSe) lens (f = 3.8 cm, Macro Optica Ltd., Moscow, Russia).

The SCMS is immersed into the liquid sample, which was kept under constant stirring. The carrier gas stream (nitrogen, 99.9 %) through the thin-walled silicone permeation (diameter: 0.5 mm, Global FIA Inc., Fox Island/WA, U.S.A.) tube is controlled via mass flow controllers (MFC 5850E, Rosemount Inc., Chanhassen/MN, USA) and a portable digital flow meter (Analyt GmbH, Wuppertal, Germany). Stainless steel tubing with a length of 400 mm and a diameter of 1/16" connects the SCMS module to the HWG gas cell.

Absorption spectra of the sample were recorded at a spectral resolution of 4.0 cm^{-1} averaging 63 scans, which corresponds to a measurement time of 30 seconds. A scheme of the experimental setup is shown in figure 1. Absorption spectra were evaluated using OPUS™ software package (Bruker Optik GmbH, Ettlingen, Germany).

Reagents and sampling procedure: Dichloromethane, chloroform and 1,4-dioxane were obtained from Sigma-Aldrich (Munich, Germany). Solutions for the calibration procedure were prepared sampling the pure substances with 0.5-10 µl or 10-100 µl micropipettes (Eppendorf–Hinz GmbH Hamburg/Germany) and further dilution for less concentrated solutions with conventional tap water.

Aqueous samples were investigated by immersing the SCMS probe directly into the sample solution under constant carrier gas flux, enabling continuous permeation and extraction of gaseous samples into the HWG cell. Different optical setups have been investigated and will be discussed in detail in the following section.

Each measurement was performed after purging the stainless steel tubing and the hollow waveguide with carrier gas, and spectroscopically ensuring that no analyte is present in the system before immersing the probe into solution. The same procedure is applied for recording the reference spectrum without sample present in the aqueous phase.

Water and CO_2 absorption bands do not interfere with the spectral features of chloroform and 1,4-dioxane in the investigated spectral range. Dichloromethane shows selective absorption bands near the CO_2 bending vibration at 667 cm^{-1}. Hence, any open optical path in the sensor setup was enclosed and flushed with nitrogen for minimized CO_2 interferences.

4.4.3 Results

For relevance to this project only results on the volatile are discussed here.

As a first test, chloroform was detected in aqueous solutions from 500 ppm down to 750 ppb with a 200 mm fiber section of type HWG 3 in a laboratory setup (one HWG connection module, flask setup with centered probe). Spectra were recorded with open aperture and scanner velocity at 7-20 KHz; acquisition mode was double sided, forward-backward.

500 ppm, 250 ppm, 100 ppm and 62.5 ppm $CHCl_3$ solutions were detected with a N_2 flow rate of 45 cm^3/min. The evaluated absorption band at 772 cm^{-1} is shown in Figure 13 (left). For lower concentrations a flow rate of 7 cm^3/min was applied. Stirring was kept constant at 750 rpm. Under these conditions, a limit of detection at 750 ppb was determined with excellent linear correlation (R = 0.98) at 20 °C.

Dichloromethane has been detected down to low ppb concentration range (experimental LOD = 500 ppb) with the laboratory setup, again showing linear behaviour (R = 0.98) over a considerable concentration range, as shown in Figure 13 (right).

Using the simulated industrial setup with the flow cell in the frequency range relevant for CH_2Cl_2 resulted in improvement of the limit of detection by more than 50 % in comparison to the laboratory setup 1.

With the presented mid-infrared gas sensing system for liquid phase analysis coupling an FT-IR spectrometer to a hollow waveguide sensor module and a supported capillary membrane sampler continuous and efficient detection and quantification of organic compounds with variable volatility in aqueous solution is provided. Response times range from few minutes for aqueous solutions of highly volatile chlorinated hydrocarbons to approx. 30 min for 1,4–dioxane representing semi-volatile target compounds, respectively. With the availability of tailored thin-walled tubular permeation materials optimization of the permeation process for compounds with variable polarity is expected. Limits of detection in the ppb (v/v) (chlorinated hydrocarbons) and ppm (v/v) (1,4-dioxane) concentration range have been achieved, respectively.

The sensor system has been optimized, in order to achieve required detection limits for both sample categories in industrial effluent monitoring applications and demonstrates continuous operation for on-line analysis of organic compounds at process conditions. Based on the achieved results a prototype system will be installed at an industrial location for continuous on-line determination of methanol in a process effluent stream. Recently, IR gas sensing utilizing the combination of hollow waveguides with quantum cascade lasers has been demonstrated [44]. This concept enables the development of miniaturized molecule specific gas sensors, extending the demonstrate principle to a microscale. Hence, hollow waveguide sensor modules coupled to FT-IR spectroscopy and a capillary membrane sampler can be considered an innovative novel approach towards spectroscopic sensing tools for on-line effluent analysis.

5 Remaining Working Plan for the 2nd Year

- Continued MIP development for solid phase (SPE) and HPLC applications and application to real world samples in collaboration with U.S.G.S. Atlanta.
- Collaboration with USGS Atlanta to coordinate real-world measurements at Rottenwood Creek with accompanying validation.

6 FIGURES AND TABLES

	1ST YEAR (QUARTERS)				2ND YEAR (QUARTERS)			
	1	*2*	*3*	*4*	*1*	*2*	*3*	*4*
WP 1	Development of chemical recognition layers based on sol-gels							
			Implementation of sol-gels as coating materials for the fiber optic evanescent wave sensor system					
	Molecular imprinting strategies for selected organic pollutants							
			Characterization of molecularly imprinted polymers and their application as novel recognition layers					
WP 2	Optimization of the FT-IR based fiber optic evanescent wave sensor prototype							
		Measurement of real-world samples						
					Field measurements at Rottenwood Creek			
WP 3			Alternative sensing concept based on IR hollow waveguide sensor combined with capillary membrane sampler					

Figure 1: Time schedule and work plan

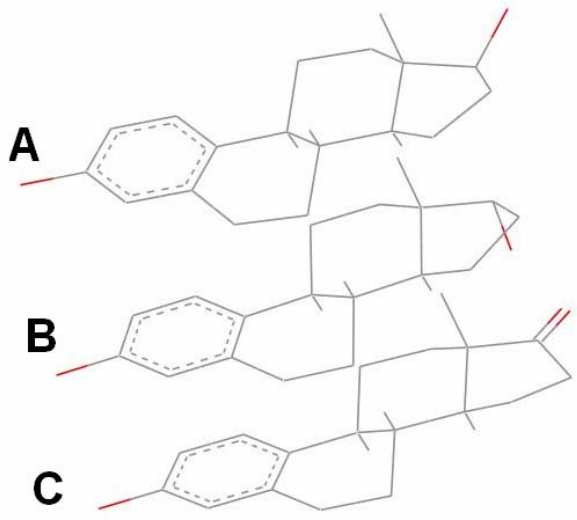

Figure 2: Structure of analytes employed in the evaluation of MIPs. A: 17β-estradiol, B: 17α-estradiol, C: estrone.

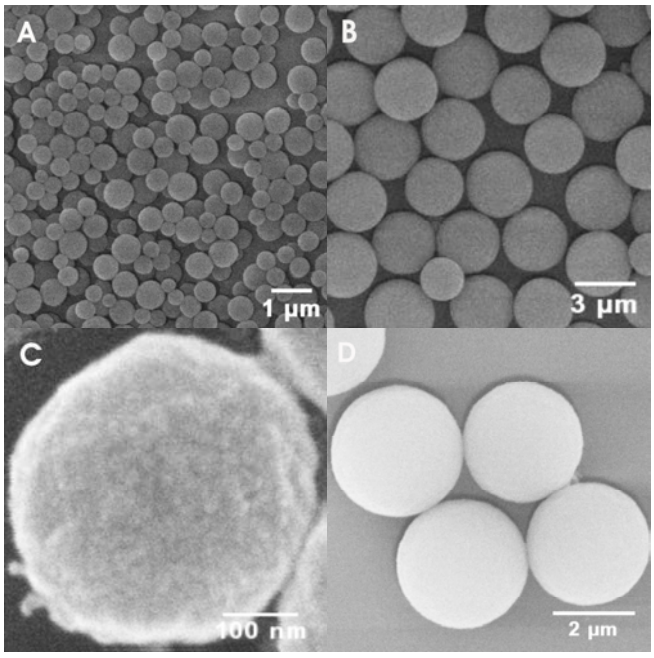

Figure 3: Scanning electron micrographs of beads (A, C, MIP1; B, D, MIP2) produced from precipitation polymerization.

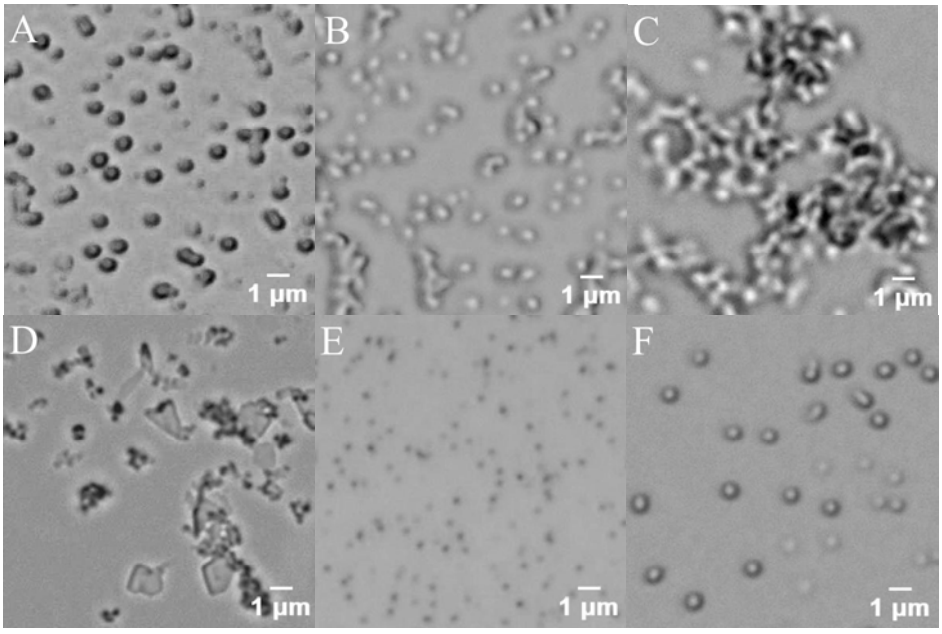

Figure 4: Optical micrographs of poly (MAA-co-EDMA) beads prepared with different monomer ratios (MAA/EDMA, A: 8/6; B: 8/10; C: 8/14; D: 8/16) and poly (MAA-co-TRIM) beads prepared at different temperatures (E: 60^{o}C, F: 70^{o}C) produced from precipitation polymerization.

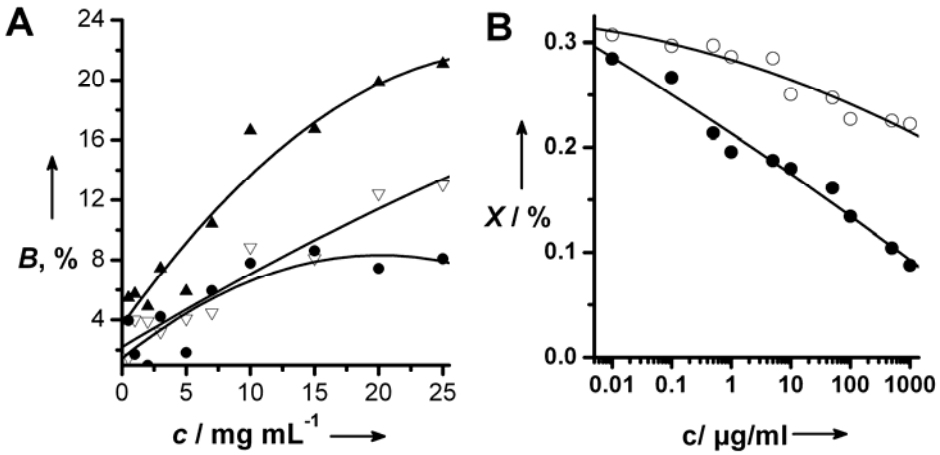

Figure 5: Radioligand binding assays. A: Binding of [^{3}H] estradiol as a function of the polymer concentration. The data points represent the binding isotherm of MIP1 (▲) and CTL1 (□). The specific binding (●) was calculated by subtracting the binding amount of CTL1 from MIP1. B: Displacement of [^{3}H] estradiol binding to MIP1 as a function of the concentration of 17β-estradiol (●) and 17α-estradiol (○). The X axis (c/ µg/ml) has a logarithmic scale.

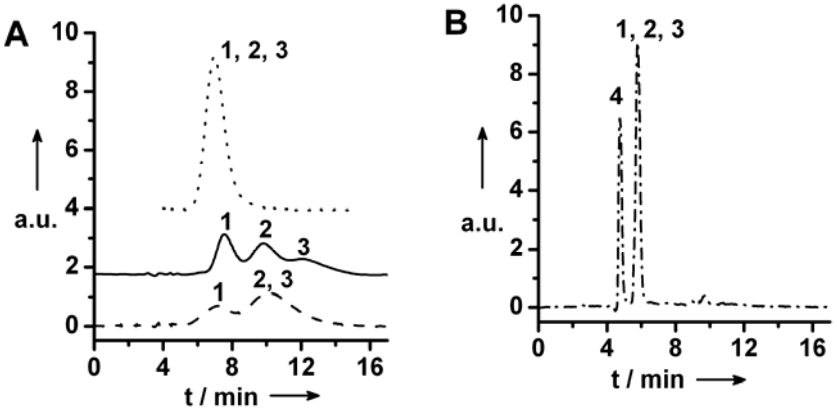

Figure 6: Comparison of chromatographic separation of estrone (peak 1), 17α-estradiol (peak 2) and 17β-estradiol (peak 3) on MIP2 (A: solid line and dotted line), different solvents were used as described below. CTL2 (A: dashed line) and Kromasil 100 C_{18} column (B: dash dot line). Mobile phase: acetonitrile containing 0.5% acetic acid (solid, dash and dash dot line), acetonitrile containing 10% pH8.5 acetate buffer (dot line). Flow rate: 0.6mLmin^{-1}; detection: 280nm. 0.2 µg of estrone, 0.2 µg of 17α-estradiol and 0.4 µg of 17β-estradiol in 20 µL acetonitrile were injected.

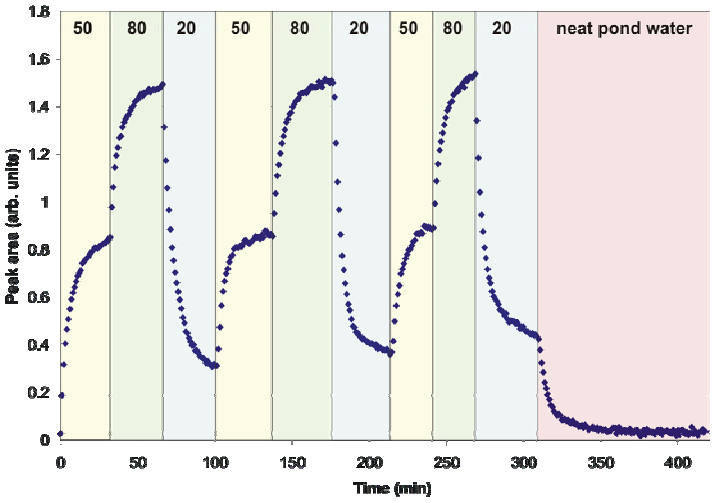

Figure 7*:* Trace of the peak area of the absorption band of o-xylene at 740 cm^{-1} with time during enrichment-based IR-ATR sensing. Concentration trace: 50 ppm; 80 ppm; 20 ppm (in pond water; the sensor was exposed to each concentration for approx. 30 to 35 min) followed by neat pond water for sensor regeneration.

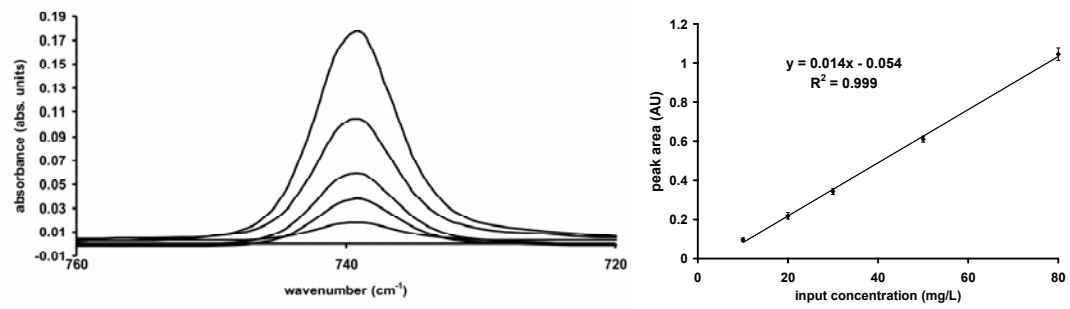

Figure 8*:* (left) The C-H out of plane vibration band of CB for 5 different concentrations (bottom to top: 10, 20, 30, 50 and 80 mg/L) after partitioning into the E/P-co layer recorded after an enrichment time of 20 min. (right) Calibration curve for 3 repetitive measurements of the calibration set of CB. Error bars are derived from the standard deviation for each data point.

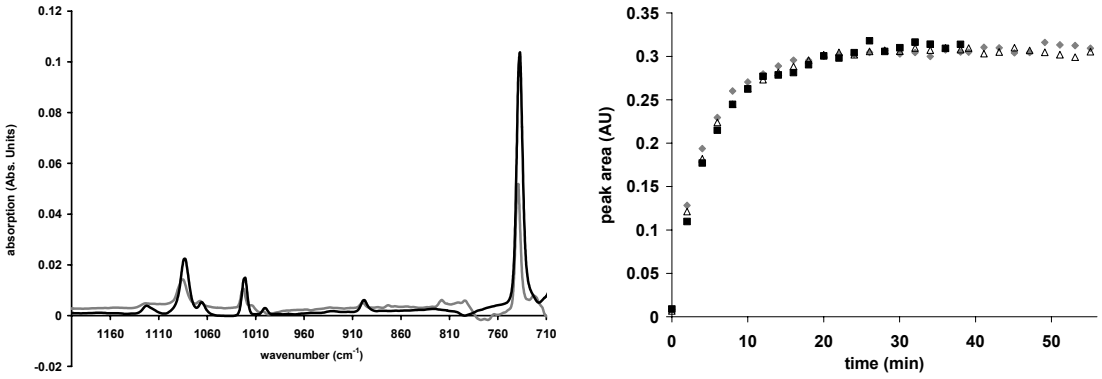

Figure 9*:* (left) Exemplary spectra of a groundwater sample from shaft 5 (grey line) and a calibration solution of 50 mg/L CB in water (black line). Spectra were recorded after 24 min of exposure time to the polymer coated transducer. The peak area of the band at 740 cm^{-1} is used for data evaluation. (right) Enrichment curves of CB from groundwater at SAFIRA site into the E/P-co layer at a flow rate of 4 mL/min. The 3 measurements were performed at 3 different days..

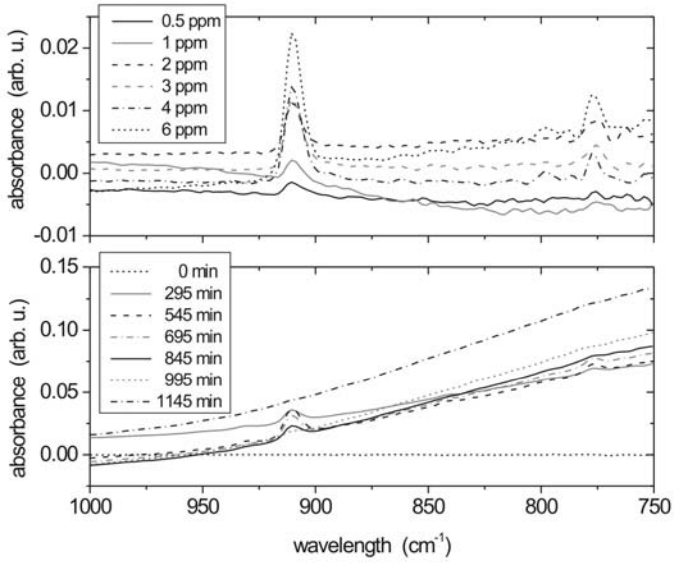

Figure 10: (top) Experimental calibration spectra obtained from aqueous TeCE samples. (bottom) measurement spectra with strong background spectrum drifts; note the different y-axis scalings.

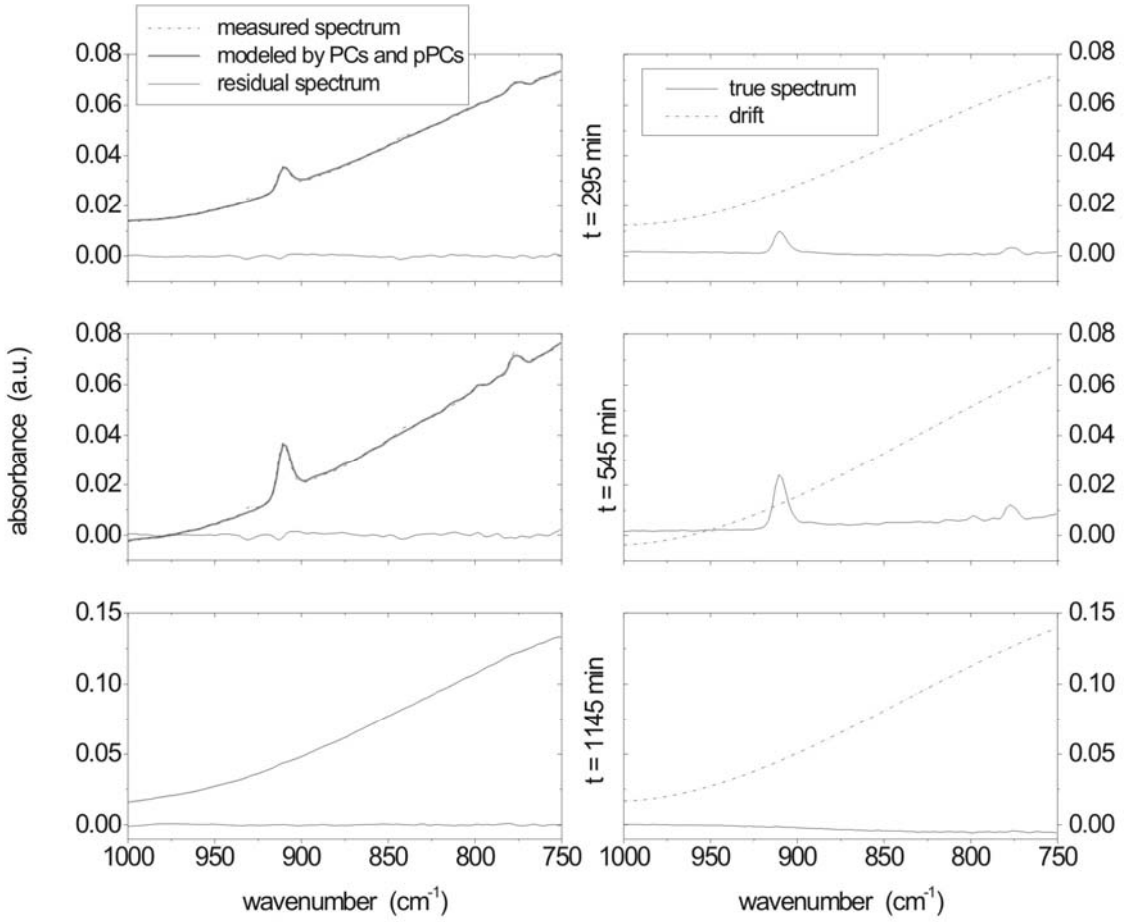

Figure 11: Comparing the the TeCE concentrations obtained with conventional PCR, pPCR, and polyPCR also shown are reference values, which were obtained by headspace gas chromatography (HSGC).

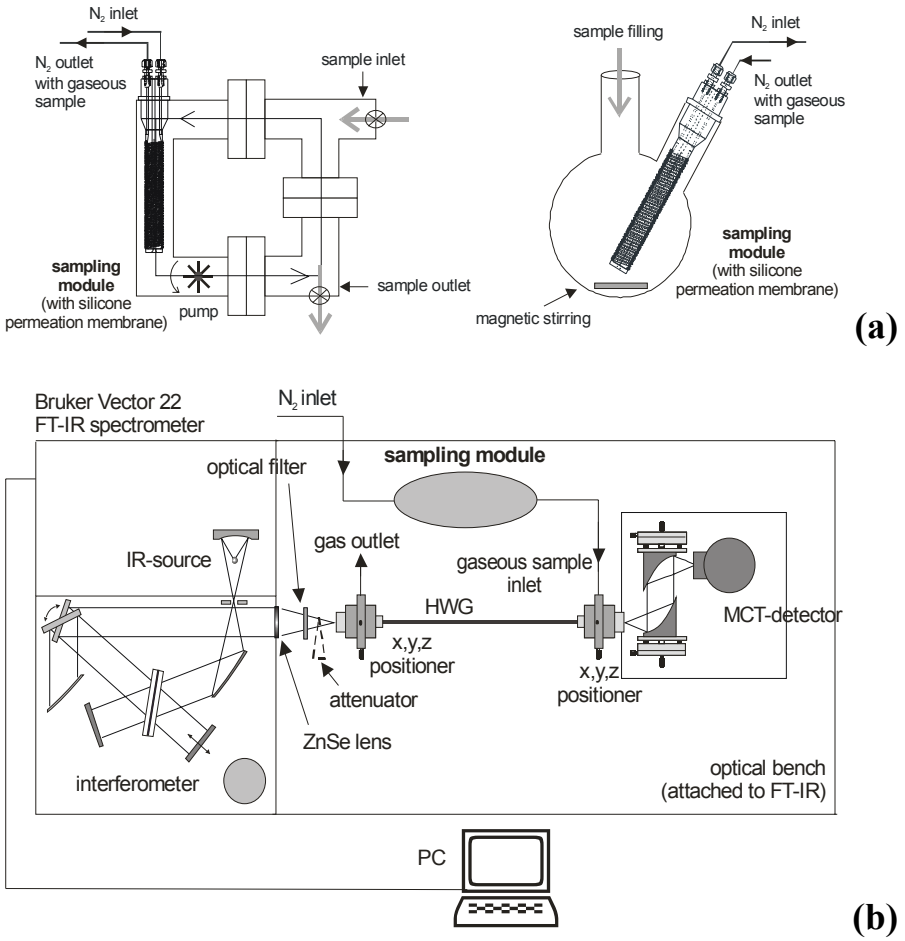

Figure 12: (a) Sampling module (left) as part of an industrial flow cell setup and (right) immersed into a flask in the laboratory setup. (b) Sensing scheme with FT-IR coupled to the hollow waveguide gas sensor module.

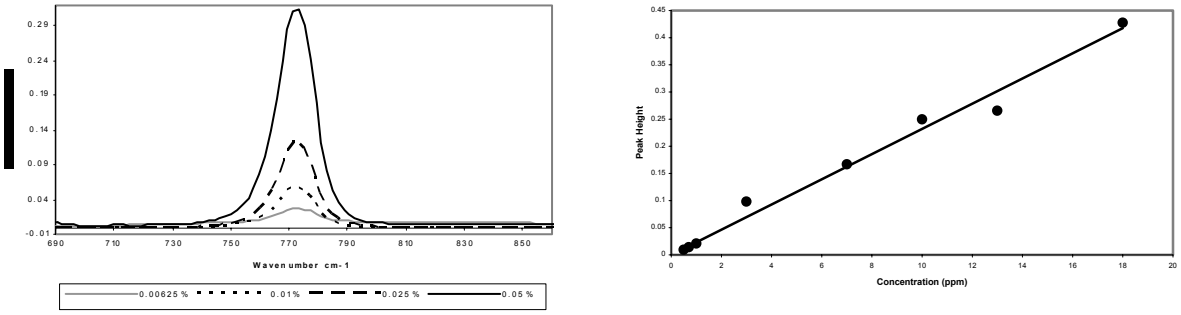

Figure 13: (a) Sampling module (left) as part of an industrial flow cell setup and (right) immersed into a flask in the laboratory setup. (b) Sensing scheme with FT-IR coupled to the hollow waveguide gas sensor module.

7 REFERENCES

1. M. Hecker, C. R. Tyler, M. Hoffmann, S. Maddix, L. Karbe, *Environ. Sci. Technol.* **2002**, *36*, 2311.
2. A. C. Johnson, J. P. Sumpter, *Environ. Sci. Technol.* **2001**, *35*, 4697.
3. A. Penalver, E. Pocurull, F. Borrull, R. M. Marce, *J.Chromatogr. A* **2002**, *964*, 153.
4. L. Zhu, L. Chen, X. Xu, *Anal. Chem.* **2003**, *75*, 6381.
5. O. Ramstroem, L. Ye, K. Mosbach, *Chem.Biol.* **1996**, *3*, 471.
6. B. Sellergren, *Molecularly Imprinted Polymers: Man-Made Mimics of Antibodies and Their Applications in Analytical Chemistry. [In: Tech. Instrum. Anal. Chem., 2001; 23]*, Elsevier, **2001**, pp.113-180.
7. J. P. Lai, X. Y. Lu, C. Y. Lu, H. F. Ju, X. W. He, *Anal. Chim. Acta* **2001**, *442*, 105.
8. A. G. Mayes, K. Mosbach, *Anal. Chem.* **1996**, *68*, 3769.
9. L. Piscopo, C. Prandi, M. Coppa, K. Sparnacci, M. Laus, A. Lagana, R. Curini, G. D'Ascenzo, *Macromol. Chem. Phys.* **2002**, *203*, 1532.
10. J. S. Downey, R. S. Frank, W.-H. Li, H. D. H. Stoever, *Macromolecules* **1999**, *32*, 2838.
11. W.-H. Li, K. Li, H. D. H. Stover, *J.Polym. Sci. Pol. Chem.* **1999**, *37*, 2295.
12. L. Ye, Y. Yu, K. Mosbach, *Analyst (Cambridge, United Kingdom)* **2001**, *126*, 760.
13 J. Janata, M. Josowicz, P. Vanýsek, D. M. DeVaney, Anal. Chem., **70**, 179R (1998)
14 J. Janata, Anal. Chem., **73**, 150A (2001)
15 H. J. Arditty, J. P. Dakin, R. T. Kersten (Editors), *Optical Fiber Sensors*, (Springer-Verlag, Berlin, 1989)
16 O. S. Wolfbeis (Editor), *Fiber Optic Chemical Sensors and Biosensors*, (CRC Press, Boca Raton, FL, 1991) Vol. 1 and 2
17 R. A. Potyrailo, S. E. Hobbs, G. M. Hieftje, Fres. J. Anal. Chem., **362**, 349 (1998)
18 B. Mizaikoff, Proc SPIE, **3849**, 7 (1999)
19 O. S. Wolfbeis, Anal. Chem., **72**, 81R (2000)
20 B. Mizaikoff, B. Lendl, Sensor Systems Based on Mid-Infrared Transparent Fibers, *Handbook of Vibrational Spectroscopy*, J.M. Chalmers and P.R. Griffiths (Eds.), (John Wiley&Sons, Ltd, 2002), Vol. 2, p. 1560
21 G. Holst, B. Mizaikoff, Optical Fiber Sensors for Environmental Applications, *Handbook of Fiber Optic Sensing Technology: Principles and Application*, José Miguel Lopez-Higuerra (Ed.), (John Wiley&Sons, Ltd, 2002), p. 729
22 Janata, *Principles of chemical sensors*, (Plenum Press, New York – London, 1989) Chap. 5, p. 242
23 J. A. Harrington; Fib. and Int. Opt., **19,** 211 (2000)
24 E. A. J. Marcantili, R. A. Schmeltzer; Bell Sys. Technol. J. **43,** 1783 (1964)
25 M Miyagi, A. Hongo, Y. Aizawa, S. Kawakami, Appl. Phys. Letters, **43**, 430 (1983)
26 Y. Matsuura, m. Miyagi, Appl. Opt., **32**, 6598 (1993)
27 A. Inberg, M. Oksman, M. Ben-David, N. Croitoru, J. Clin. Las. Med. Surg., **16,** No 2, 125 (1998)
28 T. Abel, J. Hirsch, J.A. Harrington, Opt. Lett., **19,** 1034 (1994)
29 Y. Wang, Y. W. Shi, Y. Matsuura, M. Miyagi, Opt. Las. Tech., **29** No. 8, 455 (1997)
30 S. Saito, M. Saito , M. Miyagi, Appl. Spec., **47,** 1665 **(**1993)
31 S. Saggese, J. A. Harrington, G. H. Sigel Jr., Opt. Lett., **16** No. 1, 27 (1991)
32 C. C. Gregory, J. A. Harrington, Appl. Opt., **32**, 5302 (1993)
33 N. Croitoru, J. Dror, E. Goldenberg, D. Mendlovic, I. Gannot; US Patent 4,930,863. (1990)
34 R. H. Micheels, K. Richardson, D. J. Haan, J. A. Harrington; Proc. SPIE, **3540,** 64 (1999)
35 D. J. Haan, D. J. Gibson, C. D. Rabii, J. A. Harrington; Proc. SPIE, **3262,** 125 (1998)
36 C. A. Worrell, N. A. Gallen; J.Phys D: Appl. Phys., **30,** 1984 (1997)
37 J. Yang, J. W. Her, H. S. Chen; Anal. Chem., **71,** 3740 (1999)
38 J. Yang, J. W. Her; Anal. Chem., **72,** 878 (2000)
39 K. Dasgupta, Z. Genfa, S. K. Poruthoor, S. Caldwell, S. Dong, S. Y. Liu, Anal. Chem., **70,** 4661 (1998)
40 B. Mizaikoff, R. Göbel, R. Krska, K. Taga, R. Kellner, M. Tacke and A. Katzir, Sens. Act. B, **29**, 58 (1994)
41 J. E. Walsh, B. D. MacCraith, M. Meany, J. G. Vos, F. Regan, A. Lancia, S. Artjushenko, Analyst, **121**, 789 (1996)
42 Brian R. Stallard, Appl. Spec., **5**, 625 (1997)
43 F. de Melas, V. V. Pustogov, D. K. Wolcott, D. C. Olson, A. Inberg, N. Croitoru, B. Mizaikoff, in press, Int. J. Env. Analyt. Chem. (2002)
44 L. Hvozdara, S. Gianordoli, G. Strasser, W. Schrenk, K. Unterrainer, E. Gornik, Ch. S. S. S. Murthy, M. Kraft, V. Pustogow, B. Mizaikoff, A. Inberg, N. Croitoru, Appl. Opt., **39,** No. 36, 6926 (2000)

INFORM: Integrated Forecast and Reservoir Management System for Northern California

Basic Information

Title:	INFORM: Integrated Forecast and Reservoir Management System for Northern California
Project Number:	2003GA33O
Start Date:	7/1/2002
End Date:	6/30/2005
Funding Source:	Other
Congressional District:	5
Research Category:	Climate and Hydrologic Processes
Focus Category:	Hydrology, Management and Planning, Surface Water
Descriptors:	Integrated Forecast-Decision Systems for River Basin Management
Principal Investigators:	Aris P. Georgakakos, Konstantine P. Georgakakos

Publication

1. Georgakakos, A., and K. Georgakakos, 2003. "Value of Climate and Hydrologic Forecasts for River Basin Planning and Management." Key Note Address, GEWEX Workshop, IUGG Conference, Saporo, Japan.
2. Georgakakos, A.P. and H. Yao, 2003. "Climate Variability and Change Assessments for the ACR and ACT River Basins." In Proceedings of the 2003 Georgia Water Resources Conference, April 23-24, 2003, at University of Georgia. Kathryn J. Hatcher, editor, Institute of Ecology, University of Georgia, Athens, GA.

The proposed 1st year project activities are listed below:

1. Interaction/consultation with stakeholder agencies on the scope, design, and data requirements of the Folsom and Oroville short/mid range decision support systems;

2. Development of short range and mid range decision models for Folsom and Oroville reservoirs and corresponding sub-basins;

3. Linkage with hydrologic forecasting systems for Folsom and Oroville sub-basins;

4. Development of policy assessment model for Folsom and Oroville;

5. Development of a graphical user-model DSS interface;

6. Assessment of the Folsom and Oroville forecast-decision systems;

7. Technical report and user manual writing for the Folsom/ Oroville DSS and investigations;

8. Technical workshops with the stakeholder agencies to demonstrate and implement (a beta version of) the Folsom and Oroville short/mid range DSS, provide training in model theory and use, and consider further enhancements and modifications.

Epidemiological and Environmental Malaria Information System for East Africa

Basic Information

Title:	Epidemiological and Environmental Malaria Information System for East Africa
Project Number:	2003GA34O
Start Date:	10/1/2003
End Date:	6/30/2004
Funding Source:	Other
Congressional District:	5
Research Category:	Climate and Hydrologic Processes
Focus Category:	Management and Planning, Climatological Processes, Hydrology
Descriptors:	
Principal Investigators:	Aris P. Georgakakos, Mark Benedict

Publication

The project activities focused on gathering preliminary information and developing collaborative institutional plans to address malaria control issues. The specific aims of this initial phase were (1) assess malaria related data availability and monitoring needs in East Africa, (2) conduct workshops to develop sufficient information and collaboration with East African agencies and ministries, and (3) develop a draft proposal for a malaria information system.

The project team helped organize a national workshop in Khartoum, Sudan, to address malaria control and related data and institutional needs. The workshop took place in February of 2004 with the participation of several Sudanese and international organizations. Workshop participants included: the World Health Organization (WHO); Sudan Ministries of Science and Technology, Health, and Irrigation and Water Resources; the International Atomic Energy Agency (IAEA); and the Georgia Institute of Technology. GWRI staff participated and gave presentations on their past and current involvement in the Nile Basin. Other presenters reported on the status of entomological, epidemiological and environmental data. The workshop developed recommendations that were provided to the Sudanese Government. While in Khartoum, tours and meetings were conducted with the Ministry of Science and Technology's remote sensing and GIS centers to observe the current state of technology, discuss applications to malaria control, and determine the extent of training required to support local operation of the proposed malaria information system.

Information Transfer Program

Hydrologic Engineering for Dam Design

Basic Information

Title:	Hydrologic Engineering for Dam Design
Project Number:	2003GA35O
Start Date:	10/13/2003
End Date:	10/15/2003
Funding Source:	Other
Congressional District:	5
Research Category:	Engineering
Focus Category:	Hydrology, Floods, Water Supply
Descriptors:	Continuing Education Course
Principal Investigators:	Bert Holler

Publication

Nile Decision Support Tool Applied Training Program

Basic Information

Title:	Nile Decision Support Tool Applied Training Program
Project Number:	2003GA36O
Start Date:	1/1/2004
End Date:	8/31/2004
Funding Source:	Other
Congressional District:	5
Research Category:	Climate and Hydrologic Processes
Focus Category:	Hydrology, Water Supply, Irrigation
Descriptors:	Decision Support, River Basin Planning and Management, Remote Sensing, Hydrology, Agricultural Planning, Hydropower
Principal Investigators:	Aris P. Georgakakos, Stephen Bourne, Carlo De Marchi, Amy Tidwell, Huaming Yao

Publication

Scope

Nile DST is a prototype decision support system developed for supporting planning and management decisions in the Nile Basin. The system consists of a comprehensive data base, a set of models linked to the database, and a graphical user-model interface to access data, models, and results in intuitive and meaningful ways. The models are designed to support river basin planning and management decisions, and include models for river simulation and reservoir management, crop simulation and irrigation scheduling, hydrologic watershed simulation and forecasting, and remote sensing.

The purpose of the proposed activities during the extension period is to *strengthen* the capacity of the Nile DST engineers and planners to utilize and sustain the Nile DST technology through effective participation in database development, data quality control, and model recalibration. More specifically, the following activities are envisioned:

1. Stakeholder Consultation and Assessment of Training Needs
   Assist the project office in prioritizing DST training activities through consultation with the policy makers and the national modelers of the Nile Basin countries.

2. Development of a DST Training Program
   Based on the country input, and in collaboration with the project office and AGLW, design a DST training program focusing on the identified priorities. As a minimum, the program will include technical support through the Internet and one regional workshop. The project will circulate the proposed program to the NCs and NMs for comments and concurrence.

3. Development of a stand-alone Nile DST Database Module
   As promised during the last PSC workshop, a stand-alone database system will be developed and made available to the Nile Basin countries. The cost for this activity will be provided by the Georgia Institute of Technology.

4. Implementation of Internet Support
   A set of Nile DST exercises will be developed and provided to the National Modelers through the Internet. The purpose of the exercises will be to review the software functionality, correct data discrepancies that have already been identified in the previous project phase, and perform preliminary model runs with the various Nile DST modules in preparation for the regional training workshop. Georgia Tech personnel will provide technical support through an internet communication forum that will be set-up for this purpose. Questions, answers, and comments will be accessible by all participants. Participation will be controlled by passwords and will be limited to National Modelers and other individuals designated by each country.

5. Regional Workshop
   The purpose of this workshop will be to re-convene the National GIS Experts and the National Modelers to provide in-depth, integrated, and hands-on training on all

aspects of the Nile DST including (1) data entry, management, and quality control, (2) model re-calibration with revised data, and (3) scenario analysis pertinent to the expectations of the policy makers. The duration of the workshop would be three weeks. This will be the first workshop that will bring together Database Experts *and* National Modelers to jointly address relevant water resources planning and management issues.

6. Post Workshop Training and Reporting

The purpose of this activity will be to consolidate and document the achievements of the training program through a series of advanced investigations of interest to the policy makers. Technical assistance will be provided via the Internet as in Activity 4. The output of this activity will be a comprehensive technical report summarizing the findings of the advanced investigations. The report will be co-authored by all training program participants and will form the basis for journal and conference publications and presentations.

Student Support

Student Support					
Category	**Section 104 Base Grant**	**Section 104 RCGP Award**	**NIWR-USGS Internship**	**Supplemental Awards**	**Total**
Undergraduate	0	0	0	0	0
Masters	1	0	0	0	1
Ph.D.	3	1	1	0	5
Post-Doc.	0	0	0	0	0
Total	4	1	1	0	6

Notable Awards and Achievements

Publications from Prior Projects

None